การปั่นและสมบัติของเส้นใยนาโนคอมพอสิตไอโซแทกติกพอลิพรอพิลีน/ไฮโดรโฟบิกซิลิกา

นายนที ศรีสวัสดิ์

SPINNING AND PROPERTIES OF ISOTACTIC POLYPROPYLENE/HYDROPHOBIC

SILICA NANOCOMPOSITE FIBERS

Mr. Natee Srisawat

A Dissertation Submitted in Partial Fulfillment of the Requirements

for the Degree of Doctor of Philosophy Program in Materials Science

Department of Materials Science

Faculty of Science

Chulalongkorn University

Academic Year 2009

Thesis Title	SPINNING AND PROPERTIES OF ISOTACTIC
	POLYPROPYLENE/ HYDROPHOBIC SILICA
	NANOCOMPOSITE FIBERS
By	Mr. Natee Srisawat
Field of Study	Materials Science
Thesis Advisor	Associate Professor Kawee Srikulkit, Ph.D.
Thesis Co-Advisor	Assistant Professor Manit Nithitanakul, Ph.D.

Accepted by the Faculty of Science, Chulalongkorn University in Partial Fulfillment of the Requirements for the Doctoral Degree

………………………………………….. Dean of the Faculty of Science

(Professor Supot Hannongbua, Dr.rer.nat.)

THESIS COMMITTEE

………………………………………….. Chairman

(Assistant Professor Sirithan Jiemsirilers, Ph.D.)

…………………………………………. Thesis Advisor

(Associate Professor Kawee Srikulkit, Ph.D.)

………………………………………….. Thesis Co-Advisor

(Assistant Professor Manit Nithitanakul, Ph.D.)

………………………………………….. Examiner

(Associate Professor Duangdao Aht-Ong, Ph.D.)

………………………………………….. Examiner

(Associate Professor Pranut Potiyaraj, Ph.D.)

………………………………………….. External Examiner

(Associate Professor Taweechai Amornsakchai, Ph.D.)

นายนที ศรีสวัสดิ์ : การปั่นและสมบัติของเส้นใยนาโนคอมพอสิตไอโซแทกติกพอลิพรอพิ ลีน/ไฮโดรโฟบิกซิลิกา. (SPINNING AND PROPERTIES OF ISOTACTIC POLYPROPYLENE/HYDROPHOBIC SILICA NANOCOMPOSITE FIBERS) อ.ที่ ปรึกษาวิทยานิพนธ์หลัก : รศ.ดร. กาวี ศรีกูลกิจ, อ.ที่ปรึกษาวิทยานิพนธ์ร่วม : ผศ.ดร. มานิตย์ นิธิธนากุล จำนวนหน้า 125 หน้า.

ได้ทำการเตรียมเส้นใยฟิลาเมนท์พอลิพรอพิลีนผสมอนุภาคซิลิกา โดยในอันดับแรกได้ทำ การผสมอนุภาคซิลิกาเข้าไปในพอลิพรอพิลีนโดยอาศัยวิธีผสมแบบหลอมเหลวหรือการผสมแบบ ละลายจนได้เป็นคอมพอสิตเรซิน จากนั้นนำคอมพอสิตเรซินไปอัดรีดเป็นเส้นใยมัลติฟิลาเมนท์ที่ ปั่นด้วยความเร็วต่างๆ ด้วยเครื่อง Fourne's pilot plant (ในกรณีของคอมพอสิตเรซินจากการผสม แบบหลอมเหลว) หรืออัดรีดเป็นโมโนฟิลาเมนท์ด้วยเครื่อง ThermoHaake (ในกรณีของคอมพอ สิตเรซินจากการผสมแบบละลาย) การวิเคราะห์เส้นใยคอมพอสิตที่อัดรีดออกมาได้อาศัยหลาย เทคนิค เช่น การวิเคราะห์ลักษณะทางสัณฐานวิทยา (SEM และ AFM) อุณหภูมิเกิดผลึก (DSC) โครงสร้างผลึก (XRD) และศึกษาสมบัติทางความร้อน (TGA) ความแข็งแรง การหดตัว และ สมบัติไม่ชอบน้ำโดยการวัดมุมสัมผัส จากภาพถ่าย SEM ของเส้นใยมัลติฟิลาเมนท์พบว่าอนุภาค ซิลิกายังมีขนาดในระดับไมครอนซึ่งแสดงว่าแรงเฉือนจากเทคนิคการหลอมเหลวไม่สามารถทำให้ อนุภาคซิลิกาแยกออกจากกัน ในขณะที่เทคนิคการผสมแบบละลายด้วยความดันสามารถทำให้ อนุภาคซิลิกาที่เกาะกันอยู่แยกออกจากกัน เป็นผลให้อนุภาคนาโนซิลิกาสามารถกระจายตัวใน เนื้อของพอลิพรอพิลีนอย่างสม่ำเสมอ ด้วยมีขนาดอนุภาคที่เล็กมากทำให้มีสามารถแสดงตัวเป็น สารก่อผลึกให้กับพอลิพรอพิลีน ผลจากอนุภาคนาโนที่กระจายตัวอย่างสม่ำเสมอ ทำให้เส้นใยนา โนคอมพอสิตมีสมบัติการทนการหดตัวที่ดีขึ้นอันเป็นผลมาจากการเสริมแรงของอนุภาคนาโนซิลิ กา นอกจากนี้ยังพบว่าสมบัติความไม่ชอบน้ำของนาโนคอมพอสิตเพิ่มสูงขึ้นเมื่อเทียบกับพอลิ พรอพิลีนที่ไม่ผสมอนุภาคนาโนอันเป็นผลมาจากการเพิ่มขึ้นของความขรุขระของผิวเส้นใยนั่นเอง

ภาควิชา......วัสดุศาสตร์.......................... ลายมือชื่อนิสิต..
สาขาวิชา.....วัสดุศาสตร์.......................... ลายมือชื่อ อ.ที่ปรึกษาวิทยานิพนธ์หลัก....................
ปีการศึกษา...2552................................ ลายมือชื่อ อ.ที่ปรึกษาวิทยานิพนธ์ร่วม....................

4873820123 : MAJOR MATERIALS SCIENCE

KEYWORDS : POLYPROPYLENE/SILICA NANOCOMPOSITE FIBERS / NUCLEATING AGENT / NANOCOMPOSITE FIBERS

NATEE SRISAWAT : SPINNING AND PROPERTIES OF ISOTACTIC POLYPROPYLENE/HYDROPHOBIC SILICA NANOCOMPOSITE FIBERS. THESIS ADVISOR : ASSOCIATE PROFESSOR KAWEE SRIKULKIT, Ph.D., THESIS CO-ADVISOR : ASSISTANT PROFESSOR MANIT NITHITANAKUL, Ph.D., 125 pp.

Silica particles filled polypropylene filament fibers were prepared. Firstly, melt mixing and solution (toluene) mixing were carried out to predisperse silica agglomerates, leading to composite resins. Then, the obtained composite resins were spun into multifilament fibers with various spinning speeds using the Fourne's pilot plant fiber spinning machine (for melt mixed masterbatches) and free-fall monofilaments using ThermoHaake's single screw extruder (for solution mixed resins). The characterizations of spun composite fibers including morphological analyses (SEM and AFM), crystallization temperature (DSC) and the fine structure (XRD) were studied. Properties evaluation included thermal property (TGA), tensile strength, shrinkage and surface hydrophobicity by contact angle measurement.   SEM images of multifilament fibers demonstrated that shear stress applied during melt-mixing failed to overcome cohesion force among agglomerate particles. Successfully, AFM images revealed that solution mixing via autoclave treatment could disaggregate the silica agglomerates into nanoscale particles, producing an even distribution of nanoparticles within the bulk of the fiber or on the surface. As a consequence, the presence of the nanoparticles favorably induced heterogeneous nucleation process in the free-fall filament as evidenced by DSC analysis. Hot stage images further confirmed the nucleating effect of silica nanofiller. Well dispersion of nanoparticles in PP matrix resulted in an improvement in shrinkage properties of nanocomposite fibers. Furthermore, the surface hydrophobicity of the nanocomposite fibers was found higher than neat fiber thanks to an increase in surface roughness arising from the presence of nanoparticles on the surface.

Department : ___Materials Science_____   Student's Signature _____

Field of Study : ___Materials Science_____   Advisor's Signature _____

Academic Year :_2009_____   Co-Advisor's Signature _____

ACKNOWLEDGEMENTS

I would like to express my faithful gratitude to my advisor, Associate Professor Dr. Kawee Srikulkit for his invaluable guidance and encouragement throughout this thesis. I also would like to thank my co-advisor, Assistant Professor Dr. Manit Nithitanakul, thesis committee and member of Materials Science Department for their direction and for letting me draw from his experience during many years at Chulalongkorn University. Without their vision and support, this thesis would not have been possible.

I also would like to thank my parents who support me all my life and my family on the great support, especially on my wife (Jaja) and my daughter (Denier/NuDee).

I also would like to thank all member and friends at the department of Materials Science, Faculty of Science, Chulalongkorn University and my colleague at RMUTT all a time to study, without helps and comments, this thesis would not have been completed.

I would like to extend my gratitude to National Science and Technology Development Agency, Thailand and National Center of Excellence for Petroleum, Petrochemicals, and Advanced Materials, Chulalongkorn University for financial support.

CONTENTS

LIST OF TABLES

LIST OF FIGURES

Figure   Page

Figure	Page

LIST OF ABBREVIATIONS

iPP   Isotactic Polypropylene

FDY   Fully Drawn Yarn / Fiber

Denier   Fineness of fiber, weight-per-unit-length

                 (grams of fiber / yarn in 9000 meter length)

g/den   gram force / denier (tenacity of fiber)

DR   Draw ratio: ratio of collection speed and feeding speed

CHAPTER I

INTRODUCTION

1.1 Introduction

Nanotechnology is a new sector of science that has been growing in a rapid path thanks to novelties including significantly enhanced physical, chemical, and biological properties, functions, phenomena, and process. Nanomaterials developed from nanotechnology have emerged from many scientists and the industrialized sectors. Carbon nanotube, montmorillonite, titanium dioxide nanoparticles, silver nanoparticle and silica nanoparticle, for example, are frequently used to improve the properties of many materials, especially the polymeric materials. One growing area of research activities in nanomaterials utilization is polymer-based nanocomposites which significantly offers better improvement in various properties and new functional properties, such as improved mechanical properties, heat deflection temperature (HDT), dimensional stability, and flame retardancy.

Fibers from isotactic polypropylene (iPP) are commonly found in many end-use products. Their advantageous properties are such as light weight, resistance to moisture and chemicals, low cost, sufficiency strength, and ease in processing. Furthermore, fiber's properties can be enhanced with melt mixing with particulates and fibrous materials as well as by melt blending with other polymers (Velasco et al., 1996; Amash et al., 2000; Qiu et al., 2000; Esfandiari et al., 2008; Sui et al; 2009). There is an increasing demand for novel polymeric material with improved physical properties for high tech applications. Blending of polymers and polymer composites are two important approaches towards achieving novel polymeric material. Recently, polymer nanocomposites which contain nano-sized particles at a much lower loading ratio than conventional fillers have attracted great deal of attention because they offer enhanced mechanical properties and thermal properties when compared to conventional composites (Wu et al., 2002). Nano-sized particles, particularly, carbon nanotube (CNT) (Bhattacharyya et al., 2003; Chatterjee et al., 2003) and montmorillonite (MMT) (Liu and

Wu, 2001; Gao, 2004) have taken a lead as the novel nano-fillers for plastics as well as fibers due to their high aspect ratio. Even though, the fillers with high aspect ratio are ideal for plastic reinforcement, recently silica is interesting filler widely investigated for polymeric materials and held a great potential for developing nanocomposites.

Fumed silica (silicon dioxide: SiO_2) is a nanoparticle with the size of around 8 – 12 nm. Because of tiny size, nanoscopic particles have an ultra large surface area per volume which preferably enhances adhesion capability with the polymeric matrix. As a result, produced nanocomposites show improvement in properties including toughness and impact performance, thermal stability, gas barrier properties, and electrical and thermal conductivity. Recently, fumed silica has been received considerable interest. Fumed silica is synthesized by hydrolysis of chlorosilane in an oxygen-hydrogen gas flame. It is an amorphous silicon dioxide which is claimed to be non-toxic when compared to crystalline silica.   There are many reports on the usage of silica for enhancing mechanical properties of polymer. Some articles dealt with silica as filler for polypropylene fiber (Caldas et al., 1997; Chen et al., 2006; Rottstegge et al., 2007) and other articles reported the study of silica addition to polyester and nylon-6 fibers (Liu et al., 2004; He et al., 2006; Tian et al., 2006; Mahfuz et al., 2007; Yang and Gu, 2007; Zheng and Wu, 2007). Typically, silicas are presented in an agglomerated form which, for nanocomposite applications, needs to be small enough and fully dispersed in polymer matrix in order to achieve the improved properties. In case of hydrophilic silica (untreated silica), its surface contains silanol groups connecting together through strong intermolecular hydrogen bonding. Hence, it is not easy to obtain the state of dispersion at nanoscale level. Hydrophobic silicas which are normally modified using organosilane agents make them compatible with hydrophobic polymer matrix like polypropylene.

The purpose of this study was to explore the usage of hydrophobic silica as nano-reinforcement fillers for common polypropylene fiber. Hydrophobic silica was chosen because the nanoparticle forms are commercially available. Due to its

hydrophobic characteristic the hydrophobic silica nanoparticles could easily be compatible with polypropylene matrix. Melt blending and solution blending techniques to introduce hydrophobic silica to polypropylene were studied and discussed. The effect of silica as nucleating agent was also be investigated. Isotactic polypropylene was chosen to be a fiber polymer because of its preeminent properties and economics. Melt spinning process to produce filaments was also used to obtain the fiber form. The aims of this study were to introduce hydrophobic silica into melt spun isotactic polypropylene fiber and then studying the distribution behavior of the nanoparticles in the nanocomposite fiber. Finally, fiber properties such as physical, thermal, and other were investigated.

1.2 Thesis objective

    1.2.1   Spinning isotactic polypropylene/hydrophobic silica fibers

    1.2.2   Study the effects of hydrophobic silica on nanocomposite fiber properties

1.3 Thesis outline and scope

    To study the hydrophobic silica effect as nanofiller in polypropylene fiber, multifilament and monofilament fibers were spun from melt-mixed and solution mixed composites. Melt compounding and solution mixing techniques were adopted to predisperse silica particles into polypropylene matrix. Characterizations and properties evaluation were carried out for physical properties, thermal properties, molecular structure, orientation along the fiber, and surface hydrophobicity.

CHAPTER II

LITERATURE REVIEW

This chapter is aimed to presenting the background of the material used. In first part of this chapter, the characteristic of silica, type, properties, are presented. In a second part of this chapter, background of about polypropylene, properties, are presented. In a third part of this chapter, the spinning polymers, especially on polypropylene spinning are presented. In a last part of this chapter, literature reviews in using silica to any polymers are presented.

2.1 Silica

Silica or silicon dioxide used in this study is fumed silica (pyrogenic silica) commercialized by Degussa AG (Thailand). Hydrophobic silica (Aerosil® R974) was used as filler to isotactic polypropylene (iPP), fiber form is final product. Types of synthetic silica, surface properties and surface modification are introduced in this part to understanding on silica was used in this study.

2.1.1 Types of synthetic silica

Silica is one of the most abundant components on the Earth surface, especially in the form of quartz. Silica can also be synthesized industrially. It can be crystalline (generally for natural origins) or amorphous (generally for synthetic origins) There are various synthesis routes for the manufacturing of synthetic amorphous silica.

- wet routs: sol/gel process, precipitation and

- thermal route: pyro-hydrogenation, arc, plasma
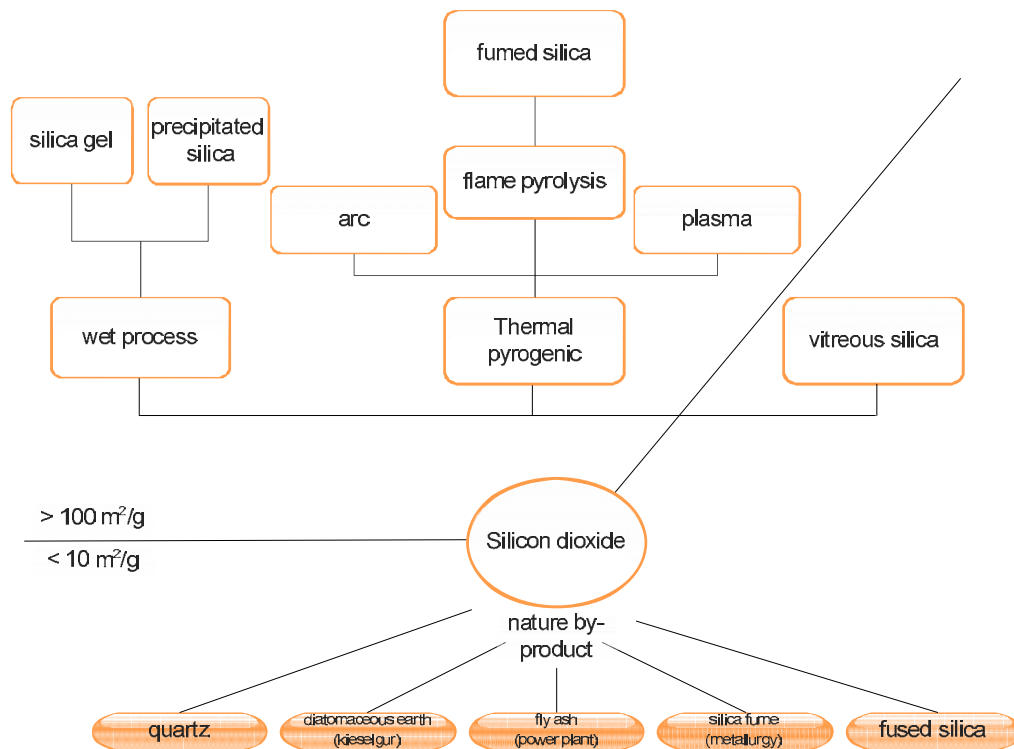
Figure 2.1 Different categories of synthetic silica

2.1.1.1 Silica sol

The sol-gel process is one of the most extensively described in the literature. It is based on the condensation of silanol groups to form a siloxane network according to the reaction:

$$\equiv Si\text{-}OH \ + \ HO\text{-}Si \equiv \ \ \text{->} \ \ \equiv Si\text{-}O\text{-}Si \equiv \ + \ H_2O$$
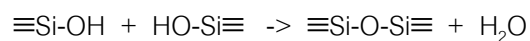
Silicate of sodium or alcoxysilanes can be used as raw materials to get silanols species by hydrolysis. The hydrolysis and the condensation take place simultaneously in an aqueous solution, forming stable colloidal particles. The condensation reaction is influenced by the addition of an electrolyte or by changing the pH of the solution. The growth of particles or the bonding of particle leading to the formation of a network can be respectively favored depending on the conditions chosen.

After the sol/gel transition, an elastic behavior appears, and a hydrogel is obtained in case the solvent is water, or respectively an alcogel in alcohol. When dried, a hydrogel provides a xerogel and an alcogel provides an aerogel. The porosity can be tailored and subsidiary thermal treatment can be necessary to stabilize the material.

The advantage of this process is to lead to pure and homogeneous silica particles under low temperature. Silica obtained by sol-gel process, so-called silica sol (or also sometimes silica gel), is generally used for the manufacture of films, fibers, powders, composite or porous material. (Bugnicourt, 2005)

2.1.1.2 Precipitated silica

The precipitated silica was developed in the 1940's as white reinforcing filler for rubbers, which is still its main application field. It is obtained by acidification of a solution of silicate of sodium in the presence of sulphuric acid or of carbon dioxide and hydrochloric acid according to the reaction

$$Na_2OXSiO_2 \ + \ H_2SO_4 \ -> \ XSiO_2 \ + \ Na_2SO_4 \ + \ H_2O$$
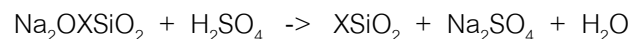
Rather individual silica particles are obtained because the gelation is avoided during the process.

2.1.1.3 Pyrogenic silica

The pyrogenic (or fumed) silica was prepared for the first time by the German chemist Klopfer, in 1941, with the same objective as for the precipitation process. Pyrogenic silica consists of a nonporous, amorphous, fine, fluffy white powder and is totally amorphous.

The main markets of fumed silica are: reinforcing filler mainly for silicone rubbers (application accounting for about 55% of the market of fumed silica), matting agent for paint and polymers, free flow agent for powders, rheological additive providing thickening or thixotropy to polymers, adhesive, paint, ink for example. The main supplier

of fumed silica worldwide are Wacker (HDK®), Cabot (Cabosil®) and Degussa (Aerosil®), with an annual world market around 150,000 tones (2004).

2.1.1.4 Silica obtained via other thermal processes

Silica can also synthesized in an electric arc: from the reduction of quartz at 2,000 °C in the presence of coke, silicon monoxide is created and then oxidized by air to form silica. This process is not widespread because of its high cost and or the poor properties of this silica compared with fumed silica. Finally, the plasma process is also rarely employed.
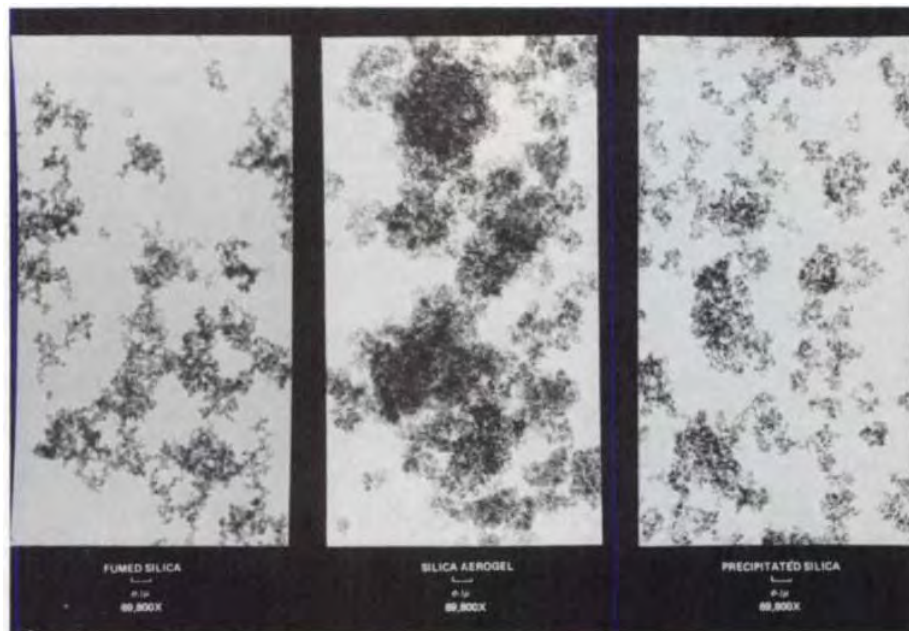
Figure 2.2 Comparative electron micrographs of fumed, gel, and precipitated silicas

Comparison of physical properties

The physical properties of the different type of synthetic silica such as the porosity, size and organization of the particle depended largely on their synthesis process. They are summarized in the Table 2.1.

Table 2.1 Physical properties of different synthetic silica depending on their process of synthesis (Katz and Milewski, 1987)

	Thermal processes		Wet processes	
	Fumed	Arc	Gel	Precipitated
Surface area, m^2/g	50–400	150–200	300–1000	60–300
Oil absorption, cc/100 g	150–250	80–120	150–250	50–250
Bulk density, g/l (compacted)	90–120	120–150	90–160	160–200
5% pH	3.6–4.3	3.5–4.2	4.0–7.5	6.5–7.5
% Moisture	<1.5	<2.0	5.0	6.0
Silanol groups/nm^2	2–4	2–3	4–8	8–10
Primary particle size, nm	7–40	—	—	10–30
Average particle size, μm	0.8	4–8	4–10	1.5–10

2.1.2 Synthesis and multi-scale organization of pyrogenic silica

Pyrogenic silica is obtained via a high temperature process. The hydrolysis of silicon tetrachloride in a flame of mixed hydrogen and oxygen, between 1,200 °C and 1,500 °C approximately, leads to the formation of silica and hydrochloric acid according to the reaction:

$$SiCl_4 + 2 H_2 + O_2 \rightarrow SiO_2 + 4 HCl$$
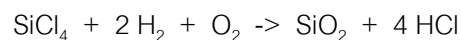
A part of the hydrochloric acid formed is evaporated but the excess remains physically absorbed on silica surface explaining its slightly acid character (3.5<pH<4.3).
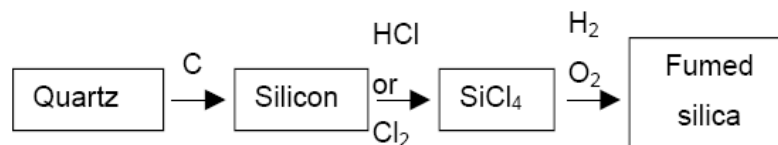
Figure 2.3 Process leading to the formation of fumed silica

The 3-scales organization of fumed silica is due to its synthesis into a flame. From the reordering of 'protoparticles', i.e. clusters of 10 – 200 silicon atoms

covered by active groups, spherical primary particles result from the first step. Their diameter is included between 10 – 20 nm depending on the combustion conditions.

Still in the molten state, these primary particles fuse (by formation of siloxane bonds between neighboring primary particles) as secondary 3-dimensional chain-like structures, i.e. sintered aggregates, which dimensions vary from 100 – 500 nm.

On cooling down, these aggregates flocculate under the effect of low physic-chemical interactions to form macroporous tertiary structure, or agglomerates, measuring up to several microns, finally building up macroscopic fluffy flocks. The size of these structures is function of the silica surface treatment that controls particle interaction (colloidal forces). This size is generally difficult to determine accurately because it depends on the balance between agglomeration and dispersion forces resulting from particles sizing techniques.
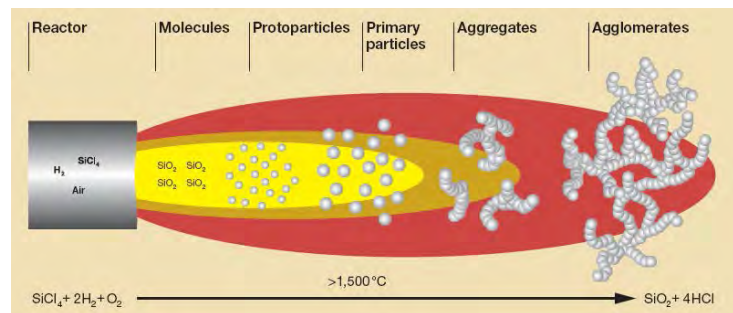
Figure 2.4 Production of fumed silica (Wacker HDK®) and different levels of organization

The size and size distribution of the primary particles, and thus the specific surface area, is controlled via the temperature and temperature gradient of the gas flow in the flame. Certainly due to diffusion aggregation limited processes, primary particles of same size tend to stick together to form the aggregates, so that size distribution of primary particles is delta like inside a given aggregate, but not is between various aggregates of the same manufacture. When the specific surface area increases,

on one hand, average size of primary particle decreases, and on the other hand, size distribution of the aggregates decreases markedly.

Silica exhibits a fractal structure. A section of the next chapter is devoted to the basics of fractals geometry and the measurements of fractal dimension of silica aggregates.
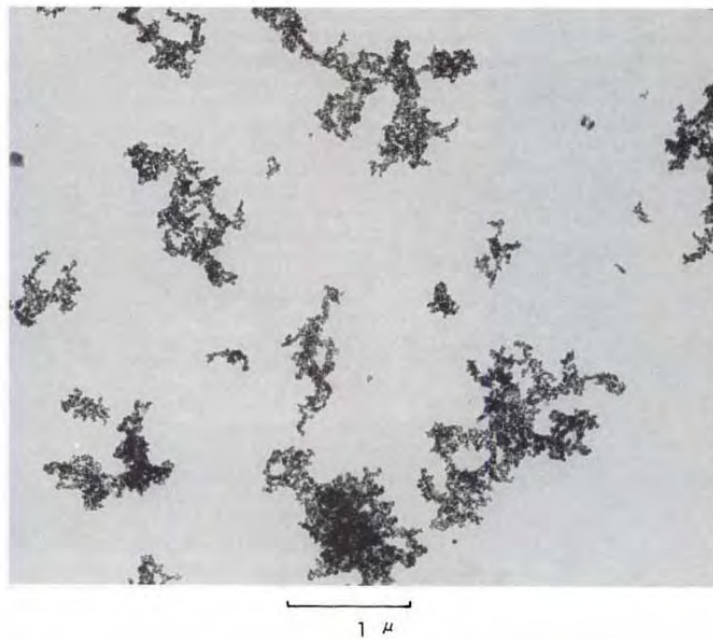
Figure 2.5 Electron micrograph of hydrophobic fumed silica (R972): average primary particle size 16 nm, BET surface area 110±20 m^2/g, Scheme of the structure of the elemental aggregate.

2.1.3 Chemical structure and surface properties

Fumed silica results from the random assembling of $SiO_{4/2}$ tetrahedrons, therefore it is amorphous and presents a lower density (ca. 2.2) than crystalline silica (ca. 2.5 to 3). The apparent bulk density is obviously much lower due to the fluffy

appearance and macroporosity of the flocks, i.e. when freshly prepared, density can go down to 0.03 g/cm^3.

Fumed silica consists of more than 99.8% of silicon dioxide, however chemical analyses also show the presence of traces of other components (Al_2O_3, Fe_2O_3, TiO_2)

Silica surface properties are related to various parameters that are defined in the following paragraphs: size and specific surface area of particles, number and distribution of surface hydroxyl groups, physically absorbed water.

2.1.3.1 Specific surface area

Due to its structure and low particle size, silica has a high surface area (from 50 to 400 m^2/g), conferring to silica a high surface of interaction with the medium. Above 300 m^2/g, fumed silica surface presents micro-porosities that modify its whole behavior.

The specific surface area is generally estimated according to BET measurements (developed by Brunauer, Emmett and Teller in 1938), by recording the isothermal adsorption of a monolayer of gas, generally nitrogen, on silica surface. For instance, from this technique, at 76 K with a single point method, using a Stroehlein volumetric equipment, Barthel et al. obtained a value of 200 m^2/g for the specific surface area of an hydrophilic untreated silica.

The drawback of this technique lies in its sensitivity to surface energy (thus to chemical modification of silica) and not only to the 'topography' of the surface. As a consequence, values obtained from this technique for hydrophobic silica are underestimated: 260 m^2/g versus 314 m^2/g for the same silica before surface modification.

In first approximation, the specific surface area (in m^2/g) of the particles can be related to the size of the primary particles by the following formula:

$$BET = \frac{6}{\rho.d}$$

where ρ is the density (2.2 g/cm^3) and d is the diameter of the primary particles.

2.1.3.2 Surface chemistry

Approximately every second silicon atom on silica surface bears a silanol group (Si-OH).
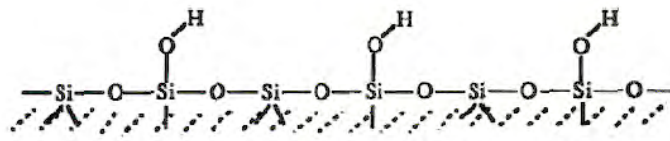
Figure 2.6 Silica surface chemistry

Various types of silanol groups, presenting different reactivities depending on their accessibility, exist on silica surface: Isolated silanol group, accounting for approximately 85% of the silanols, Geminal silanol groups (2 silanols carried by the same silicon atom) and Vicinal silanol groups (2 silanols carried by adjacent silicon atoms).
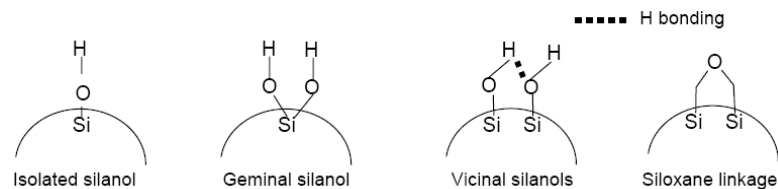
Figure 2.7 Various types of silanol groups

In the literature, the values found for silanol density on silica surface lie between 1.9 and 4.6 per nm^2 depending on the measurement method used, i.e. if every type of surface silanols are taken into account or not. The silanol content can generally be determined by acid base titration, thermo-gravimetric analysis, infra-red spectroscopy or proton nuclear magnetic resonance. For fumed silica the values are

generally lower than for other types of silica, due to the structure that makes a part of the surface no accessible. Warcker Co. provides the following data for hydrophilic untreated fumed silica (reference HDK® N20): density of silanols around 1.8 Si-OH per nm^2 independent on specific surface area (measured by acid base titration against aqueous sodium hydroxide, method not accounting for geminated silanols).

The high silanol density on silica surface induces a high potential interactivity (i.e. formation of hydrogen bond readily) between particle or between the particles and the medium, or reactivity (groups chemically available for covalent bonding). As it is detailed in paragraph surface modification concerning the organo-modification of the silica surface.

It is also the reason for the high surface energy of hydrophilic silica which is greater than 72 mJ/m^2 and is thus wettable by water. For a given surface modification, the surface energy is related to the content of residual silanols on the silica surface. And can go down to c.a. 33 mJ/m^2 in case of a polydimethylsiloxane modification. (Barthel, 1995)

2.1.3.3 Interaction with water

Another important parameter characterizing the silica surface properties is the quantity of physisorbed water attracted by surface groups (estimated to approximately 0.5 – 2.5 wt.% in a standard atmosphere).
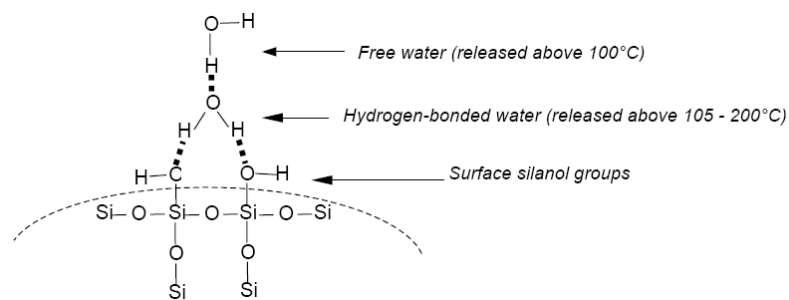
Figure 2.8 Simplified scheme of the physisorption of water on silica surface

After thermal treatment above 120-200°C under standard pressure, the water and the silanol groups can be removed from the silica surface by dehydratation followed by dehydroxylation, i.e. formation of a siloxane bond according to the process illustrated in the Figure 2.9.
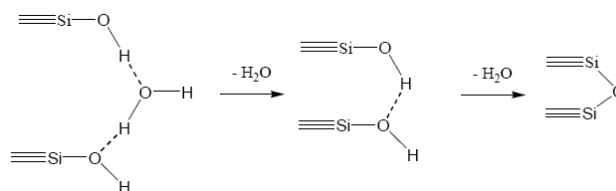
Figure 2.9 Dehydratation and dehydroxylation of silica surface

2.1.3.4 Summery of properties

The values concerning the structure, size and surface properties of the fumed silica detailed in the previous paragraphs are summarized in the Table 2.2.

Table 2.2 Properties for pyrogenic silica

	General values for pyrogenic silica	Values for an unmodified fumed silica of surface BET=200m^2/g (Aerosil®200)
Primary particle size (nm)	5-40	12
Aggregate size (nm)	200-1500	170-230
Agglomerate size (μm)	-	10-100
BET (m^2/g)	50-400	200
Silanol content (nm^{-2})	2-4	1.8
Density (primary particle SiO$_2$)	2.2	2.2
pH (5%solution)	3.6-4.5	3.8-4.3
Refractive index, n	1.45	1.46
Surface energy (mJ/m^2)	80	<72
Moisture (wt.%)	0.5-2.5	<2 (loss wt% in 2h at 1000°C)
Softening point (°C)	1667	-

Table 2.3 Fumed silica properties

Colour	White
Structure	X-ray amorphous
Surface area	50-380 m^2/g
Silanol group density	2-4 SiOH/nm^2
Refractive index	1.45
Primary particle size	7-40 nm

2.1.4 Surface modification

Silica is hydrophilic by nature, but additional chemical treatment can make the surface hydrophobic or reactive.

2.1.4.1 Principle

The chemical modification (or silanization) of silica, generally done via grafting of organo-silanes on silanols sites, is realized in order to increase the compatibility of silica with an organic medium. The aim can be: 1) to obtain adhesion with the matrix, 2) to tune the viscosity of the filled medium, 3) to improve damping properties.

Figure 2.10 General scheme of the silanisation of silica surface silanols
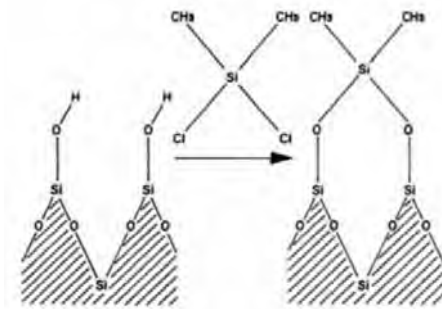
Figure 2.11 Preparation of hydrophobic silica

The general form of organo-silanes is the following one: R_n-Si-X_{4-n}, where R is an organic function potentially reactive with the polymer generally separated from the silicon atom by a methylene or propylene spacer and X is a hydrolysable function. The thickness of the layer can vary depending on n. The length of the spacer largely influences the reactivity of the organo-silane.

Many chemical natures of organofunctional silanes are available: chloroprypyl-, (di)amino-, epoxy-, vinyl-, methyl-, phenyl-, cationic styryl-, methacrylate-, mercapto-, isocyanate-, alkoxy-functional silane.

The maximum grafting yield is limited because of the steric hindrance. The resulting grafting content can be measured either by titration of the silanes fixed (for example by elemental analysis of carbon content), or by acid base titration of the residual silanols. The grafting of silica can be achieved in solution or vapor phase as it is presented in the following paragraphs.

2.1.4.2 Grafting in solution

The grafting in solution is generally performed in an aqueous solution or in an organic solvent (most often in a water/alcohol mixture). Silanes are hydrolyzed to give rise to silanol groups that can directly react with the silica surface silanols first by hydrogen bonding then by covalent bonding condensate between each other to from siloxane bonds. Many parameters influence the quality and rate of the grafting

controlled by a balance between hydrolysis and condensation rate (relative concentration, acid basic character, presence of a catalyst for the hydrolysis). The thickness of the silane layer obtained results sometimes difficult to control, but this process is the easiest to carry out.

2.1.4.3 Grafting in vapor phase

The grafting in vapor phase is more complicated to carry out, but the results are generally more controlled, and the grafting is more homogenous on the silica surface. The silane is introduced in gaseous state in a reactor containing the silica, under static or dynamic conditions. Therefore, this process requires working at high temperatures, under high vacuum, or with highly volatile products (low weight chloro- or alkoxy- silanes). The silane condensates on the silica surface by forming covalent bonds with silanols.

2.1.5 Synthetic silica supplier, general applications and future uses

The suppliers of synthetic silica are listed in Table 2.4. The general applications of synthetic silicas are listed in Table 2.5. Synthetic silicas offer unique properties and functions. Growth is expected in the following market: the waste treatment industry; the selective adsorption of ions, including nuclear waste cleanup; catalyst support applications; the oil recovery area; support material for industrial chromatography; plastic and polymer reinforcement and property enhancement applications; the cosmetic and fragrance industry for selective water adsorption and free flow application; and unique applications in the fiber glass reinforced plastics industry.

Table 2.4 Synthetic silica suppliers

Manufacturer	Product Name	Surface Treatment	Address
		Fumed silica	
Degussa	Aerosil 200	No	Degussa, Pigments Division,
	Aerosil R972	Yes	Teterboro, NJ 07608
Cabot	Cab-O-Sil M-5	No	Cabot, Box 188, Tuscola, IL 61953
	Cab-O-Sil N70-TS	Yes	
Wacker	N-20	No	Wacker, Chemie GmbH
	H-20	Yes	Postfach, D8000 München 22,
			Federal Republic of Germany
		Arc silica	
Degussa	TK 900	No	Degussa, Frankfurt Main,
			West Germany
		Silica gel	
Davison	Syloid 244	No	W. R. Grace, Davision Chemical
	Syloid 169	Yes	Division, P.O. Box 2117,
	Sylox 2	No	Baltimore, MD 21203
Glidden	Silcron G-100	No	SCM, Glidden Pigments, SMC Corp.,
			Baltimore, MD 21226
		Precipitated silica	
PPG	Hi-Sil 233	No	PPG Industries, One Gateway
			Center, Pittsburgh, PA
J. M. Huber	Zeothix® 265	No	J. M. Huber Corporation,
	Zeothix 177	No	P.O. Box 310,
			Havre de Grace, MD 21078
PQ	Quso	No	PQ Chemicals, P.O. Box 840,
	WR-50	Yes	Valley Forge, PA 19482
Degussa	HK 125	No	Degussa, Frankfurt Main,
	OK 412	Yes	West Germany

Table 2.5 General applications of synthetic silicas

Function	Application area
Reinforcement	Silicone rubber, natural and synthetic rubber, polymer and plastics
Thixotrope	Unsaturated polyester, expoxy, phenolic, and PVC dispersion resins
Thickening	Paints, inks, coating, wire cable jacketing
Rheology control	Cosmetic, pharmaceuticals, toothpaste, and liquids
Matting	Paints, coatings, PVC and plastic
Dry-up liquids	Flavor, fragrances, foods, cosmetics
Filler	Plastics
Plate-out	Thermoplastics
Anti-blocking	Foods, plastics, resins
Abrasive and polishing agent	Toothpaste

2.2 Polypropylene

2.2.1 Polypropylene

Polypropylene (PP) was very fast growth production. In comparison to other thermoplastic has been encouraged by significant advances in catalyst and process development and by the attractive combination of features which characteristics such as low density, heat distortion temperature above 100°C, extraordinary versatility in terms of properties, applications and recycling in addition to a low cost. PP is a vinyl polymer obtained, by means of organo-metallic catalysts, from polypropylene (CH_2-CH-CH_3) through the reaction:
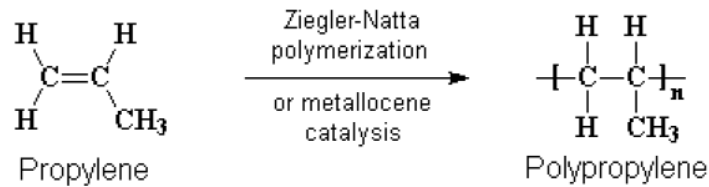
Depending on the organization of CH_3 groups along the backbone, three configurations can be distinguished: isotactic, syndiotactic and atactic. When all the groups are on the same side of the chain, PP is isotactic: in this case chains have a very regular arrangement; consequently they can pack easily together in a crystal structure. Thus, the higher the amount of isotactic phases in the polymer, the higher the degree of crystallinity in the solidified PP. In syndiotactic configuration, methyl groups are alternatively on either side of the carbon chain. This structure yields a highly flexible PP. No order at all is present in atactic PP: the side groups are randomly situated on either side of the backbone and therefore the polymer has a very low degree of crystallinity. Compared to isotactic PP, the syndiotactic isomer 'exhibits higher impact resistance and improved adhesion on organic surfaces or glass fillers. However, PP is semi-crystalline, which means it always has two phases, an amorphous and a crystalline one. When cooling is slow enough, molecular chains have time to arrange themselves in 'lamellar' fibrils. These structures grow out from a central nucleus in the three dimensions yielding an organization with a spherical symmetry. The whole assembly is called ' spherulite ' and is illustrated in Figure 2.12.
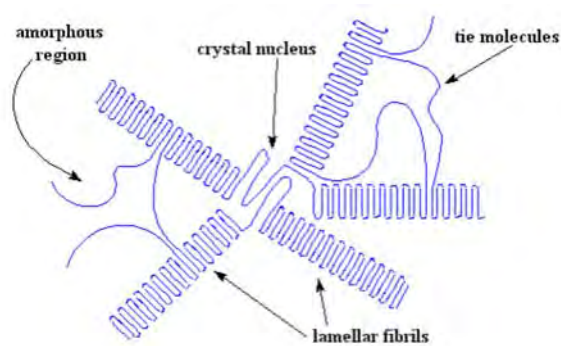
Figure 2.12 Schematic illustration of chains organization in PP spherulites

Thus it is possible to distinguish: spherulites on the largest scale, the lamellar structure on the intermediate level and the crystal structure on the smallest scale. PP is a polymorphic material. This means its crystals can be arranged in several forms: monoclinic a, hexagonal, triclinic or smectic. The formation of a certain crystal form will depend on the crystallization conditions. However PP is usually produced and commercialized as a copolymer: in this case different monomers are used as raw materials. Ethylene is the monomer most commonly copolymerized with propylene. Copolymerization level and kind (random, block, alternate) strongly affect the final material properties: for instance if 5% of ethylene is random copolymerized, the crystallinity degree is already markedly reduced.

2.2.2 Polypropylene properties

'Polypropylene' is a very versatile polymer, thus an exhaustive discussion of all its features would be too vast and inappropriate in the present work. Moreover PP is a well known material, hence, in this paragraph, only the properties which might be useful for a deeper comprehension of the subject of this thesis will be briefly outlined.

The PP mechanical properties, as stiffness and ductility, are strongly affected by its crystallinity degree. The latter, though, does not depend only on tacticity but it is influenced by thermal history as well: for instance, quenching the polypropylene, the biggest part of polymer will be 'frozen' in an amorphous arrangement, more the few crystals formed will be small. Such a material will be less stiff than the slowly cooled one. Consequently several variables could be moved in order to 'set' the final material properties according to our need. For this reason it is necessary, in listing PP general features, either to state what grade of material we are dealing with or to refer to 'average' values.

For a 100% isotactic PP the significant numbers are

- Melting temperature: 174°C

- Glass transition temperature: -17°C

- Amorphous density at 25°C: 0.85 g/cm^3

- Crystalline density at 25°C: 0.95 g/cm^3

- Average tensile yield strength: 30.7 MPa

- Average Young's modulus: 1.9 GPa

- Service temperature up to 120°C

In general, PP can be considered chemically 'inert': namely its very stable structure provides a good chemical resistance, except for aromatic hydrocarbons at elevated temperatures and halogens. It can even withstand most inorganic acids, except nitric and sulphuric, and inorganic salt solutions. On the other hand PP is unsuitable, due to swelling, to be used with most organic solvents. These features, together with water resistance, low density and good price/property ratio, give to PP its great industrial importance. As an example Table 2.6 gives the mechanical properties and relative cost of some plastics.

Table 2.6 Principle properties and relative cost of commercial polymer

Material	Tensile strength (MPa)	Elastic modulus (GPa)	Density (kg/m^3)	Relative cost
Polypropylene	35	1.5	900	1.0
Polyvinyl chloride	55	3.5	1400	1.0
Polyethylene	12	0.2	900	0.7
PTFE	21	1.0	2100	20.0
GRP polyester	100	7.0	1500	2.0
GRP epoxy	250	14.0	1800	3.3

However, PP is more commonly commercialized as copolymer and/or loaded with fillers: in fact its brittleness at low temperature and its low resistance to oxidation with light, heat and oxidants restricts the use of the neat polymer. Nonetheless, Table 2.6 shows PP big advantage: it is a cheap polymer; therefore, major efforts have been dedicated to improve its properties instead of looking for a different polymer. That is why PP is currently toughened through the already mentioned ethylene copolymerization and the problems coming from its low stiffness, low heat distortion and its high mould shrinkage are overcome by incorporating glass and mineral fillers (such as talc at a micro scale).

Before paragraph said polypropylene's molecular formula is $(CH_2\text{-}CH\text{-}CH_3)_n$. It can assume isotactic, syndiotactic, or atactic configurations. Only the atactic form is used in fiber production because it allows the chains to pack closely to form crystals. The Ziegler-Natta catalysts developed in the 1950s made the atactic formation possible. While polypropylene fibers were first manufactured in Italy in 1957 and U.S. production began in 1962, these fibers did not truly thrive until the 1970-80s, when antioxidants and thermal and ultraviolet stabilizers overcame the polymer's susceptibility to oxidation and radiation induced degradation. The following table summarizes typical properties of textile grad polypropylene fibers.

Table 2.7 Properties of Polypropylene Fibers

Tensile Strength (gf den-1)	3.5-5.5
Elongation (%)	40-100
Abrasion Resistance	Good
Moisture Absorption (%)	0-0.05
Elastic Recovery (after 30s at 2% elongation)	
Immediate (%)	91
Delayed (%)	9
Glass Transition Temperature (°C)	-15 to −20
Softening Point (°C)	140
Melting Point (°C)	165
Chemical Resistance	Generally Excellent
Relative Density	0.91
Thermal Conductivity	6.0 (with air as 1.0)
Pyrolytic Stability (°C)	350
Electrical Insulation	Excellent
Resistance to Mildew, Moth	Excellent

In textile applications, the typical melt flow rates range between 15-25 g/10min, corresponding to moderate molecular weights, are used. High molecular weights in the range of 3-5 g/10min are used in more technical applications. The polydispersity ranges from 2-12 or greater. A polydispersity 3 is considered ideal for high speed spinning

2.3 Melt Spinning Technique for Forming of Polypropylene Fiber

Beginning in 1940 with the commercial production of nylon 6,6, melt spin processing of fibers has proved to be an efficient, cost effect method to produce high quantity and quality fibers. Today it dominates all other fiber forming technologies. Melt spin processing begins with the feeding of polymer chips (or melt in a continuous

process) into the extruder. There are multiple designs/configurations for extruders. Usually a single or twin screw encompassed in a barrel is used to melt the polymer chips and transport the melt along the length of the barrel under pressure. Melting is achieved not only through the heating of the screw and barrel but by the mechanical shearing of the polymer. As the diameter of the screw decreases, the melt becomes more mixed and compressed. The polymer's viscosity during processing is affected by its molecular weight and by the temperature and pressure within the system. Polymer melts experience shear thinning; as the shear rate increases, the viscosity of the polymer decreases.

The polymer passes through a pre-filter before entering the spinning head. The pre-filter is composed of sand particles ranging from 20-80 microns held in place by a series of stainless steel, gauze-like screens of different sizes. Filtration removes partially degraded polymer gels, foreign matter such as metal particulates, and gaseous bubbles. After filtration, the polymer enters the gear pump which tightly measures exact amounts of polymer and releases them into the spin pack. After passing through another filter of fine sand or alumina held in place by metal sintered disks, the polymer finally reaches the spinneret. The spinneret is a metal plate, 3-30 microns thick with various size holes that influence the size and shape of the spun fibers. Upon exit from the spinneret the melt experiences die swell, a phenomenon where the polymer recovers its stored elastic energy after being released from the high-pressure confinement of the spin pack. The melt is now in the quench chamber, where it is cooled and wound onto a package.

Important Factors, the factors that influence a spun fiber's orientation in order of decreasing impact are: polymer material, extrusion temperature, take up velocity, mass output rate (through put speed), cooling conditions, spinneret channel dimensions, number of filaments, and the spinning path. Typical extrusion temperatures for polypropylene range from 230- 290 °C, well above the average melting temperature

of 165 °C. Typical take up speeds for PP range from 100-4000 m/min depending on the length of the quench chamber.

The relationship between spinning conditions and spun orientation is important because a fiber's molecular orientation, crystallinity, and morphology are directly responsible for a fiber's mechanical and electrical properties. How the melt is stretched and cools along with the crystallization kinetics of the polymer determines if crystallization takes place during spinning.

Crystallinity in a fiber is influenced by its crystallization rate and cooling conditions. The rate of crystallization for polypropylene is very fast. Polypropylene has three crystalline geometries, which can form, depending on the processing conditions: α monoclinic, β hexagonal and γ triclinic. The crystalline phases co-exist with the amorphous phase. Polypropylene can also display a "smectic" form that is an intermediate phase between the amorphous and crystalline. The following figure shows the results of an X-ray diffractogram for polypropylene with different crystals.
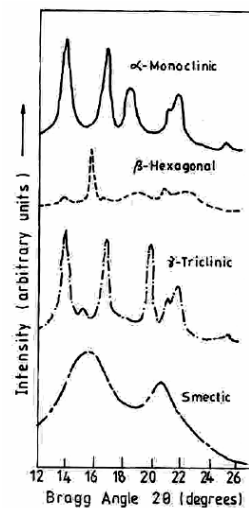
Figure 2.13 X-ray diffractogram of polypropylene crystal structures

Spinning speed affects the geometry of the crystals formed; the greater the speed, the greater the tendency to form the more stable crystalline structures. The

following figure shows the tendency to form the α monoclinic crystal form, which is the most stable configuration for polypropylene.
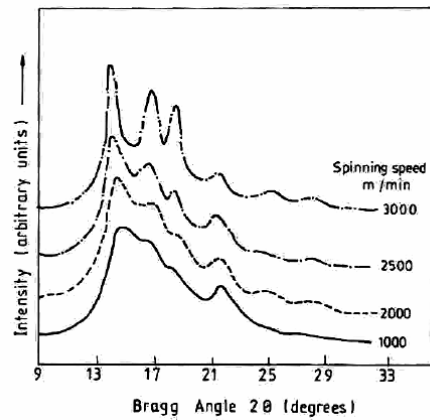
Figure 2.14 Crystalline structure at different spinning speeds

Similarly, plotting the crystalline orientation function of polypropylene verses take up velocity, shows how the orientation of crystals on each axis changes as the take up speed increases. See figure 2.15 f_c represents the axis parallel to the fiber axis. f_b represents the axis perpendicular to the fiber axis and f_a represents the axis 45 degrees to the fiber axis.

In terms of fiber morphology, this accounts for the change in formation of spherulitic crystals to row nucleatated with twisted lamenllae to, finally, row nucleated with untwisted lamellae.
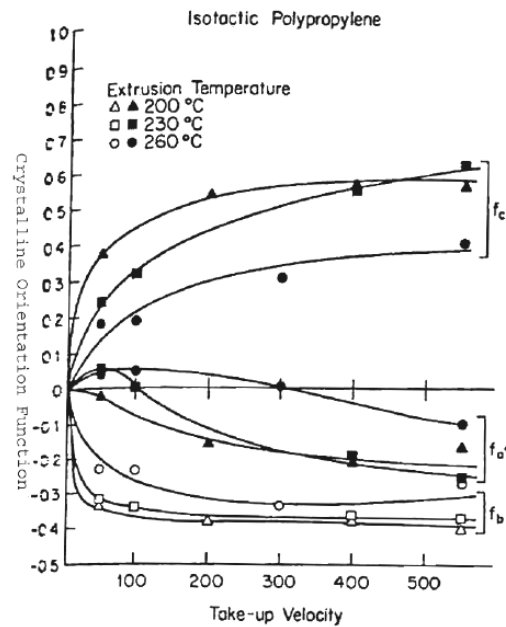
Figure 2.15 Effects of Temperature and Take-Up Velocity on the Crystalline Orientation

Function of Polypropylene

Figure 2.16 shows how the mechanical properties of polypropylene are affected by take up velocity. As take up velocity increases, the tenacity of the fibers increases, while the percent elongation to break decreases. It suggests that for this particular fiber and spinning conditions, the 1000-3500 m/min take up velocity produces the best fiber.
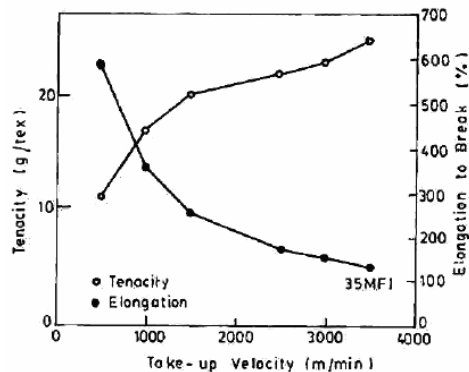
Figure 2.16 Effect of Take-Up Velocity on Fiber Mechanical Properties

2.4 Nanocomposites manufacturing techniques

Nanocomposites (plastics) have their origin in the 1970's with the use of sol-gel technology to form homogeneous dispersions of small sized inorganic particles throughout a polymer matrix. In such system, the inorganic phase may or may not be chemically attached to the organic phase. These Generation I nanocomposites have been found to be useful in coating application. In the 1980's Generation II nanocomposite emerged with resurgence in the use of fine particle, mineral and clay fillers for plastics. Limited compatibility between the filler and polymers as well as complex polymer processing requirements are needed to from these nanocomposites. In the 1990's and beyond, a new form of nanocomposite has emerged. These so-called Generation III nanocomposites are polymeric materials that are reinforced with nanofibers such as carbon nanotubes, SiC whiskers, colloidal silica, nano-clay particles and the like. In all such work, the technical challenge is the need to obtain intimate blending of these nanofibers and particles into the polymer matrices. The problems exist: 1) the need to blend and distribution individual nanofiber species into the bulk polymer matrix and 2) induce chemical compatibility (adhesion) between the nanfibers and the polymer media. Most form of nanofibers are agglomerated entities. They exist as bundles of nanoparticles and are very difficult to separate and keep separated.

Now a day, nanocomposite manufacturing is a keen point in the development of multi-functional nanocomposites. Uniform dispersion of nanoparticles and improved adhesion at the interface nanofillers-matrix that are critical issues in processing of nanocomposites. There are many techniques used to prepare nanocomposites. For example are as followed.

2.4.1 Shear-mixing method

The rheological properties of a thermoplastic like polypropylene allow the use of extrusion as manufacturing process of nanocomposites. This process consists in mechanical dry mixing of the mixture containing thermoplastic polymer and nanofillers, and use of a screw extruder to melt and improve the mixing of the compound. Many researchers use this method to produce thermoplastic polymer containing different concentrations of nanofillers. This method, although very simple, has not given good improvement of mechanical properties and of dispersion of nanofillers in the polymeric matrix.

2.4.2 Solution process

The use of ultrasound can improve the dispersion of nanofillers like carbon nanotubes in the matrix, through a solvent compatible with both nanofillers and polymer. Ultrasonic activators use sound waves at high frequency, which produce a cavitation effect responsible for the formation of millions of microscopic bubbles at low pressure. Many studies used this method to disperse nanofillers in a polymer. They have used to disperse the nanofillers in solvent mix with polymer solution. Ultrasound has been used to improve mixing. After removal of solvent in vacuum furnace or the oven, nanocomposite could be received in this method. However, the using the ultrasound used to improve the dispersion of nanofillers before mix to polymer matrix. A solvent used should to compatible with both fillers and polymers

2.4.3 Coagulation method

This method consists in dispersing the nano-fillers in solvents using a ultrasound bath. Then appropriate amount of polymer is dissolved in the mixture. The suspension is dripped in a large amount of distilled water (coagulated solution). Due to insolubility of solvent in water, polymer precipitates and entraps the nanofillers and prevent them form agglomerating in bundles. After vacuum drying, raw nanocomposite has been processed in an extruder. For example of this method, carbon nanotube/polymethylmetacrylate (PMMA) nanocomposite, this method consists in dispersing the nanofillers in dimethylformamide (DMF) using a ultrasonic bath. Then appropriate amount of PMMA is dissolved in the mixture. The suspension is dripped in a large amount of distilled water. Due to insolubility of DMF in water, PMMA precipitates and entraps the carbon nanotube and prevent them from agglomerating in bundles. After vacuum drying, raw nanocomposite has been compounded in an extruder.

2.4.4 in-situ formation or polymerization

In-situ formation of nanoparticles or the polymerization of monomers in the presence of nanoparticles can be make nanocomposite same method of polymerization just as nanofillers was added in like additive in polymerization. Nanofillers or nanoparticles were mixed into the monomer or added as additives in polymerization process. So, nanoparticles were infused into polymer

2.5 Prior work

Bhattacharyya, A.R., Sreekumar, T.V., Liu, T., Kumar, S., Ericson, L.M., Hauge, R.H. ,and Smaaley, R.E. (2003) studied crystallization behavior of melt-blended polypropylene (PP)/single wall carbon nanotube (SWNT) composites using optical microscopy and differential scanning calorimetry. Polypropylene containing 0.8 wt% SWNT exhibited faster crystallization rate as compared to pure polypropylene. PP/SWNT fibers have been spun using typical polypropylene melt spinning conditions. The PP

crystallite orientation and the SWNT alignment in the fibers have been studied using X-ray diffraction and polarized Raman spectroscopy, respectively.

Bikiaris, D.N., Papageorgiou, G.Z., Pavlidou, E., Vouroutzis, N., Palatzoglou, P. ,and Karayannidis, G.P. (2006) studied two series of isotactic polypropylene (iPP)/SiO$_2$ nanocomposites containing 1, 2.5, 5, 7.5, and 10 wt % SiO$_2$ nanoparticles were prepared by melt-mixing on a twin-screw corotating extruder. In the first series untreated fumed silica nanoparticles were used, whereas in the second nanoparticles were surface-treated with dimethyldichlorosilane. In both cases, the average size of the primary nanoparticles was 12 nm. Tensile and impact strength were found to increase and to be affected mainly by the type and content of silica nanoparticles. A maximum was observed, corresponding to samples containing 2.5 wt % SiO$_2$. These findings are discussed in light of the SEM and TEM observations. By increasing the amount of nanoparticles, large aggregates of fumed silica could be formed, which may explain the reduction of mechanical properties with higher concentrations of SiO$_2$. However, it was found that surface-treated nanoparticles produced larger aggregates than did those derived from untreated nanoparticles, despite the increased adhesion of the iPP matrix, as was postulated from yield strength. This behavior negatively affected mechanical properties. In addition, an effort was made to determine if toughening theories, mainly the critical interparticle distance for rubber toughening or composites, also might be applicable in nanocomposites. From DSC measurements it was demonstrated that silica nanoparticles acted as effective nucleating agents, increasing the crystallization rate and the degree of crystallinity of iPP.

Bikiaris, D.N., Vassiliou, A., Pavlidou, E. ,and Karayannidis, G.P. (2005) studied a series of iPP/SiO$_2$ nanocomposites, containing 1, 2.5, 5, 7.5, 10 and 15 wt% SiO$_2$ nanoparticles, were prepared by melt mixing in a twin screw co-rotating extruder. Poly(propylene-g-maleic anhydride) copolymer (PP-g-MA) containing 0.6 wt% maleic anhydride content was added to all nanocomposites at three different concentrations, 1,

2.5 and 5 wt%, based on silica content. Mechanical properties such as tensile strength at break and Young's modulus were found to increase and to be mainly affected by the content of silica nanoparticles as well as by the copolymer content. For the tensile strength at break as well as for yield point, a maximum was observed, corresponding to the samples containing 2.5–5 wt% SiO_2. At higher concentrations, large nanosilica agglomerates are formed that have as a result a decrease in tensile strength. Young's modulus increases almost linearly on the addition of SiO2, and takes values up to 60% higher than that of neat iPP. Higher concentrations of PP-g-MA resulted in a further enhancement of mechanical properties due to silica agglomerate reduction. This finding was verified from SEM and TEM micrographs. Evidently the surface silica hydroxyl groups of SiO_2 nanoparticles react with maleic anhydride groups of PP-g-MA and lead to a finer dispersion of individual SiO_2 nanoparticles in the iPP matrix. The enhanced adhesion in the interface of the two materials, as a result of the mentioned reaction, has been studied and proved by using several equations. The increased Vicat point of all nanocomposites, by increasing the PP-g-MA content, can also be mentioned as a positive effect.

Broda, J., and Wlochowicz, A. (2007) reported WAXS and DSC of the structure of uncoloured and coloured polypropylene fibres. Two organic pigments: a phthalocyanine and a quinacridone with different nucleating abilities were used for the colouring of fibres. The fibres were formed at various take-up velocities, and heat stabilized at temperature in the range 120±160°C. It was stated, that two polymorphic forms α and β occur in uncoloured fibres spun at extrusion velocity. Fibres spun at small and medium take up velocity contain the mesophase, whereas fibres spun at high take-up velocity contain the crystalline a-form. In the fibres coloured with a phthalocyanine the α-form occurs independently of the take-up velocity. Fibres coloured with a quinacridone contain both forms α and β. A great content of b-form occurs in ®bres spun at the lowest take-up velocity. The observed changes of the structure of Fibres are connected with the change of nucleation mechanism. During heat stabilization perfecting of a-form occurs. The mesophase and a hexagonal b-form transform into a

monoclinic α-form. The degree of transformation depends on the stabilization temperature. For coloured fibres the structure of unstabilized fibres is more perfect and undergoes smaller changes during stabilization than the structure of uncoloured fibres.

Broda, J., Gawlowski, A., Slusarczyk, C., Wlochowicz, A. ,and Fabia, J. (2007) studied the influence of two organic pigments and two flame retardants on the structure of polypropylene fibres. It was found that by spinning at low velocities in the presence of pigments a highly crystalline structure is formed. In fibres coloured with quinacridone the rarerly encountered β-form of polypropylene was observed. Utilizing low take-up velocities, the addition of flame retardants leads to an increase in fibre crystallinity. In the case of fibres formed at higher velocities the influence of additives on fibres structure was less visible. For all fibres, independent of additives, a similar structure containing the a form of polypropylene was obtained.

Caldas, V., Brown, G.R., Nohr, R.S., Macdonald, L.G. ,and Raboin, L.E. (1997) reported the surfaced modified silica/silicone copolymer additive act as an effective nucleating agent for isotactic polypropylene. This result in a reduction in the size of the crystalline entities, hence a more homogeneously distributed crystalline phase and load-bearing 'tie' molecules. TEM show that the crystalline entities are substantially smaller at the surface and mid-radius of fibers prepared with additive containing isotactic polypropylene. Furthermore, the bond points of the resulting spunbonded fabrics have a dramatically increased nucleation density and smaller crystalline dimensions.

Chan, C.M., Wu, J., Li, J.X. ,and Cheung, Y.K. (2003) studied preparing polypropylene composites with CaCO3 nanoparticles (~44 nm). The notched fracture toughness of the nanocomposites under either quasi-static or impact loading conditions was found substantially higher than that of the pure PP. The TEM study showed that the nanoparticles were distributed in the PP matrix uniformly and little particle agglomeration was found at 4.8 and 9.2 vol%. Thermal analysis and SEM studied on the PP and nanocomposites revealed that the CaCO3 nanoparticles are and effective nucleating

agent that causes the absence of detectable spherulites. Fractography of the broken specimens from the J-integral tests suggested that the nanoparticles introduce a massive number of stress concentration sites in the matrix and promote cavitation at the particle-matrix boundary when loaded. The cavities, in turn, release the plastic constraint and trigger large-scale plastic deformation of the matrix, which consumes fracture energy.

Chatterjee, A., and Deopura, B.L. (2003) studied crystallization behaviour of blends of different MFI isotactic polypropylenes (PP), and blends of PP with carbon nanofibre investigated by DSC and polarizing optical microscope. Both higher MFI PP component and the carbon nanofibre in the blend influence the nucleation activity of the melt during non-isothermal crystallization. In presence of carbon nanofibre, the sherulitic growth rate was highly disturbed. The calculation of nucleation activity indicates that carbon nanofibres act as active substrate for heterogeneous nucleation.

Chen, M., Tian, G., Zhand, Y., Wan, C. ,and Zhang, Y. (2006) studied the crystallization and melting behavior of isotactic polypropylene (iPP) and polypropylene copolymer (co-PP) containing silicon dioxide (SiO_2) by differential scanning calorimeter (DSC). SiO_2 had a heterogenous nucleating effect on iPP, leading to a moderate increase in the crystallization temperature and a decrease in the half crystallization time. However, SiO_2 decreased the crystallization temperature and prolonged the half crystallization time of co-PP. A modified Avrami theory was successfully used to well describe the early stages of nonisothermal crystallization of iPP, co-PP, and their composites. SiO_2 exhibited high nucleation activity for iPP, but showed little nucleation activity for co-PP and even restrained nucleation. The iPP/SiO_2 composite had higher activation energy of crystal growth than iPP, indicating the difficulty of crystal growth of the composite. The co-PP/SiO_2 composite had lower activation energy than co-PP, indicating the ease of crystal growth of the composite. Crystallization rates of iPP, co-PP, and their composites depended on the nucleation. Because of its high rate of nucleation, the iPP/SiO_2 composite had higher crystallization rate than iPP. Because of

its low rate of nucleation, the *co*-PP/SiO$_2$ composite had lower crystallization rate than *co*-PP.

Cho, J.W., and Paul, D.R. (2001) studied nylon 6 - organoclay nanocomposites prepared via direct melt compounding using a conventional twin screw extruder. The mechanical properties and morphology of these nanocomposites were determined and compared to similar materials made by an in situ polymerization process. The organoclay was well exfoliated into the nylon 6 matrix when compounded with the twin screw extruder but use of a single screw extruder was far less effective. The mechanical properties of the organoclay nanocomposites were significantly increased with marginal decrease of ductility and showed much greater values than glass fiber composites.

Choi, S., Jeong, Y., Lee, G.W., and Cho, D.H. (2009) examined the thermal and mechanical properties of polypropylene filaments reinforced with multiwalled carbon nanotubes (MWNTs). The MWNTs were functionalized with maleic anhydride polypropylene to increase the interfacial interactions between the CNTs and polypropylene. PP/MWNT composites with different concentrations of MWNTs were prepared by melt compounding using a twin screw extruder. The composites of the filament were then post drawn and heat treated. Tensile tests showed increased strength with the addition of only 0.1 wt% while there were only slight changes in elongation. The thermal properties were also slightly enhanced by the MWNTs.

Garcia, M., G. van Vliet, Jain, S., Schrauwen, B.A.G., Sarkissov, A., W.E. van Zyl, and Boukamp, B. (2004) studied compoounding polypropylene-SiO$_2$ nanocomposites using twin-screw extruders. The properties of the nanocomposites were studied using two different inorganic fillers: colloidal (sol) and powder silica nanoparticles. Reinforcing and toughening effects of the nanoparticles on the polymer matrix were found at a loading of 4.5 wt.%, which is lower than for most particulate filled composites. The use of silica nanoparticles led to different microstructure when compared with that of the pure polymer. Addition of colloidal silica to the polymer matrix

produced good filler dispersion while the use of powder silica resulted in aggregated silica particles in the polymer matrix. There was no noticeable improvement of the mechanical properties when powder silica was added to the pure polymer. On the contrary, the presence of silica-sol nano-particles in the polymer matrix led to an increase of both Young modulus and impact strength, from 1.2 GPa to 1.6 GPa and from 3.4 kJ/m^2 to 5.7 kJ/m^2 respectively.

Hasan, M.M., Zhou, Y., Mahfuz, H. ,and Jeelani, S. (2006) investigated the effect of SiO$_2$ nanoparticle on the thermal and mechanical properties of nylon-6. Firstly, nanoparticles with 0, 1, and 2 wt.% loading were dry-mixed with nylon-6 by mechanical means and extruded into filaments using a single screw extruder. Then, tensile tests were performed on the single filament at the strain rate range of 0.02–2 min^{-1}. Experimental results show that both neat and nanophased nylon-6 were strain rate strengthening materials. The tensile modulus, yield strength, and ultimate tensile strength (UTS) all increased with increasing strain rate. Experimental results also show that infusing nanoparticles into nylon-6 can increase tensile modulus, yield strength, hardening modulus, and UTS. Forty-five percent enhancement in tensile modulus and 26% enhancement in UTS were observed in the 2 wt.% system as compared with neat nylon-6. At the same time, thermal properties of neat and nanophased nylon-6 were characterized by TGA and DSC. TGA thermograms have shown that the nanoparticle infused systems are more thermally stable. DSC studies also have indicated that there is a moderate increase in Tg without a distinct shift in the melting endotherm for the nanophased systems. At last, based on the tensile test results, a nonlinear constitutive equation was developed to describe strain rate sensitive behavior of neat and nanophased nylon-6.

Huang, L., Zhan, R. ,and Lu, Y. (2006) studied, polypropylene (PP)/nano-silica (nano-SiO$_2$) composites were prepared by a melt blending process. Here, a novel surface treatment method which uses combined dispersant and a coupling agent is developed to treat the nano-SiO$_2$ which is uniformly dispersed into the PP matrix. To

treat the surface of nano-SiO$_2$, the optimal content of the dispersant (SDBS) is 2.0% and the optimal amount of the coupling agent (KH-550) is 1.5%. The mechanism and synergistic effect of the combined dispersant and coupling agent are discussed based on their chemical structures. The fractography of PP/nano-SiO$_2$ composites after notched impact testing observed by the scanning electron microscope (SEM) proves the uniform dispersion of nano-SiO$_2$ in the PP phase. The mechanical testing results show that after surface treatment, both the tensile and notched impact strength of nanocomposites enhance markedly. The tensile strength reaches its maximum with the 4.0% of nano-SiO$_2$ and the notched impact toughness achieves its maximum with the 5.0% of nano-SiO$_2$. The crystallization behavior characterized by the differential scanning calorimetry (DSC) and the crystalline structure observed by the polarizing microscope (PM) indicated that nano-SiO$_2$ has a nucleation role in the crystallization of PP which results in a higher crystallization temperature, a higher degree of crystallinity, and a smaller size of spherulites.

Janigova, I., and Chodak, I. (1995) studied kinetics of isothermal crystallization of low density polyethylene (LDPE) filled with silica (Ultrasil) and crosslinked by peroxide investigated by a DSC method. It is suggested that the addition of high-surface-area silica as a filler results in a significant adsorption of LDPE chains on the filler surface, which plays an important role in the kinetics of isothermal crystallization. The isothermal crystallization of filled and crosslinked LDPE is influenced simultaneously by adsorption, nucleation, retardation and formation of pre-ordered structure.

Kearns, J.C., and Shambaugh, R.L. (2002) studied the strength properties of polypropylene fibers enhanced with single-wall carbon nanotubes (SWNTs). Solvent processing was used to disperse SWNTs in a commodity polypropylene. After the solvent was removed, the solid polymer was melt-spun and postdrawn into fibers of unusual strength. For a 1-wt % loading of nanotubes, the fiber

tensile strength increased 40% (from 9.0 to 13.1 g/denier). At the same time, the modulus increased 55% (from 60 to 93 g/denier)

Kumar, S., Doshi, H., Srinivasarao, M., Park, J.O. ,and Schiraldi, D.A. (2002) studied fiber from polypropylene and polypropylene/vapor grown nano carbon fiber composite spun using conventional melt spinning equipment. At 5 wt% nano carbon fiber loading, modulus and compressive strength of polypropylene increased by 50 and 100%, respectively, and the nano carbon fibers exhibited good dispersion in the polypropylene matrix as observed by scanning electron microscopy.

Liu, W., Tian, X., Cui, P., Li, Y., Zheng, K. ,and Yang, Y. (2004) studied poly(ethylene terephthalate) (PET)/silica nanocomposites fabricated by direct polymerizing PET monomer dispersed with organic modified silica nanoparticles. The characteristics and properties of these nanocomposites were investigated by the transmission electron microscopy, differential scanning calorimetry, and Thermogravimetric analysis, respectively. The results show that (1) the nanoparticles have been well dispersed in the polymer matrix; (2) the addition of nanoparticles can speed up the crystallization and melting point; and (3) the addition has no significant effect on the synthesis process.

Ma, H., Zeng, J., Realff, M.L., Kumar, S. ,and Schiraldi, D.A. (2003) studied poly(ethylene terephthalate) (PET) resin compounded with carbon nanofibers. The amount of carbon nanofibers utilized in each case was 5 wt.%. Compounding methods included ball-milling, high shear mixing in the melt, as well as extrusion using a twin-screw extruder. PET/CNF composite resins were melt-spun into fibers using the conventional PET fiber spinning conditions. Morphology and mechanical properties of these composite fibers have been studied. The results show that CNFs can be incorporated into PET matrix with good dispersion. Compressive strength and torsional moduli of PET/CNF composite fibers were considerably higher than that for the control PET fiber.

Mahfuz, H., Hasan, M.M., Rangari, V.K. ,and Jeelani, S. (2007) studied spherical silica nanoparticles infused into nylon-6 and drawn into filaments through a melt-extrusion process. The idea was to improve the strength and stiffness of the resulting filaments by utilizing the interactions between the nanoparticles and the polymer. The focus was to increase the fracture strain of the filaments, as this had not been possible earlier with the infusion of carbon nanotubes. It has been observed that with the infusion of silica nanoparticles, the strength and Young's modulus of the nylon filament can be enhanced in the 28 to 36% range without any loss of fracture strain. The source of this improvement has been traced to the formation of stronger amide and carbonyl bonds, nucleated by the presence of SiO_2 nanoparticles during polymerization. Moreover, calculations based on basic theories of inclusions show that the Young's modulus of the nanophased filament is within 5% of the upper bound predicted by the micromechanical theory.

Moore, E.M., Ortiz, D.L., Mara, V.T., Shambaugh, R.L. ,and Grady, B.P. (2004) studied single-walled carbon nanotubes added to two different grades of polypropylene to produce composites. The composites were then melt-spun into fibers, and the fibers were tested with both a conventional tensile pull tester and dynamic mechanical analysis. The changes in tensile properties were related to the grade of polypropylene used. In addition to fibers being made from the mixes, coarse extrudates (i.e., undrawn, gravity-spun filaments) were also produced. Density measurements on these extrudates showed that the addition of nanotubes increased the composite density in a highly nonlinear manner, which suggested interaction between the polypropylene and the carbon nanotubes.

Papageorgiou, G.Z., Achilias, D.S., Bikiaris, D.N. ,and Karayannidis, G.P. (2005) studied isothermal and non-isothermal crystallization kinetics of polypropylene (PP)/surface-treated SiO_2 nanocomposites. Analysis of the isothermal crystallization showed that the phenomenon is characterized by faster rates as the amount of silica is increased. In the case of non-isothermal crystallization, it was found that the Ozawa

analysis was rather inapplicable for the nanocomposites. In contrast, the modified Avrami method, as well as the method proposed by Mo was applied giving satisfactory results. The effective energy barrier for non-isothermal crystallization was estimated as a function of the relative degree of crystallinity using the isoconversional analysis of calorimetric data. This was found to vary with the degree of conversion, as well as with the presence of filler. Finally, the nucleation activity of the silica nanoparticles on the polymer matrix was explored and it was proved that when the content of filler exceeds 7.5 wt.% the nucleation is not drastically improved.

Peng, Z., Kong, L.X. ,and Li, S.D. (2005) studied poly(vinyl alcohol) (PVA)/silica (SiO2) nanocomposite prepared with a novel self-assembled monolayer technique, and its morphology and thermal properties were studied with different material characterization instruments. The treated SiO2 nanoparticles were dispersed in the PVA matrix homogeneously, and the thermal properties of the nanocomposite were markedly improved in comparison with those of pure PVA. Under the same isothermal heating conditions, the decomposition of the nanocomposite was delayed significantly in comparison with that of PVA. The thermal degradation of the nanocomposite was a two-step reaction, including the degradation of the side chain and main chain. The products of side-chain degradation were mainly carboxylic acid, whereas main chain degradation primarily produced carbon dioxide and low-molecular-weight conjugated polyene.

Qu, C., Yarg, H., Liang, D., Cao, W. ,and Fu, Q. (2007): Morphology and Properties of PET/PA-6/SiO2 Ternary Composite studied composite properties of hydrophilic nano-SiO_2/poly(ethylene terephthalate)/polyamide-6 (PA-6) blends. Melt-blended composites were prepared at various component ratios and different nano-SiO_2 levels. Mechanical, morphological, dynamic mechanical, and thermal tests were carried out to characterize the properties, morphology, and compatibilization of the composites. Increased impact strength, tensile strength, and modulus were observed by adding nano-SiO_2 particles in the blends. The nano-SiO_2 particles were found to be preferentially dispersed in PA-6, resulting in an increase of glass transition temperature

and crystallization of PA-6. The mechanism of morphology and properties changes was discussed based on the selective dispersion of nano-SiO$_2$ particles in the blends.

Rosso, P., Ye, L., Friedrich, K. ,and Sprenger, S. (2006) studied the influence of adding 5 vol % of silica nanoparticles, obtained via a sol–gel process, on an Araldite-F epoxy. To characterize toughening effects, compact tension specimens were used to obtain K_{IC} and G_{IC}. Additionally, tensile strength and E-Modulus were measured as well as differential scanning calorimetry and dynamic mechanical thermal analysis were carried out to evaluate the influence on the thermal properties of the epoxy because of addition of the particles. Electronic microscopy was used to check dispersion quality and fracture surfaces, in transmission mode and scanning mode, respectively. The addition of 5 vol % silica-nanoparticles could improve the stiffness and the toughness of an epoxy resin at the same time.

Rottstegge, J., Zhang, X., Zhou, Y., Xu, D., Han, C.C. ,and Wang, D. (2007) reported the nanocomposite powders and fibers from polypropylene filled with surface modified and unmodified fumed silica. Nanocomposites prepared from polymer solution to achieve improved mixing and have been forwarded to fiber melt spinning. The surface of the fumed silica was modified with dodecyl alkoxy silanes. Result are untreated fumed silica filled polypropylene shown a shear thinning and an increased crystallization velocity of the polymer melt, while only minor changes were detected in the presence of modified fumed silica particle. Two king of fumed silica can increase the crystallinity of polypropylene. Fibers from unmodified fumed silica/polypropylene composites had mechanical properties stronger than modified fumed silica/polypropylene composites.

Supahol, P., Thanomkiat, P., Junkasem, J. ,and Dangtungee, R. (2007) investigated on the effect of the addition of titanium(IV) oxide (TiO$_2$) with diverse surface characteristics [i.e. neat, silica (SiO$_2$)-coated and stearic acid-coated] and various contents (ranging from 5 to 30 wt%) on non-isothermal melt-crystallization, subsequent melting behavior and mechanical properties of filled isotactic polypropylene (iPP). The

cooling rate used ranged between 5 and 30 °C/min. The crystallization exotherm for all of the samples investigated became larger and shifted towards a lower temperature as the cooling rate increased. The crystallization peak temperature (Tp) values for all of the iPP samples filled with neat TiO2 nanoparticles were slightly greater than those of the neat iPP and were not affected by the variation in the filler content. For iPP samples filled with stearic acid-coated TiO_2 nanoparticles, the Tp values were not much different from those of the neat iPP. For iPP samples filled with 5, 20, and 30wt% SiO_2-coated TiO_2 nanoparticles, marked differences in the Tp values in comparison with those of the neat iPP were observed. Together with the Avrami analysis, the nucleation ability of the various fillers investigated can be ranked as follows: SiO_2-coated TiO_2 nanoparticles > neat TiO2 nanoparticles > stearic acid-coated TiO_2 nanoparticles. Lastly, the presence of the nanoparticles caused the rigidity of the resulting composites to increase especially when the filler content was greater than or equal to 20 wt%.

Tian, X., Zhang, X., Liu, W., Zheng, J., Ruan, C. ,and Cui,P. (2006) used silica infuse in poly(ethylene terephthalate) via in situ polymerization using the compatibility between silica nanoparticles and ethylene glycol (EG). TEM micrographs revealed that the silica nanoparticles were about 10 nm with narrow distribution, and there existed strong interaction between the particles and the polymer chains. DSC results indicated that the thermal properties of PETS with 2 wt% silica (PETS-2) are different from those of pure PET (PETS-0). The properties of as-spun fibers show that the tenacity and LASE-5 (load at a specified elongation of 5%) of PETS-2 were higher than those of PET-0, while the heat shrinkage of PETS-2 was lower than that of PETS-0. They suggest that the increasing of crystallinity and the strong interface interaction tenacity and LASE-5 but also to have lower heat shrinkage.

Vladimirov, V., Betchev, C., Vassiliou, A., Papageorgiou, G. ,and Bikiaris, D. (2006) studied polypropylene/fumed silica nanocomposites prepared via melt mixing using a twin-screw co-rotating extruder. To improve the dispersion degree of the nanoparticles, maleic anhydride grafted polypropylene (PP-g-MA) was used as a

compatibilizer. From transmission electron microscopy it was found that agglomerations of silica particles into the PP matrix increased in average size with increasing silica contents whilst they decreased at higher PP-g-MA amounts. Storage modulus values of prepared nanocomposites measured by DMTA were sensitive to the microstructure of the nanocomposites. Higher silica contents resulted in higher storage modulus, evidence revealing that the material became stiffer. By adding the PP-g-MA copolymer a further increase of storage modulus was observed due to the finer dispersion of the filler in the matrix and the increased interfacial adhesion. Both permitted a much more efficient transfer of stresses from the polymer matrix to the SiO_2 nanoparticles. Crystallization rates were found to increase by increasing silica nanoparticles as well as PP-g-MA content. In fact for a given PP-g-MA content increasing the silica content up to 5–7.5 wt% accelerated the crystallization. Further increase of the nanoparticles amount did not have any effect. Permeability rates of O_2 and N_2 through films of iPP/SiO_2 were also measured. Lower rates were observed compared to pure iPP, most notably for O_2, which decreased with increasing concentrations of silica. This was attributed to the more tortuous path which must be covered by the gas molecules, since silica nanoparticles are considered impenetrable by them.

Wang, Z., Li, G., Xie, G. ,and Zhang, Z. (2005) studied TiO_2 nanoparticles introduced into linear low-density polyethylene (LLDPE)/low-density polyethylene (LDPE) composite films in the form of master batch where TiO_2 was pre-dispersed in LDPE by melt compounding. The dispersion behavior scanning electron microscopy (FE-SEM). The Rheology results show that the viscosity of LDPE/TiO_2 masterbatch is lower than that of LLDPE/LDPE composites. Energy dispersive X-ray spectrometer (EDS) composition distribution map indicates that TiO_2 nanoparticles were dispersed randomly in the master batch. Scanning electron microscopy (SEM) images show that LDPE/TiO_2 master batch is crushed into micro scale dispersed phases due to the shear stress during the blow-forming process. Subsequently, TiO_2 nanoparticles in the dispersed phases are released into the ambient matrix and form a wide ring composed of monodispersed particles. The sizes of spherical crystals decrease due to the presence of TiO_2

nanoparticles in LLDPE/LDPE/TiO$_2$ nanocomposites. The transparency of LLDPE/LDPE/TiO$_2$ composite films decreases little compared to that of LLDPE/LDPE composite films.

Wu, C.L., Zhang, M.Q., Rong, M.Z. ,and Friedrich, K. (2003) studied low nanoparticles filled-polypropylene composites properties. This paper found beforehand that low nanoparticles loaded polymer composites with improved mechanical performance can be prepared by conventional compounding technique in which the nanoparticles are pre-grafted by some polymers using irradiation. To examine the applicability of the approach, a tougher polypropylene (PP) was compounded with nano-silica by industrial-scale twin screw extruder and injection molding machine in the present work. The results of tensile tests indicated that the nanoparticles can simultaneously provide PP with stiffening, strengthening and toughening effects at a rather low filler content (typically 0.5% by volume). The presence of grafting polymers on the nanoparticles improves the tailorability of the composites. Due to the viscoelastic nature of the matrix and the grafting polymers, the tensile performance of the composites filled with untreated and treated nanoparticles is highly dependent on loading rate. With increasing the crosshead speed for the tensile tests, the dominant failure mode changed from plastic yielding of the matrix to brittle cleavage.

Yang, F., and Nelson, G.L. (2006) studied three polymer/silica nanocomposites prepared by a single-screw extrusion approach: poly(methyl methacrylate), polystyrene and polycarbonate/silica nanocomposites. The resulting nanocomposites were subjected to comprehensive studies of mechanical, thermal and flammability properties. All materials showed improved mechanical performance and thermal stabilities, although they are not strictly flame retardant when subjected to fire tests like Oxygen Index or horizontal Bunsen burner tests. However, the nanocomposites showed reduction in peak heat release rates and total heat release when evaluated by cone calorimetry. Moreover, the polycarbonate showed improvement in flammability according to vertical burning tests. All polycarbonate materials subjected

to vertical burning testing are V2 rated, but after flame times with 1% silica were significantly reduced. A flame retardant mechanism is proposed in order to understand the relationship between interfacial interaction and flammability of polymer/silica nanocomposites.

Yang, F., Ou, Y. ,and Yu, Z. (1998) studied polyamide 6 (PA 6)/silica nanocomposite obtained through a novel method, *in situ* polymerization, by first suspending silica particles in e-caproamide under stirring and then polymerizing this mixture at high temperature under a nitrogen atmosphere. The silicas were premodified with aminobutyric acid prior to the polymerization. The effects of the addition of unmodified and modified silicas on the dispersion, interfacial adhesion, isothermal crystallization, and mechanical properties of PA 6 nanocomposites were investigated by using scanning electron microscopy, dynamic mechanical analysis, differential scanning calorimetry, and mechanical tests, respectively. The results show that the silicas dispersed homogeneously in the PA 6 matrix. The addition of silicas increases the glass transition temperature and crystallization rate of PA 6. The mechanical properties such as impact strength, tensile strength, and elongation at break of the PA 6/modified silica nanocomposites showed a tendency to increase and decrease with increase of the silica content and have maximum values at 5% silica content, whereas those of the PA 6/unmodified silica system decreased gradually.

Yang, Y., and Gu, H. (2007) studied PET/silicon dioxide nanocomposite by in situ polymerization and melt-spun to fibers. TEM micrographs show nanoparticles well disperse in the PET matrix at a size level of 10-20 nm. The DSC results indicated that the silica nanoparticles might be as a marked nucleating promoting the crystallization of the PET matrix from melt but which inhibited the crystallization from the glassy state, owing to the 'crosslink' interaction between the PET and silica nanoparticles. The tensile strength of 5.73 MPa was obtained for the fiber from PET/0.1 wt% silica, with was 17% higher than that of the pure PET. Fibers were treated with aqueous NaOH. SEM photographs showed that more and deeper pits were introduced

onto PET fibers, which provided shortcuts for disperse dye and diffused the reflection to a great extent. According to the K/S values, the color strength of the dyeing increased with increasing silica content. It is found that the deep dyeability of PET fibers war improved greatly.

Yoon, C.S., and Ji, D.S. (2003) studied siloxylated polypropylene fibers composed of polypropylene (PP) and aluminosiloxane (AS) prepared by melt blending followed by spinning. The effects of blend compositions on the thermal behaviors, surface and tensile properties of PP/AS blend fibers were investigated by DSC, WAXD, SEM, static honestometer, etc. The heat of fusion of PP/AS blends decreased with increasing AS contents. In addition, the peak intensity of PP/AS blends in X-ray diffraction patterns decreased with increasing AS contents. It was observed that the silicone molecules exist and well distribute on the surface of siloxylated polypropylene fibers. From the results of the half-life period measurements, the anti-static properties of PP fibers siloxylated with AS was found to be significantly modified.

Zhang, X., Yang, M., Zhao, Y., Zhang, S., Dong, X. ,and Liu, X. (2004) studied polypropylene (PP)/organomontmorillonite (OMMT) nanocomposites prepared by melt intercalation by using the conventional method of twin-screw extrusion and subsequently submitted for melt spinning. The structure and properties of the PP/clay nanocomposites and hybrid fibers were characterized by scanning electron microscopy (SEM), transmission electron microscopy (TEM), X-ray diffraction (XRD), differential scanning calorimetry (DSC), and crystallization dynamics, etc. The organoclay layers were found to disperse in the PP resin at the nanometer level. The nanoscaled OMMT layers, dispersed in the PP matrix, actually played the role of heterogeneous nuclei species in the process of PP crystallization and increased the nucleation speed of the composites, hereby leading to the increase of crystallization rate of the as-spun fiber. Meanwhile, it was found that the crystallinity of PP/OMMT hybrid fibers is much higher than that of pure PP fiber at the same draw ratios, whereas the orientation of PP/OMMT hybrid fibers is much lower than that of pure PP fiber at the same draw ratios. Because

of the effective intercalation of OMMT into PP matrix, the nanocomposites have good spinnability, and the moisture absorption of the final PP fiber is improved.

Zheng, H., and Wu, J. (2007) reported using of silica in poly(ethylene terephthalate) via in situ polymerization. Silica nanoparticles were uniformly dispersed in the process of polymerization. By means of hot-stage polarization microscope and DSC, the influence of nanosilica on the crystallization of PET/silica nanocomposites has been clarified. The results show that nanosilica does not behave as a nucleating agent in PET but postpones the appearance of crystalline. This phenomenon is very favor to improve spinnability. The investigation on melt spinning of PET/silica nanocomposites also shows that it is advantageous to spinning with descending the spinning temperature.

CHAPTER III

EXPERIMENTAL

3.1 Scope of experiment

The scope of this experiment was to prepare nanocomposite polypropylene fibers to improve properties of isotactic polypropylene (iPP) fiber, particularly its solidification behavior, mechanical and surface properties. Typically, iPP is a semicrystalline polymer which crystallizes slowly into a large crystal of spherulitic structures. Practically, the addition of a nucleating agent is employed to achieve an increase in solidification rate of iPP. The increase in solidification rate is accompanied with a decrease in the crystalline size which consequently improves the tensile properties of the material. Recently, an incorporation of a nanoscale filler has been received a great attention. It was reported that the introduction of silica nanoparticles in iPP matrix can improve the structure and properties of iPP (Caldas et al., 1997; Garcia et al., 2004; Chen et al., 2006; Hung et. al., 2006; Vladimirov et al., 2006; Supahol et al., 2007; Rottstegge et al., 2007). To achieve this improvement, nano-silica must be fully dispersed throughout and connected to the iPP matrix. Hydrophobic silica, modified surface properties from hydrophilic to hydrophobic properties by silane, was used in this study. Commercial hydrophobic silica was selected for iPP. Direct melt-mixing and solution mixing were adopted to investigate the particle dispersability. In this study, iPP and hydrophobic silica/iPP composite resins were spun into fibers including preform and drawn fiber). Materials and methods used in this study are as follows:

3.2 Materials

Commercial polypropylene chip under the trade name of Moplen® HP561R was bought from HMC Polymer Company (Thailand). Moplen® HP561R, isotactic polypropylene homopolymer (iPP) has melt flow index (MFI) of 25 g/10 min at 230 °C (multifilament grade). Silica powder (SiO_2) used in this experiment was provided

by Degussa AG (Germany). Two types of silica powder, Aerosil® R974, hydrophobic silica, and Aerosil® 200, hydrophilic silica, were chosen. Their specification details are given in Table 3.1. Toluene (CARLO ERBA reagents: analysis grade) was used to dissolve iPP and nano-silica.

Table 3.1 Specification of the Nano-silica (Aerosil® R974 and Aerosil® 200)

	Surface	BET surface area (m^2/g)	Primary particle size (nm)	Ignition loss (%)	pH in water:methanol = 1:1	Purity (% of silicon dioxide)
Aerosil® R974	Hydrophobic (dimethyl dichlorosilane)	170±20	12	<2	3.7-4.7	99.8
Aerosil® 200	Hydrophilic	200±25	12	<1	3.7-4.7	99.8

3.3 Mixing and Compounding Masterbatches

In this study, two methods of blending, direct melt-mixing and solution mixing were carried out.

3.3.1 Direct Melt-Mixing

Hydrophilic silica or hydrophobic silica/iPP composite resins were prepared by melt mixing via twin screw extruder from Saree Masterbatch Company (Thailand). Aerosil® and iPP powder (grinds from chip) were physically mixed with a high speed mixer prior to feeding into twin screw extruder. The mixture was melt mixed by a twin screw extruder operating at 180-210 °C and 120 rpm using co-rotating mode to obtain resin masterbatch containing silica particles of 5.61 wt% (measured by TGA). It should be noted that fumed silicas was too fluffy to prepare high concentration masterbatch. The obtained resin was later employed for fiber spinning. The masterbatch preparation is diagrammatically shown in Fig. 3.1.
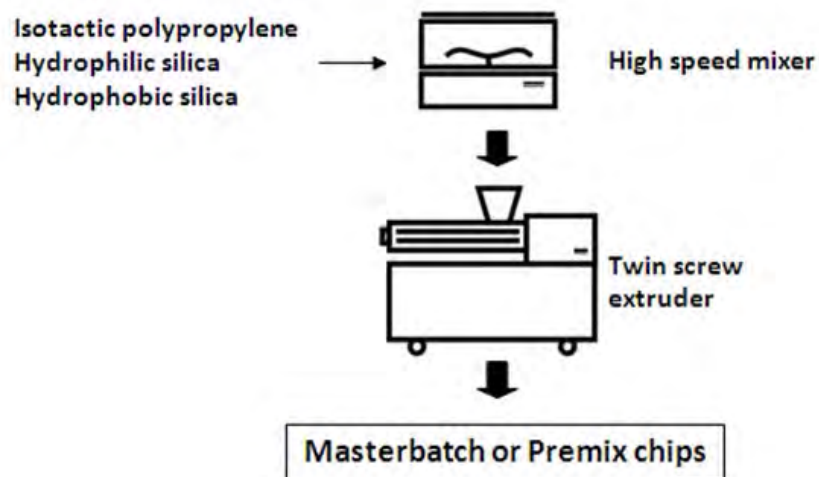
Figure 3.1 Scheme on making of masterbatch

3.3.2 Solution Mixing

In this recipe, only hydrophobic silica was employed as follows: Weighed AROSIL[®] R 974 was suspended in a beaker containing toluene. The beaker was sonicated at 80 °C for one and a half hour. Then the beaker was placed onto a hot plate and admixed with iPP powder. The mixture was heated to 140 °C and stirred with a glass rod for 30 minutes in silicone bath. After the completion of iPP solubilization, the solvent was allowed to evaporate and the resultant composite resin was ground into white powder. The dissolution method is diagrammatically shown in Fig. 3.2. In this case, hydrophobic silica/iPP composite resins loaded with 0.25, 0.5, 0.75, and 1.0 wt% of silica on iPP, were prepared.

In a separate experiment, AROSIL[®] R 974 (1 wt% based on iPP) in ml of toluene was cooked in an autoclave set the temperature of 140 °C and cooking time of one hour (Fig. 3.3). The autoclave was removed and left standing for several hours to reduce the pressure before opening-up the vessel. Then the silica dispersion was admixed with polypropylene. The mixture was stirred in a hot bath for 30 minutes. The obtained solution was poured onto an aluminum tray to allow toluene to evaporate for at least 2 days. 1 wt% silica/iPP nanocomposite resin as a white sheet was obtained. The

resin was ground into powder prior to spinning. The preparation method is diagrammatically shown in Fig. 3.4.
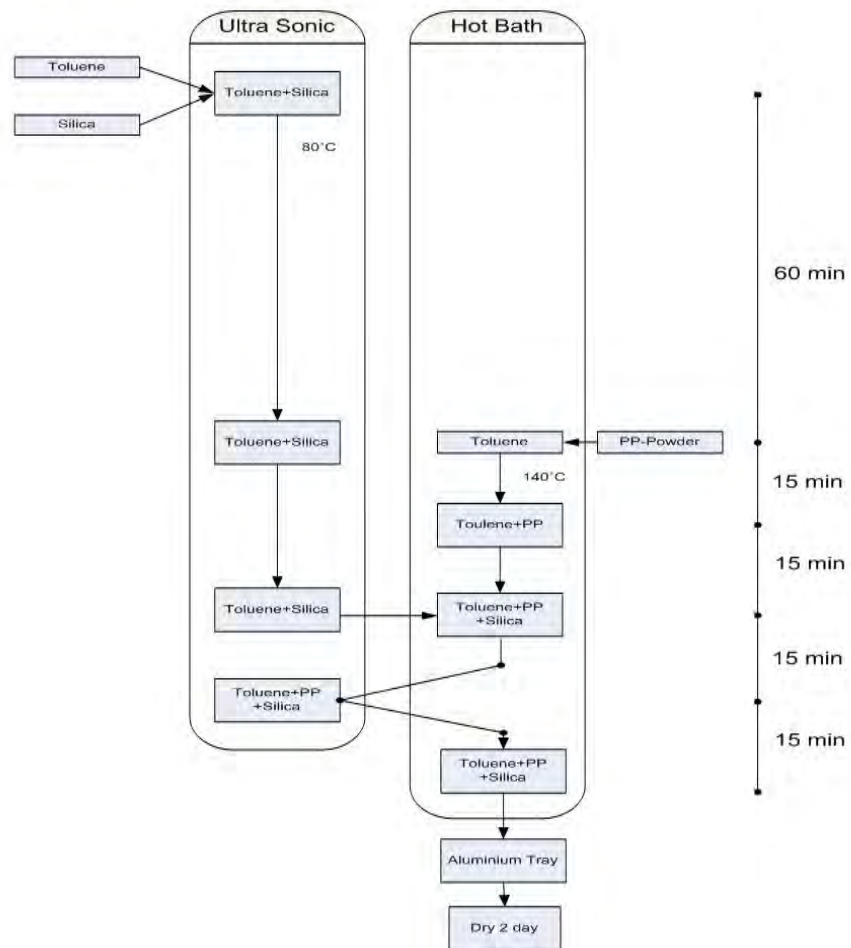

Figure 3.2 Preparation process of silica/iPP nanocomposite via solution blending method: original method (normal pressure)
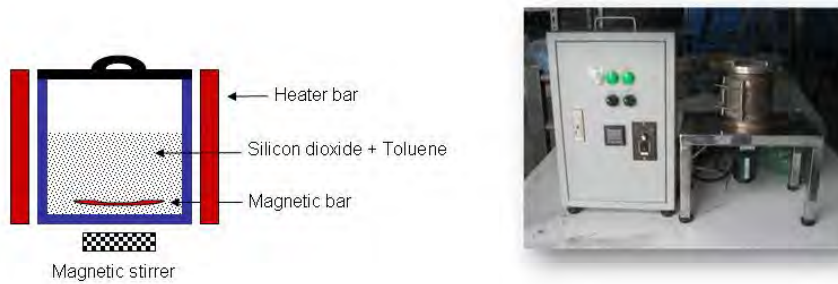
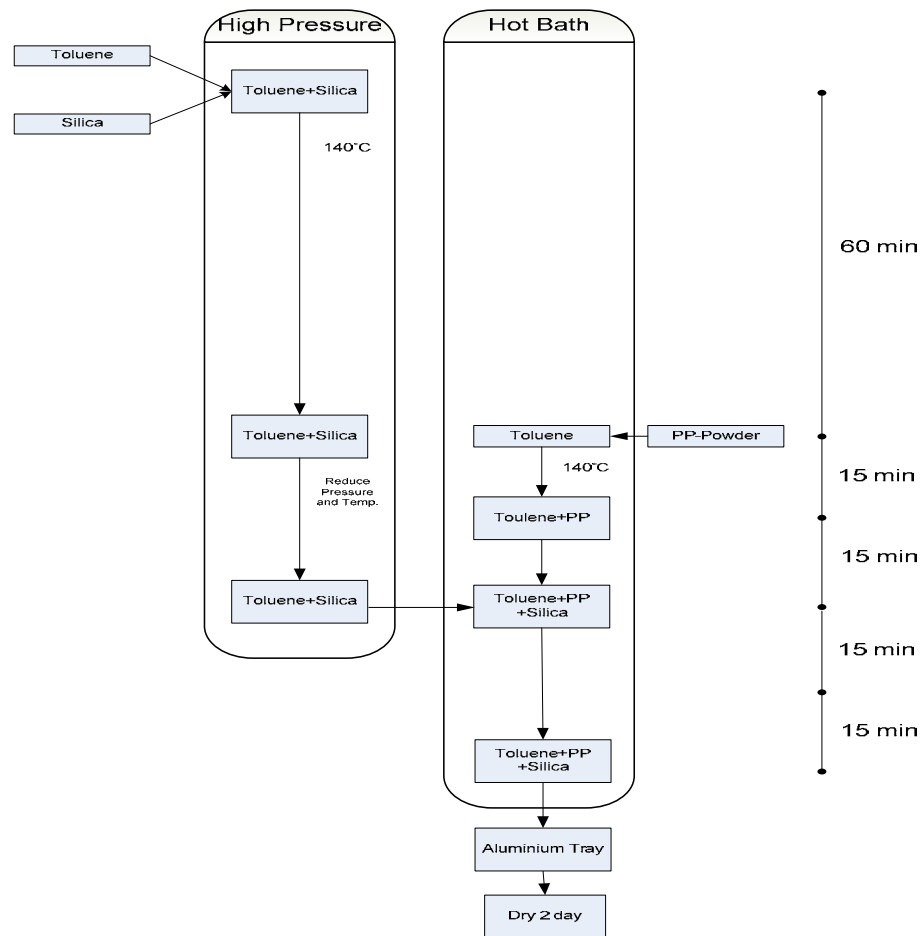Figure 3.3 High pressure vessel for solution mixing under high pressure (autoclave)

Figure 3.4 Preparation of silica/iPP nanocomposite via solution mixing in

pressurized vessel (autoclave)

3.4 Spinning of silica/iPP composite fibers

Spinning of fiber from melt mixed nanocomposite resins

In case of the masterbatch resin obtained from melt mixing, the 5.6 wt% as-extruded composite pellet (dried at 80 °C for 4 hours before usage) was admixed with virgin iPP pellet at the various ratios in the hopper of Fourne' pilot plant fiber spinning machine. After that, the mixed pellet was fed into the spinning machine having the spinneret with 24 nozzles of 0.32 mm diameter to produce filament fibers. In this experiment, a series of filament fibers containing 0.5, 1.0, 2.5 wt% silica were spun. For a typical example, the calculated amount of as-extruded resin was physically mixed with virgin iPP prior to feeding into spinning machine's extruder where barrel zone temperatures were set at 210, 220 and 230 °C for extruder zone 1, 2, and 3, respectively. Fibers with take-up speeds of 300, 500 and 1100 m/min were produced in this experiment. Three sets of godet were used to heat drawing of the filaments. The filament was heat drawn using conditions as shown in Table 3.2. The Fourne' pilot plant fiber spinning machine is diagrammatically illustrated in Figure 3.5. Condition 1, 2, and 3 are low, medium, and high spinning speed, in the other words were low, medium, and high drawn dawn ratio. Whereas, condition 4 was FDY (Fully drawn yarn) process. Low spinning speed was set in the first godet (equal to condition 1) and then increase speed to the winder. Winder speed of condition 4 was equaled to winder speed of condition 3. Different between conditions 3 and 4 is draw down ratio and solid fiber dawn ratio. Behavior of PP and their composites on fiber melt spinning could be measured in these 4 conditions.

Table 3.2 Fiber spinning conditions

|	Condition	1	2	3	4
Setting conditions	Spin pump speed (rpm) , 1.2 cc/rev.	11.4	11.4	11.4	11.4
	Extruder pressure (bar)	75	75	75	75
	Extruder temp. Z1 (°C)	210	210	210	210
	Extruder temp. Z2 (°C)	220	220	220	220
	Extruder temp. Z3 (°C)	230	230	230	230
	Measuring head temp (°C)	230	230	230	230
	Melt pipe temp (°C)	230	230	230	230
	Pump block temp (°C)	230	230	230	230
	Spin block temp (°C)	230	230	230	230
Setting speed	1st godet speed (m/min) / temp (°C)	300 / 50	500 / 50	1100 / 50	300 / 50
	2nd godet speed (m/min) / temp (°C)	320 / 50	520 / 50	1150 / 50	750 / 90
	Duo godet speed (m/min) / temp (°C)	330 / 50	540 / 50	1170 / 50	1170 / 90
	Transverse (double stoke / min)	300	300	300	300
	Friction speed (take up speed) (m/min)	300	500	1100	1100
	turns on godet (G1/G2/G3)	6,7,7	6,7,7	6,7,7	6,7,7
	Quench air (rpm/°C)	1000/25	1000/25	1000/25	1000/25
	Oil pump (rpm)	8	8	8	8
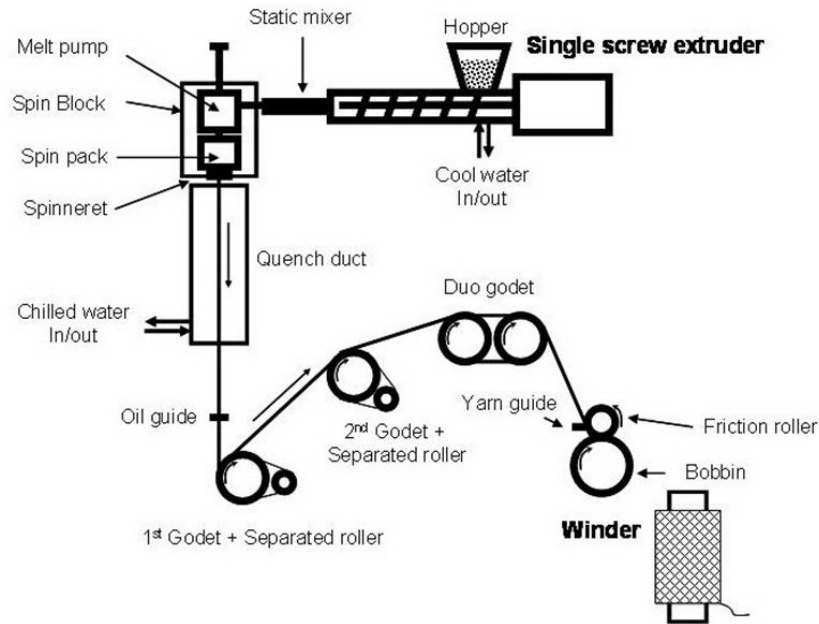
Figure 3.5 The Fourne' pilot plant fiber spinning machine

Spinning of monofilament fiber from solvent mixed nanocomposite resins

Due to the small amount of resin produced from solution mixing method, ThermoHaake® single screw extruder was employed for spinning fibers from resins obtained from solution mixing. In this case, a free-fall and drawn monofilament fibers was produced. The composite resin was fed directly into the hopper of the extruder. Spinning conditions were set as follows: screw speed : 4 rpm, 1st godet speed: 25 m/min, heater temperature: 110°C, 2nd godet speed: 51 m/min and winding speed: 50 m/min, and die hole diameter : 0.5 mm. The temperatures of extruder zone 1, zone 2, and zone 3 were 170°C, 180°C and 190°C, respectively. Throughput was 0.4224 g/min. The diagram of ThermoHaake® single screw extruder is shown in Fig. 3.6.
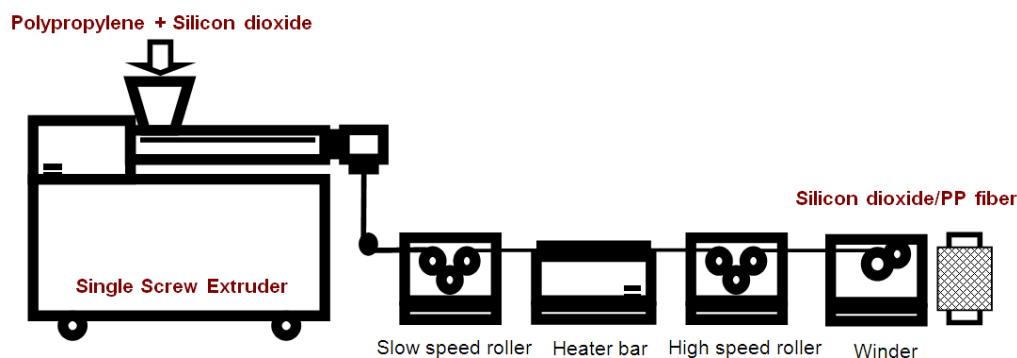
Figure 3.6 Single screw extruder and monofilament spinning line

3.5 Testing and Characterizations Technique

3.5.1 Linear density

Instrument/machine: Sartorius AC211S balance and warp reel machine

The fiber linear density in denier was determined using warp the yarn by warp reel machine in 90 meter yarn length and measured the weight of yarn to calculate the linear density (denier: 1 denier means yarn in 9000 meter long has 1 gram weight).

3.5.2 Differential scanning calorimetry (DSC)

Instrument/machine: DSC 200 F3 from NETSCH, Germany

Differential scanning calorimetry was performed using DSC 200 F3 (NETZSCH, Germany) to determine the percent crystallinity, crystallization temperature (Tc) and melting temperature (Tm). A sample was heated from 30 to 200 °C with a heating rate of 10 °C/min and kept for 5 minutes to eliminate the thermal history. Then, the sample was cooled down to 30 °C at a cooling rate of 10 °C/min under nitrogen gas at constant flow rate of 20 ml/min. From heating scan the on-set temperature, Tm and heat of fusion (ΔHf) of the fibers were measured. The crystallinity of the sample was calculated by using ΔHf for 100% crystalline iPP of ΔHf= 170 J/g. (Rottstegge et al., 2007). From the cooling scan, Tc was measured.

To measure the non-isothermal crystallization, a sample was heated from 30 to 200 °C with a heating rate of 10 °C/min and held at that temperature for 5 minutes to eliminate the thermal history and then cooled down to 25 °C at cooling rate 5, 10, 15, 20 °C/min. The exothermal curve of heat flow, as a function of temperature, was recorded to analyze the non-isothermal crystallization process. Consequently, sample was heated from 25 °C to 200 °C at heating rate 10 °C/min to collect the melting point and heat of fusion in second heating scan, then also kept for 5 minutes. Sample was cooled down to 30 °C at a cooling rate of 10 °C/min. The second crystallization temperature was recorded.

3.5.3 Thermogravimetic analysis (TGA)

Instrument/machine: Thermogravimetic analysis TG209 F1 Iris® from NETZSCH, Germany

To measure thermal degradation behavior of iPP and composite fibers, thermogravimetric analysis (TGA) was used. The results were acquired with a heating rate of 10 °C/min from room temperature to 600 °C under nitrogen gas at constant flow rate of 20 ml/min. The weight samples were used around 10 mg.

3.5.4 X-ray diffractometer (XRD)

Instrument/machine: Bruker – D8 Advance model with CuKα radiation

To obtain XRD pattern was operated by Bruker - D8 Advance model with CuKα radiation at the wave length of 1.54 angstrom. The diffraction spectrogram was registered for the fiber samples in 2θ (2 theta) range 10-50°.

3.5.5 Scanning electron microscope (SEM)

Instrument/machine: Hitachi® S-3400 SEM

SEM images were taken from chip to nanocomposite and fibers with a Hitachi® S-3400 SEM with carbon coating. Samples were fixed to the substrate by means of conductive adhesive tapes. The accelerating voltage of the applied field emission gun was about 20 KV, the working distance about 10 mm applying 1,000X – 10,000X.

3.5.6 Transmission electron microscope (TEM)

Instrument/machine: JEOL 2101 TEM

To observe size and distribution of nanosilica particle, TEM was used. Hydrophobic silica nanoparticles were prepared by original solution method and high pressure solution method compared with silica from packaging. Dried silica was dispersed in methanol in an ultrasonic for 10 min. TEM 200 kV was used. TEM micrographs of three samples of silicas were taken in 10,000X and 20,000X.

3.5.7 Atomic force microscope (AFM)

Instrument/machine: SPA 400 model from SEIKO Instruments

To observe size and distribution of nano-silica particle on the surface of fiber, AFM was used. AFM images take from the surface of the preform (free fall fiber).

3.5.8 Hot stage (for crystal image analysis)

Instrument/machine: Polarized microscopy (Olymplus® SZ40) equipped with a hot stage (Mettler Toledo® FP82HT)

The crystallization and spherical crystal size of silica/iPP nanocomposite were observed by polarized microscopy (Olymplus® SZ40) equipped with a hot stage

(Mettler Toledo® FP82HT). The particle size was evaluated by Image-ProExpress 6.0 image software. Samples were heated from 50 to 200 °C with a heating rate of 10 °C/min and cool down to 50 °C with cooling rate 10 °C/min after hold them at 200 °C for 5 min.

3.5.9 Mechanical testing

Instrument/machine: Instron® tensile tester 5500 model

Tensile measurements of fiber were performed via a Instron® tensile tester 5500 model with gauge length of 25 mm at a crosshead speed of 20 mm/min. The tensile properties of yarn were also used the Instron® tensile tester 5500 model with gauge length of 250 mm at a crosshead speed of 500 mm/min. Maximum force to breaking fiber (gram force) and elongation at break (%) were taken. Result received from the average of 10 specimens.

3.5.10 Fiber shrinkage

Instrument/machine: oven and hot water bath

Hot air shrinkage was measured in a hot air oven at 110°C for 30 min and boiling water for 30 min. The lengths of fiber before and after were measured. Result received from the average of 5 specimens. The percent shrinkage was calculated using the following equation:

$$Shrinkage\ (\%) = \frac{l_0 - l}{l_0} \times 100$$

Where, l_0 is initial fiber length, and l is the fiber length after treatment.

3.5.11 Sonic modulus

Instrument/machine: Dynamic Modulus Tester PPM-5R.

Sonic modulus technique with Dynamic Modulus Tester PPM-5R from Lawson-Hemphill Company was used to evaluate molecular orientation along fiber length. Dynamic Modulus Tester PPM-5R was applied with the LH-551 DMT Fiber Scanner Option. Fiber from 16 to 20 centimeters length were used to calculate the sound velocity then conversed to sonic modulus, E, (young's modulus of elasticity). The constant conversion factor is 11.3. The formula equation used as follow.

$$E = C^2K = C^2\ 11.3$$

$$C = \frac{Distance\ (centimeters)x\ 10^{-5}}{Transit\ Time\ (microseconds)x\ 10^{-6}}$$

C = sound velocity in km/sec

K = a constant conversion factor = 11.3

E = young's modulus of elasticity in grams/denier

3.5.12 Contact Angle

Instrument/machine: OCA-Series with dosing system from DataPhysics

Surface property of the nanocomposites was observed by contact angle measurement using OCA-series from Data Physics with dosing system. Contact angle values were obtained by automatic measurement. Sample prepared by compression on the melt mixing fiber and composites powder of silica and iPP on the solution mixing. Compression temperature and time 220°C / 3 minute was used to prepare samples.

CHAPTER IV

RESULTS AND DISCUSSION

4.1 Introduction

Fibers from isotactic polypropylene (iPP) are commonly found in many end-use products thanks to their advantageous properties such as light weight, resistance to moisture and chemicals, low cost, sufficient strength and ease in processing. Furthermore, PP's properties can be enhanced by melt mixing with particulates and fibrous materials as well as by melt blending with other polymers. Recently, polymer nanocomposites which contain nano-sized particles at a much lower loading ratio than conventional fillers have attracted great deal of attention because they offer enhanced mechanical properties and thermal properties when compared to conventional composites. Nano-sized particles, particularly, carbon nanotube (CNT) and montmorillonite (MMT) have taken a lead as the novel nano-fillers for plastics as well as fibers thanks to their high aspect ratio. Even though the fillers with high aspect ratio are ideal for plastic reinforcement, recently silica has been widely investigated for polymeric materials and held a great potential for developing nanocomposites. Particularly, fumed silica has been received considerable interest. Fumed silica is a nanoscale particle which is synthesized by hydrolysis of chlorosilane in an oxygen-hydrogen gas flame. It is amorphous silicon dioxide which is claimed to be non-toxic when compared to crystalline silica. There are many reports on the usage of silica for enhancing mechanical properties of polymer. Some articles dealt with silica as filler for polypropylene fiber and other articles reported the study of silica addition to polyester and nylon-6 fibers. Typically, silicas are present in agglomerate form which, for nanocomposite applications, needs to be small enough and fully dispersed in polymer matrix in order to achieve the improved properties. In case of hydrophilic silica (untreated silica), its surface contains silanol groups connecting together through strong intermolecular hydrogen bonding. Hence, it is not easy to obtain the state of dispersion at nanoscale level. Hydrophobic silicas which are normally modified using organosilane

agents make them compatible with hydrophobic polymer matrix like PP.

The scope of this work was to prepare nanocomposite polypropylene fibers in order to improve properties of isotactic polypropylene fiber, particularly its sodification behavior, mechanical and surface properties. Practically, the addition of a nucleating agent is employed to achieve an increase in solidification rate of iPP. The increase in solidification rate is accompanied with a decrease in the crystalline size which consequently improves the properties of the material. Surprisingly, an incorporation of nanoscale filler has demonstrated this improved performance. However, to achieve this improvement, nanosized silica must be fully dispersed throughout and connected to the iPP matrix. In this study, direct melt-mixing and solution mixing were adopted to investigate the particle dispersability. From melt-mixed masterbatches, a series of multifilament fibers containing 0.5, 1.0, 2.5 wt% silica were spun using Fourne' pilot plant fiber spinning machine. Fibers spun with take-up speeds of 300, 500 and 1100 m/min were produced in this experiment. In case of solution-mixed resins, free-fall monofilament was spun using ThermoHaake® single screw extruder. Then, characterizations of obtained composite fibers including morphological analyses (SEM), crystallization temperature (DSC) and the fine structure (XRD) were studied. The results are compared and discussed as follows:

4.2 SEM analyses of composite fibers spun from melt-mixed masterbatches and solution-mixed resins

The morphological images (longitudinal view) of neat PP and silica/PP composite multifilaments from melt-mixed masterbatches observed by SEM, are shown in Fig. 4.1. In all cases, the longitudinal images exhibit continuous, smooth and regular surfaces. These indicate that spinnability of polypropylene composites at high speed spinning rate up to 1100 m/min was affected by the presence of silica particles. The silica particle sizes present in PP bulk are in micron-sized range of micron-sized range as revealed in Fig. 4.2. As can be seen, silica particles still exist in aggregate form. Apparently, an increase in percent silica loading is accompanied with an increase in the

number of silica particles. This indicates that shear stress applied during melt-mixing failed to overcome cohesion force among agglomerate particles. As a result, the dense agglomerates of silica nanopowders remain as micron-sized particle clusters in the PP matrix. Despite its presence in micron-sized range the melt spinnability of the composite resin was not severely impaired thanks to the low aspect ratio of silica particle.
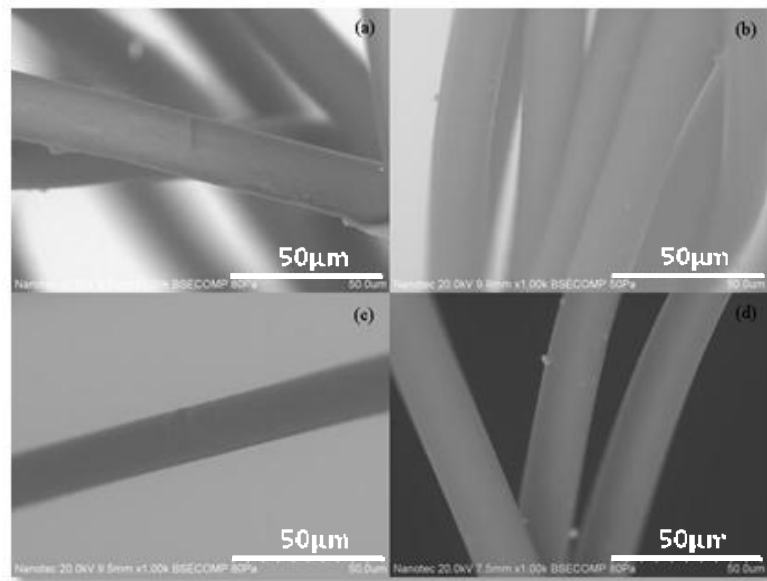

Figure 4.1 SEM longitudinal views of composite fibers spun from melt-mixing resin (a) neat PP (b) 0.5 wt% SiO$_2$/PP (c) 1.0 wt% SiO$_2$/PP (d) 2.5 wt% SiO$_2$/PP
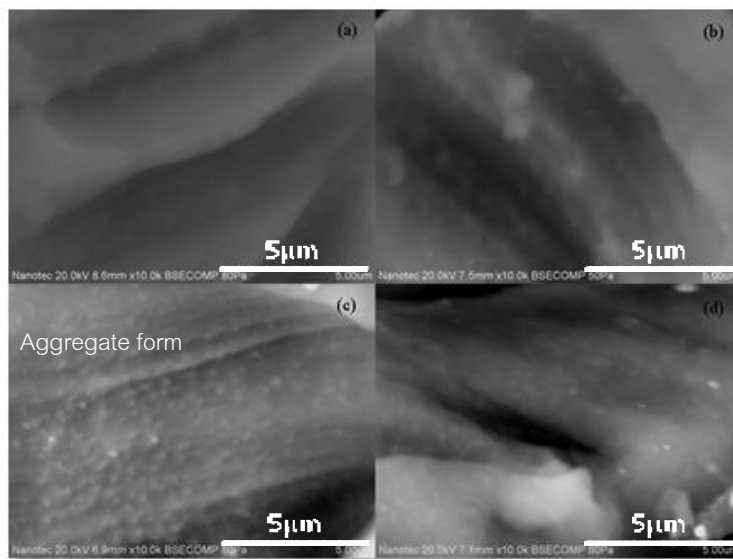
Figure 4.2 Distribution of silica agglomerate in PP bulk (a) neat PP fiber, (b) 0.5 wt% SiO$_2$/PP fiber (c) 1.0 wt% SiO$_2$/PP, (d) 2.5 wt% SiO$_2$/PP

SEM analysis of monofilament fibers spun from solution-mixed resins was conducted in a similar manner to multifilament fiber. It should be noted that due to the small amount of resins produced from solution mixing method ThermoHaake® single screw extruder was employed for spinning fibers from resins obtained from solution mixing. In this case, a free-fall monofilament fiber and a monofilament fiber with draw ratio of 2 was produced. In contrast to multifilament fibers, the monofilaments spun from solution (toluene) mixed resins exhibit very smooth fiber surfaces in accompany with no detection of silica particles judged from SEM analysis (Fig. 4.3). This indicates that solution mixing method results in the extremely fine particle dispersion. By this method, it indicates that dissolution means could overcome the binding force, leading to the breakup of micron-sized aggregates into nanoscale particles. Hence, it can be said that toluene solvent is more effective than shear stress in deagglomerating the cluster of hydrophobic silica.
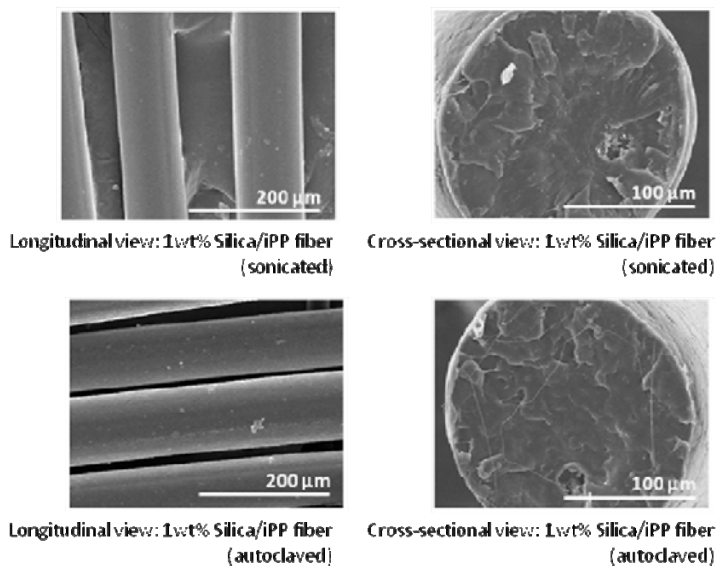
Figure 4.3 SEM images of surface of iPP: 1%silica prepared by sonication and autoclave
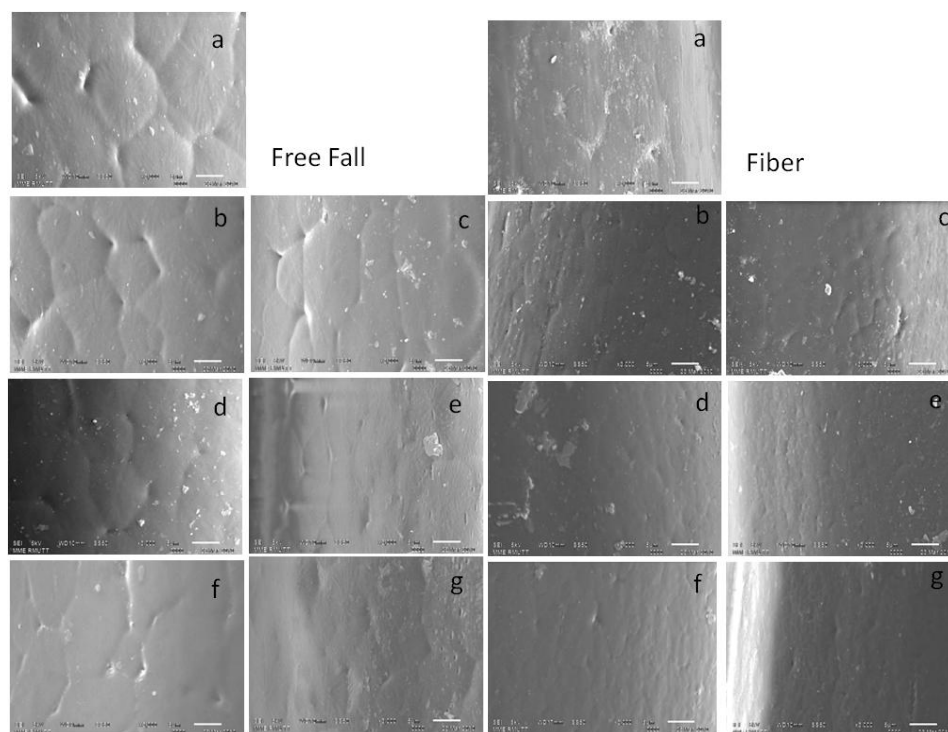

Figure 4.4 SEM surface images (3000X) of free-fall fibers of neat PP (a), PP-toluene

(control) (b), sonicated 0.25 wt%SiO$_2$/PP (c), sonicated 0.5wt% SiO$_2$/PP (d), sonicated

0.75wt% SiO$_2$/PP (e), sonicated 1.0wt% SiO$_2$/PP (f) and autoclaved 1.0wt% SiO$_2$/PP(g)

(scale bar = 5 μm)

Figure 4.4 shows SEM surface images of free-fall and drawn fibers taken at 3000X. It is found that SEM analysis at high magnificence could reveal information of the crystal structure of PP. The large spherulite crystal can be obviously seen on the surface of neat free-fall fiber. Then, the trend of decreasing crystal size as percent silica loading increases is observed. Since the free-fall fiber describes the spun fiber obtained by the only gravity force change in the crystal size is likely to be affected by the presence of silica loading. Subsequent heat drawing of free-fall fibers was carried-out. As seen, spherulite size of heat-drawn neat fiber is altered with a decrease in growth. Change in spherulite size is obvious in case of nanocomposite fibers particularly 0.75 and 1 wt% silica loading where spherulite crystal is invisible with SEM analysis. Based on these results, it can be said that crystallization phenomena of polypropylene were induced by two factors namely shear stress and heterogeneous nucleating agent. In conclusion, the combination of shear stress and heterogeneous nucleating agent could favorably enhance nucleation performance of polypropylene.

In order to prove the dispersion of silica particles in the nanoscale level, TEM micrographs of as-received silica, toluene mixed silica (under ultrasonication) and autoclave treated silica (high pressure treatment) are shown in Fig. 4.5. It can be seen that silica particles are densely packed and adhered tightly together since the surface nature of nanoparticles is highly active so that they aggregate tightly, creating a micron-sized cluster. Ultrasonication treatment of hydrophobic silica in toluene could reduce the aggregate sizes. As observed, the densely packed particles become loosely packed particles after having ultrasonication treatment. Additional treatment of sonicated silica in autoclave could further break down nanoparticle agglomerates into nanoscale particles. It was expected that sonicated silica and autoclave silica would uniformly disperse in polymer matrix
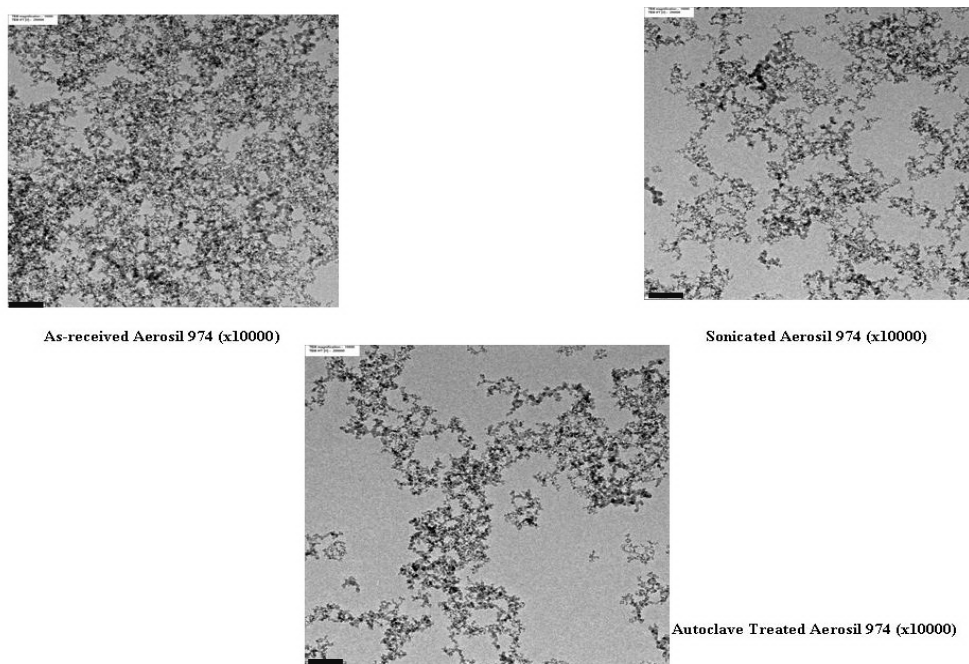
As-received Aerosil 974 (x10000)

Sonicated Aerosil 974 (x10000)

Autoclave Treated Aerosil 974 (x10000)

Figure 4.5 TEM images of silica particles prepared by solution mixing methods

(scale bar = 200 nm)

4.3 AFM analysis of nanocomposite fibers

In order to obtain information of nanoscale silica particles dispersion in PP matrix, AFM analysis was carried-out. Taping mode AFM images of fiber surfaces are presented in Fig. 4.6.   The images reveal that an incorporation of silica nanoparticles leads to apparent surface modification. As seen, raised feature surfaces are observed at the surfaces of silica/PP nanocomposite fibers. Contrarily, the neat fiber surface is found smooth with the absence of raised feature is found. The result also shows that raised features are predominantly present on the fiber surface spun from the autoclave mixed nanocomposite. This indicates that high pressure mixing could produce an even distribution of nanoparticles within the bulk of the fiber or on the surface. To a less extent, solvent mixing in hot toluene results in relatively uneven distribution of nanoparticles, judged from lesser presence of nanoparticles on the fiber surface. The

Ra value of 1 wt% sonicated silica/PP fiber and 1 wt% autoclaved silica/PP fiber are 2.089E+01 and 2.505E+01, respectively.

1 wt% sonicated silica/PP Fiber Surface

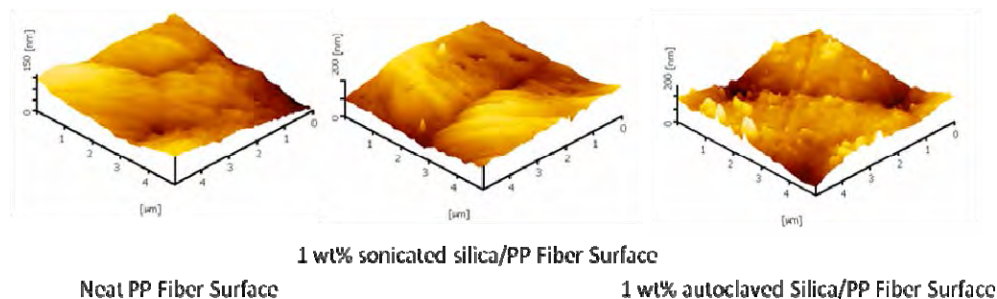Neat PP Fiber Surface

1 wt% autoclaved Silica/PP Fiber Surface

Figure 4.6 AFM images of PP fiber surfaces, 1%SiO$_2$/PP-ultrasonic and 1%SiO$_2$/PP-autoclave

4.4 X-ray Analyses of composite fibers and nanocomposite fibers

X-ray patterns of neat PP fibers and 1 wt% silica/PP composite fibers from melt-mixed masterbatch are shown in Fig. 4.7-4.8 and overlaid in Fig. 4.9. For the neat fiber taken at low spinning speed (300 m/min), the broad peak is observed which is indicative of poor crystallinity. It is thought that spinning speed rate of 300 m/min was too fast to allow crystallization of PP. Due to the fact that PP fiber was solidified before crystallization took place the neat PP fiber exhibits poor crystallinity. In case of silica infused PP fiber, the crystalline peaks appear in x-ray pattern of fiber drawn with low take-up speed (300 m/min), indicating that infused silica particle is capable of acting as a nucleating agent for isotactic PP. An increase in spinning speed leads to an appearance of α form crystals via reflections at 2θ = 13.7, 16.5, 18.1, and 21.1° corresponding to (110), (040), (130), and (111) crystal planes, respectively, which reach the strongest intensity with the fiber spun with take-up speed of 1100 m/min. However, at the take-up speed of 1100 m/min, the α-form crystallinity peaks are found identical to those of highly drawn neat PP, implying that take-up speed plays a dominant role in increasing molecular orientation along fiber axis. At the high speed state, silica filler

seems to lose its influence. It could be said that fiber take-up at high speed results in the fiber with the crystallization to the fiber. Overlaid XRD patterns in Fig. 4.9 show before and after heat drawn fiber from condition 4 (or FDY process). XRD patterns shown in the paracrystalline (smectic form) all of before heat drawn fiber. When heat drawn they move towords the more stable form in α-form. This effect found in the same effect when fiber passed annealed process. (Gupta and Kothari, 1997)
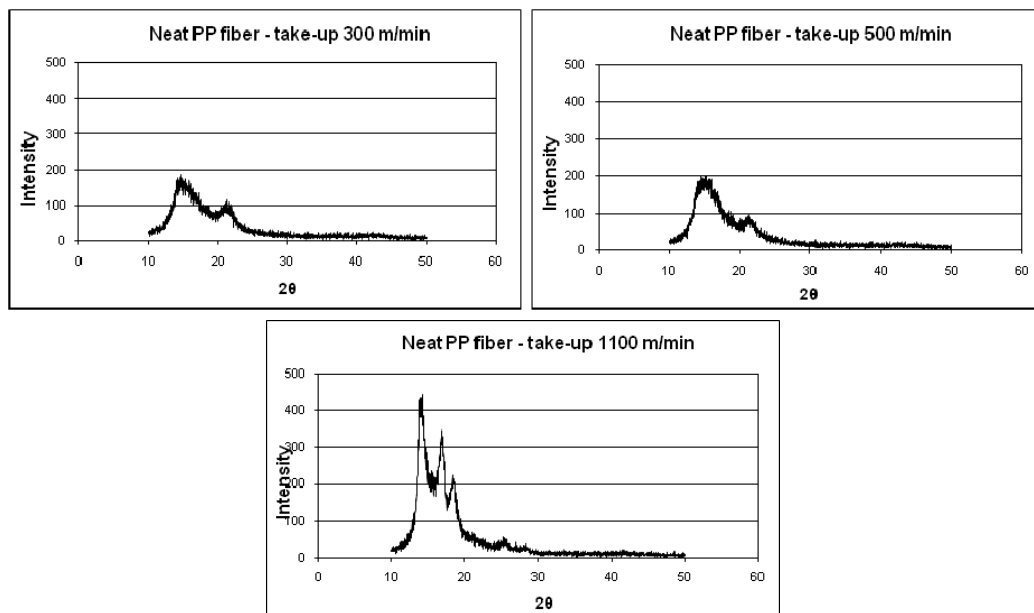

Figure 4.7 XRD patterns of neat PP fibers drawn at take-up speeds of
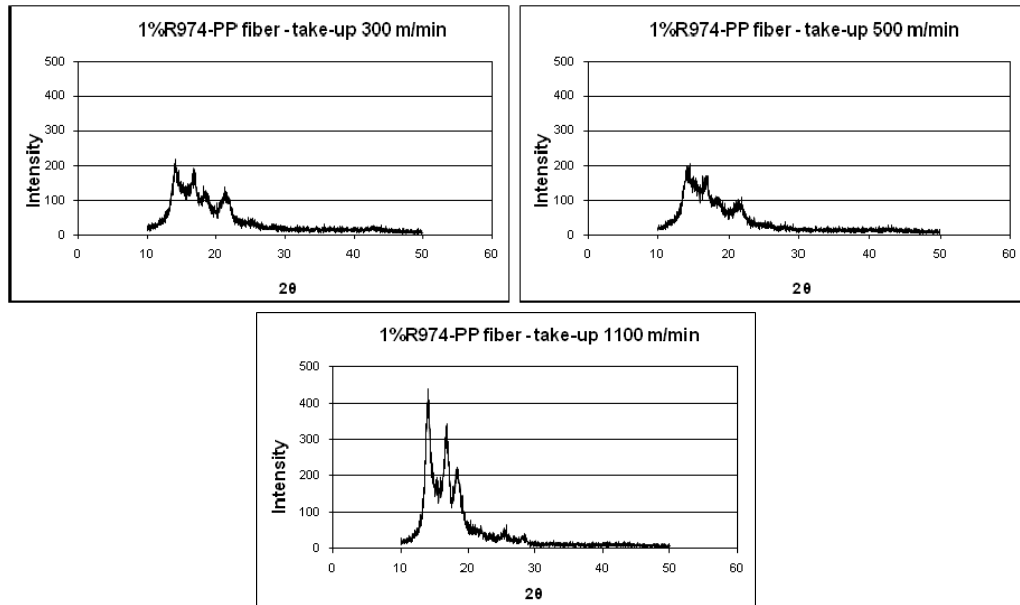
300, 500, and 1100 m/min

Figure 4.8 XRD patterns of 1wt% silica/ PP composite fibers drawn at take-up speeds of 300, 500 and 1100 m/min
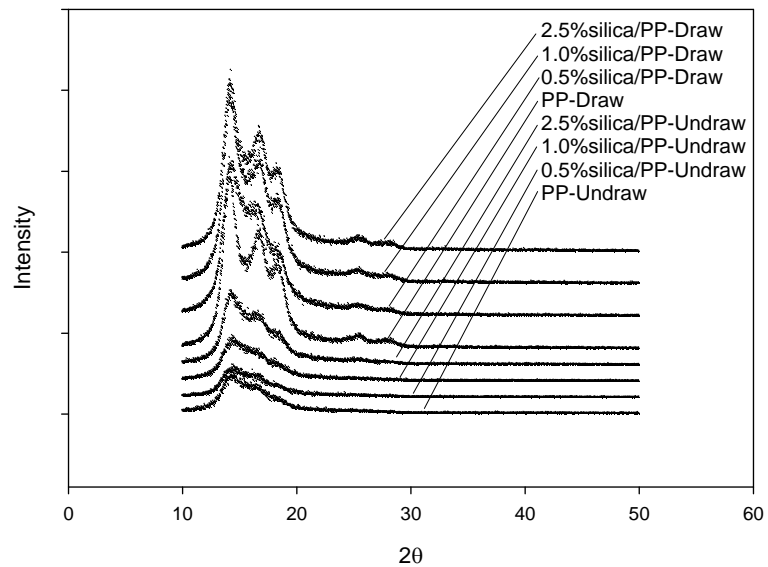

Figure 4.9 Overlaid XRD Peaks

X-ray patterns of neat PP monofilament fiber and sonicated silica/PP monofilament fibers and 1 wt% autoclaved silica/PP monofilament fiber are shown in Fig.4.10. It can be seen that neat free-fall fiber exhibits strong α-form crystallinity when compared to neat PP fiber obtained from spinning speed at 300 m/min. The reason is that free-fall fiber was solidified slowly with the absence of take-up speed, consequently allowing crystallization of polypropylene to take place. As seen, PP fiber mainly has three crystalline forms including monoclinic α, hexagonal β, and orthorhombic γ. Figure 4.10 indicates that PP and sonicated silica/PP free-fall and drawn fiber crystallize primarily in the monoclinic α form via reflections at 2θ = 13.7, 16.5, 18.1, and 21.1° corresponding to (110), (040), (130), and (111) crystal plane, respectively, in XRD diffractograms, reflecting its high content. However, in case of the sonicated silica/PP fiber, the intensity of α crystallinity at 2θ = 16.5° tends to increase, indicating that sonication treated silica could induce change in the proportions of α-form contents. This was probable due to the effect of size reduction of silica particle. In case of autoclaved silica/PP nanocomposite fibers, an appearance in the intensity of β crystalline form (the presence of the hexagonal β form via reflections at 2θ=15.6° corresponding to (300) crystal plane) is clearly observed. This indicates that the autoclave treated silica particles are able to enhance the crystallization of isotactic PP fiber, arising from the reduction of their sizes into nanoscale. The relative proportion of the β form was determined by the following equation: (Chen et al., 2006). The calculated values of k_β, $k_{\alpha 1}$, $k_{\alpha 2 \text{ and }} k_{\alpha 3}$ are listed in Table 4.1.

$$k_\beta = \frac{I_\beta}{I_\beta + I_{\alpha 1} + I_{\alpha 2} + I_{\alpha 3}}$$

where I_β is the intensity of the (300) peak, and $I_{\alpha 1}$, $I_{\alpha 2}$, and $I_{\alpha 3}$ are the intensities of the (110), (040), and (130) peaks of the α form, respectively. Similarly, the relative proportion of the three α forms can be calculated.

$$k_{\alpha_1} = \frac{I_{\alpha_1}}{I_\beta + I_{\alpha_1} + I_{\alpha_2} + I_{\alpha_3}}$$

$$k_{\alpha_2} = \frac{I_{\alpha_2}}{I_\beta + I_{\alpha_1} + I_{\alpha_2} + I_{\alpha_3}}$$

$$k_{\alpha_3} = \frac{I_{\alpha_3}}{I_\beta + I_{\alpha_1} + I_{\alpha_2} + I_{\alpha_3}}$$

Typically, a high content of β-form crystallinity is desirable since it governs the balance between stiffness and flexibility of PP fiber. From Table 4.1, only autoclaved silica (which was conducted under severe condition) exhibited the notable β-form nucleating agent, indicating that extremely high pressure was required in order to produce the extremely fine particle enough for exhibiting nucleation performance. Due to its large surface area and high surface activity, the nanoparticle underwent inducing nucleation process easily when compared to a micron-sized particle as in case of composite fibers spun from melt-mixed resin.
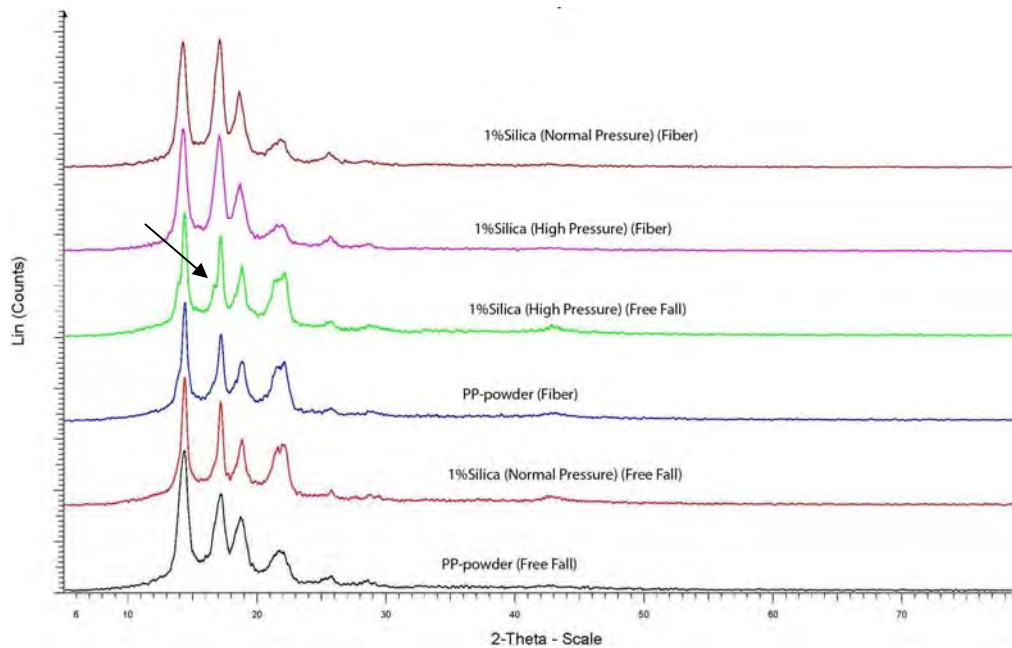

Figure 4.10 Overlaid XRD pattern of various PP fiber

Table 4.1 Proportion of iPP crystals in solution mixed 1 wt% silica/PP monofilament fibers (sonication and autoclave treatment).

Samples	k_{a1}	k_{a2}	k_{a3}	k_b
iPP-free-fall	0.445	0.306	0.249	-
iPP- drawn fiber	0.447	0.329	0.224	-
1%SiO$_2$/PP free-fall (sonication)	0.428	0.346	0.226	-
1%SiO$_2$/PP-Fiber-(sonication)	0.378	0.384	0.239	-
1%SiO$_2$/PP-free-fall-(autoclave)	0.342	0.277	0.206	0.175
1%SiO$_2$/PP-Fiber-(autoclave)	0.399	0.381	0.220	-

4.5 TGA analysis

4.5.1 TGA analysis of composite fibers spun from melt-mixed masterbatch

The TGA was performed to evaluate thermal stability of the fibers as well as particle-matrix interaction. Fig. 4.11 shows TGA thermograms of neat fiber and silica filled composite fibers from melt-mixed masterbatches. The onset temperatures of degradation are given in Table 4.2. The neat fiber starts to decompose at 416 °C. When compared to the neat fiber, the hydrophobic silica filled fibers begin to decompose at relatively higher temperatures of ca. 430 °C and, in the similar manner, their degradation temperatures recorded at 50 % residual weight are found above the temperature of 455 °C. In this scenario, the reason for an additional increase in onset temperature is that extra energy is required to break down adhesion force at polymer-silica interface. Therefore, the interfacial interaction plays an important role in degradation of polymer nanocomposites. In case of good interfacial interaction, particles are capable of restricting the movement of a polymer chain, making the scission of a polymer chain harder at lower temperature. As a consequence, the degradation temperature of the composites shifts to higher temperature (Yang and Nelson, 2006). In contrast, the 1 wt% hydrophilic silica (A200) filled fiber exhibits a

marginal increase in the decomposition temperature compared to neat fiber as a result of poorer hydrophilic particle-hydrophobic matrix interaction. These results provide indicative information on the relationship between interfacial interaction and degradation temperature. Above 0.5 wt% hydrophobic silica content, there is insignificant difference in degradation temperature, indicating further silica loading plays no part in increasing the on-set temperature of degradation. As seen in SEM images, micro-sized particles are observed in fibers with melt-mixed silica/PP composite fiber. Micro-sized fillers are prone to exhibit poor adhesion to polymer matrix due to their relatively small surface area. As a result, the effect of their presence on degradation temperature is minuscule.

Table 4.2 The degradation temperatures of composite fibers

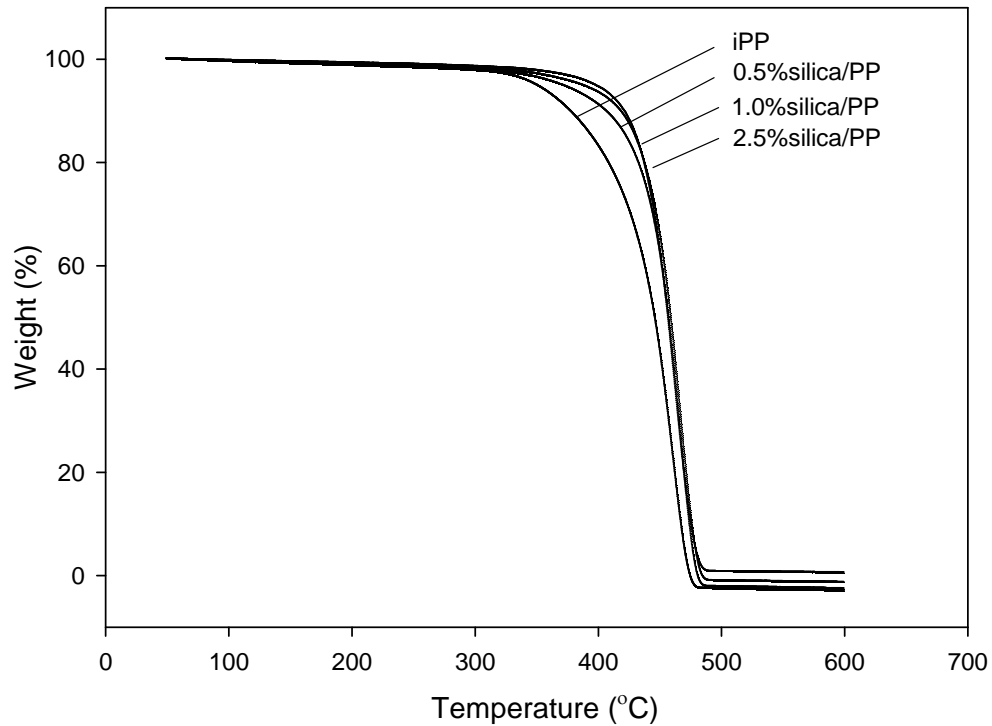| SiO_2 (wt%)	On-set Temp. (°C)	Temp. at 50% weight loss (°C)
0	416.20	446.33
0.5 (R974)	436.94	457.33
1.0 (R974)	438.53	459.33
2.5 (R974)	435.15	457.00
1.0 (A200)	417.53	459.33

Figure 4.11 TGA thermograms of neat fiber and silica filled fibers spun from

melt-mixed masterbatch

4.5.2 TGA analysis of nanocomposite fibers spun from solution-mixed resins

Figure 4.12 shows TGA thermograms of PP-toluene, sonicated 1wt% silica/ PP and autoclaved 1 wt% silica/PP monofilament fibers. In similar manner to neat PP fiber shown in Fig. 4.11, PP-toluene fiber exhibits lowest heat stability. An incorporation of silica nanoparticles results in an increase in thermal stability of nanocomposite fibers. In comparison, the results illustrate that the thermal stability is not affected by methods of dispersion (sonication or autoclave). However, solution mixed silica/PP nanocomposite fiber and melt-mixed silica/PP composite fiber behave indifferently in terms of thermal degradation pattern. This indicates that silica particle size (neither nanosize nor microsize) has no effect on thermal stability of polypropylene.
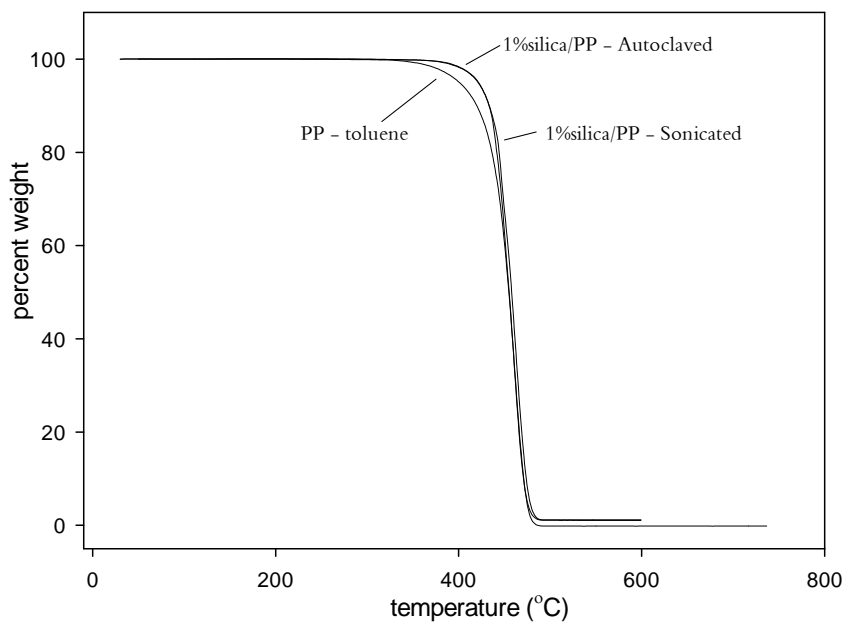
Figure 4.12 TGA thermograms of nanocomposite fibers from toluene solubilized PP resin

(PP-toluene, control) and sonicated silica/PP and autoclaved silica/PP resins

Table 4.3 The degradation temperatures of nanocomposite fibers:

SiO$_2$ (wt%)	On-set Temp. (°C)	Temp. at 50% weight loss (°C)
0 (toluene)	416.20	455.00
1.0 (sonication)	438.25	458.00
1.0 (autoclave)	437.11	455.33

4.6 Differential scanning calorimetry (DSC) analysis

4.6.1 DSC analysis of composite fibers from melt-mixed masterbatch

DSC curves of composite fibers from melt-mixed masterbatch are plotted as shown in Fig. 4.13 – Fig. 4.14. The crystallization temperatures (Tc) are recorded. Tc values of neat PP fibers appear at 113.59 °C, 113.39 °C, and 116.09 °C for fibers with spinning speeds of 300, 500, and 1100 m/min, respectively.   An increase in Tc values

with an increase in spinning speed is related to an increase in PP crystalline orientation along fiber axis which is induced by spinning speed. For the composite fibers, their Tc values are found higher than that of neat PP fiber. For example at spinning speed of 300, 500, and 1100 m/min, PP fibers filled with hydrophobic silica loadings of 1.0 wt% have Tc values of 115.79 °C , 116.99 °C , and 117.70 °C, respectively, indicating that the crystallization of PP occurred more rapidly when compared to neat fiber in accompany with release of latent heat. As the crystallization behavior of infused silica fiber is found to be affected by the presence of silica dispersion, the result indicates that silica particles play a nucleating role in inducing the faster crystallization process (Bikiaris et al., 2006; Garcia et al., 2004). From the figure, hydrophobic silica tends to induce a slightly faster crystallization process of PP than hydrophilic silica counterpart. It can be said that the interaction of hydrophobic silica with PP matrix is capable of more than what hydrophilic silica is. This finding leads to conclusion that apart from the speed of spinning, change in degree of molecular orientation could arise from interactions between the filler and fiber polymer matrix.
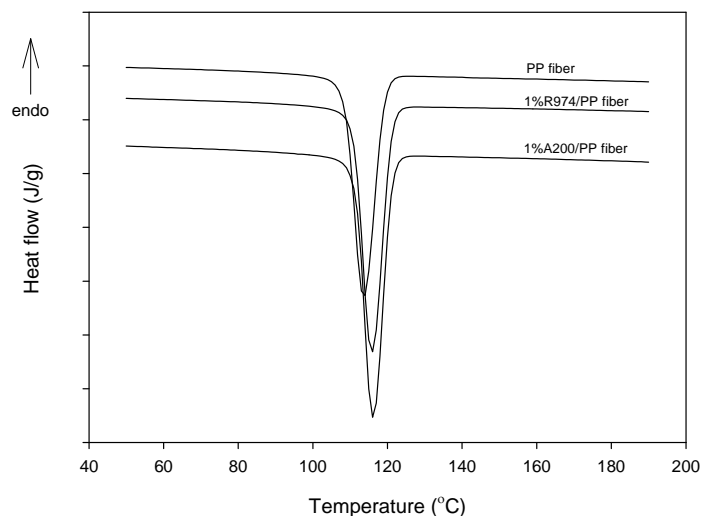

Figure 4.13 DSC cooling curve for neat PP fiber, 1 wt% A200/PP fiber and 1 wt% R974/PP fiber (spinning speed of 300 m/min)
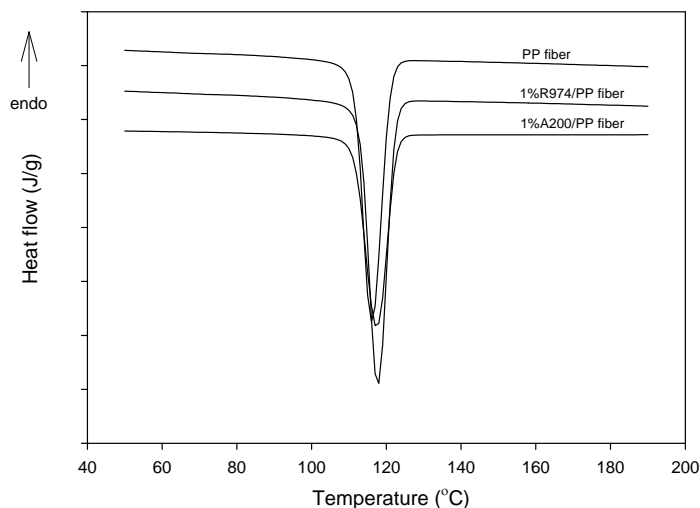
Figure 4.14 DSC cooling curve for neat PP fiber, 1 wt%A200/PP fiber and 1wt%R974/PP
fiber (spinning speed of 1100 m/min)

4.6.2 DSC analysis of nanocomposite fibers from solution-mixed resins

DSC measurement was performed using DSC 200 F3 from NETZSCH. A
sample was heated from 30 to 200 °C with a heating rate of 10 °C/min and kept for 5 min
to eliminate the thermal history. Then, the sample was cooled down to 30 °C at a cooling
rate of 10 °C/min under nitrogen gas at constant flow rate of 20 ml/min. From heating
scan the on-set temperature, the melting temperature (Tm) and heat of fusion (ΔHf) of
the fibers were measured. The crystallinity of the samples was calculated by using ΔHf
for 100% crystalline iPP of ΔHf = 170 J/g (Rottstegge et al, 2007). From cooling scan,
the crystallization point (Tc) was measured. DSC curves of the nanocomposite fibers are
shown in Fig. 4.14 – Fig. 4.15 and their DSC data shown in Table 4.4. Tc values of neat
PP fiber (free fall), sonicated1 wt% silica/PP fiber (free-fall), and autoclaved 1 wt%
silica/PP fiber (free-fall)   appear at 113.5 °C, 115.1 °C and 118.3 °C, respectively. Neat
PP has Tc value of 113.5 °C which is a typical Tc value for iPP. An increase in Tc value
of PP above 113.5 °C can be found only when loading with a nucleating agent such as
the case of nanocomposite. It is desirable to achieve an increase of Tc value of PP due

to its reflection of the fast rate of crystallization. Therefore, from these results, it can be said that nanocomposite fibers were successfully prepared by solution mixing method. As found, autoclaved 1 wt% silica/PP fiber exhibits the highest crystallization rate followed by sonicated 1 wt% silica/PP fiber (free-fall). The finding results illustrate that when the state of nanoscale dispersion was achieved iPP exhibited an increase in solidification performance. An increase in solidification rate was accompanied with a decrease in the crystalline size as revealed by SEM analysis. As a consequence of crystalline size reduction, the properties of the nanocomposite fiber including boundary crack and shrinkage are expected to be altered. Results and discussion concerning these aspects are presented in later sections.

Table 4.4 DSC data of sonicated / autoclaved silica/PP nanocomposite fibers

| Fiber	Melting temp (onset)	Melting Temp. (peak) (°C)	Heat of Fusion (J/mg)	% Crystallinity	Crystallization Temp. (°C)
Neat PP (free-fall)	159.0	167.5	72.27	42.51	113.1
PP-toluene (free-fall)	160.9	167.0	71.53	42.08	113.5
Sonicated 0.25%Silica/PP (free-fall)	159.4	167.6	78.14	45.96	115.1
Sonicated 0.50%Silica/PP (free-fall)	159.2	167.3	77.26	45.45	114.9
Sonicated 0.75%Silica/PP (free-fall)	159.3	166.7	69.07	40.63	115.0
Sonicated 1.0%Silica/PP (free-fall)	160.0	167.9	66.81	39.30	115.1
Autoclaved 1.0%Silica/PP (free-fall)	158.5	169.7	72.33	42.55	118.3
Neat PP (drawn)	155.5	165.1	75.69	44.52	114.6
PP-toluene (drawn)	155.6	165.6	71.92	42.31	115.8
0.25%SilicaPP Fiber	156.0	166.7	77.53	45.61	117.5
0.50%SilicaPP Fiber	157.0	166.5	75.91	44.65	117.4
0.75%SilicaPP Fiber	156.2	165.5	69.88	41.11	117.6
1.0%SilicaPP Fiber	155.9	166.7	66.75	39.26	117.6
1.0%SilicaPP Fiber (autoclave)	155.0	166.2	68.37	40.22	118.4
1.0%SilicaPP Free Fall Heat Rate 20°C/min	159.3	167.6	69.35	40.79	110.8
1.0%SilicaPP Free Fall Heat Rate 20°C/min(Autoclave)	156.3	166.8	75.82	44.60	114.0
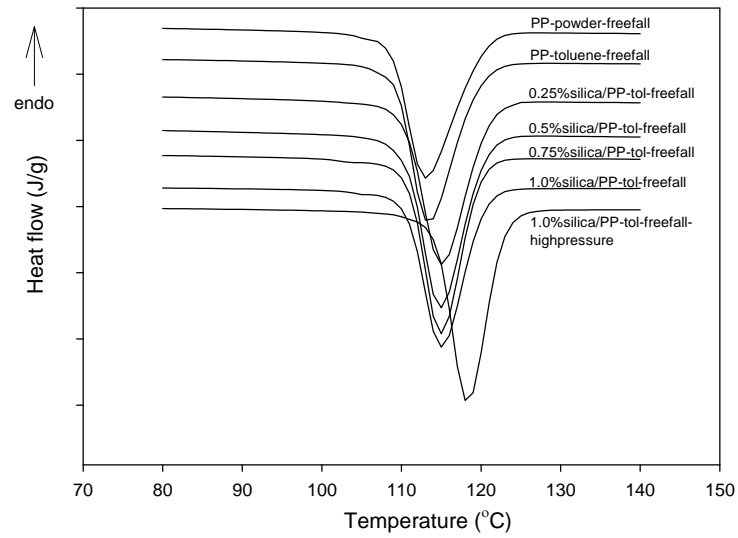
Figure 4.15 DSC cooling curve for neat PP free-fall fiber, toluene treated PP free-fall

fiber, 0.25 to 1.0 wt% silica/PP free-fall fiber (sonication) and

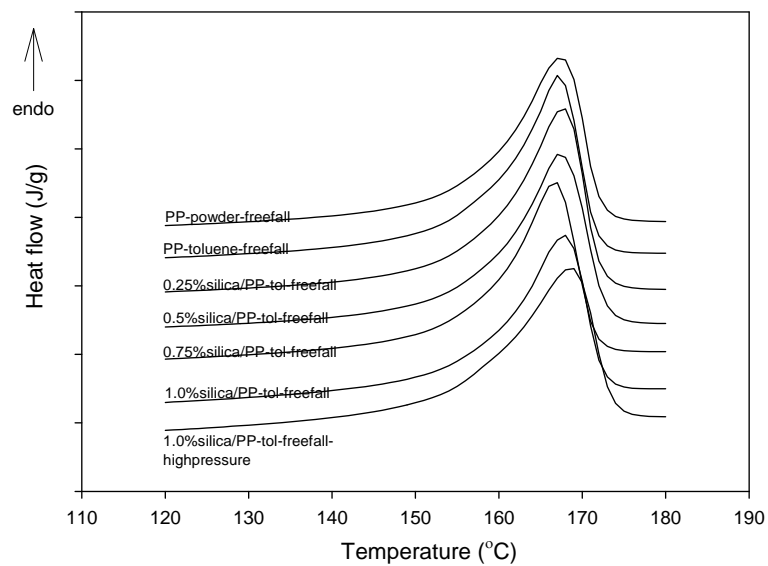1.0 wt% silica/PP free-fall fiber (autoclave)

Figure 4.16 DSC heating curve for neat PP free-fall fiber, toluene treated PP free-fall

fiber, 0.25 to 1.0 wt% silica/PP free-fall fiber (sonication) and

1.0 wt% silica/PP free-fall fiber (autoclave)

4.6.3 Non-isothermal crystallization study of solution mixed silica/PP fibers

Non-isothermal crystallization studies was carried out in order to imitate the crystallization of real processing (Chatterjee and Deopura, 2003; Li et al., 2003; Bhattacharyya et al., 2003). The sample was heated from 30 to 200 °C with a heating rate of 10 °C/min and held at that temperature for 5 min to eliminate the thermal history and then cooled down to 25 °C at cooling rate 5, 10, 15, 20 °C/min. The exothermal curve of heat flow, as a function of temperature, was recorded to analyze the non-isothermal crystallization process. After that, sample was heated from 25 °C to 200 °C at heating rate 10 °C/min to collect the melting point and heat of fusion in second heating scan, then also kept for 5 min. Sample was cooled down to 30 °C at a cooling rate of 10 °C/min. The second crystallization temperature was collected.

Figure 4.18 shows subsequent reheating DSC curves of free-fall PP fiber, sonicated 1 wt% silica/PP free-fall and autoclaved 1 wt% silica/PP free-fall fibers. Following an increasing cooling rate, subsequent melting peak becomes narrow peak, implying the reduction of lamellar thickness of iPP. In case of neat free-fall fiber with the high cooling rate (20 °C/min), there is a broad peak on the right side of the subsequent melting peak which is attributed to the re-crystallization of originally formed imperfect crystals during the fast cooling process. As for 1 wt% silica/PP free fall shown in Figure 4.18 b and c, melting peaks of recrystallized PP are narrow with irrespective of the cooling rates. These hint that no large lamellar crystal was formed in case of 1 wt% silica/PP free-fall fiber. The narrow peak with no broad signifies that silica/PP free-fall nanocomposite exhibits relatively more uniform crystallization than neat PP due to the effect of heterogeneous nucleation of nanosized silica. The crystallinity of iPP is calculated from the melting curve as shown in Table 4.4.

Table 4.5 The parameters determined from the DSC exothermal curve

	Φ (°C/min)	To(°C)	Tp (°C)	Te (°C)
PP-toluene	5	121.67	116.84	113.25
	10	117.87	112.87	108.93
	15	115.96	110.68	105.42
	20	114.45	109.00	102.59
Sonicated 1%SiO2/PP	5	123.12	119.02	116.06
	10	120.04	115.09	111.01
	15	118.19	112.81	107.33
	20	116.64	110.89	104.86
Autoclaved 1%SiO2/PP	5	125.80	121.85	118.90
	10	122.83	118.18	114.17
	15	120.70	115.71	111.05
	20	119.29	113.74	107.79

Φ = cooling rate (°C/min), To = on set of cooling curve, Tp = crystallization

temperature, Te = end point of cooling curve
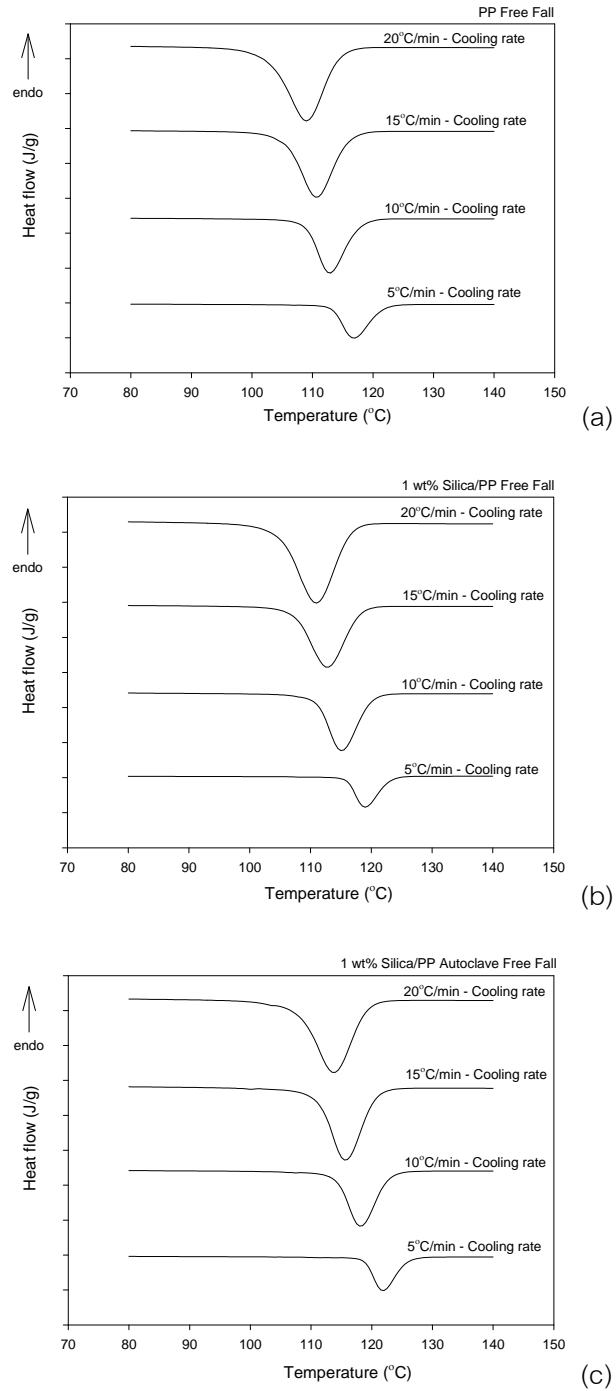
Figure 4.17 DSC cooling curve of non-isothermal crystallization at difference cooling rate; 5°C/min, 10°C/min, 15°C/min and 20°C/min, of PP free-fall fiber, 1 wt% silica/PP free-fall fiber-prepared by sonication and 1 wt% silica/PP free-fall fiber-prepared by autoclave
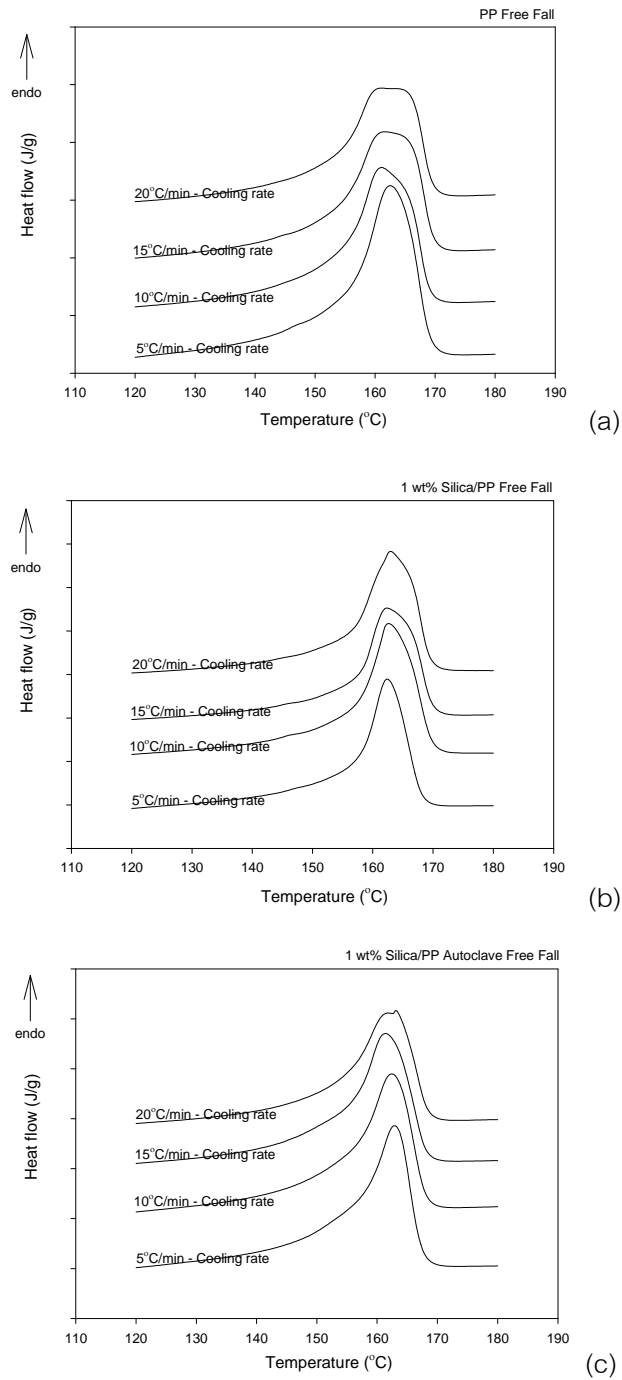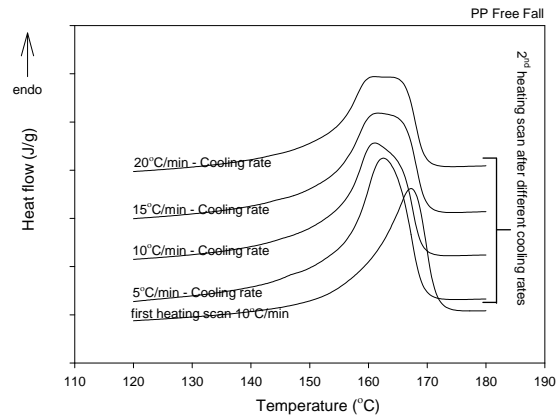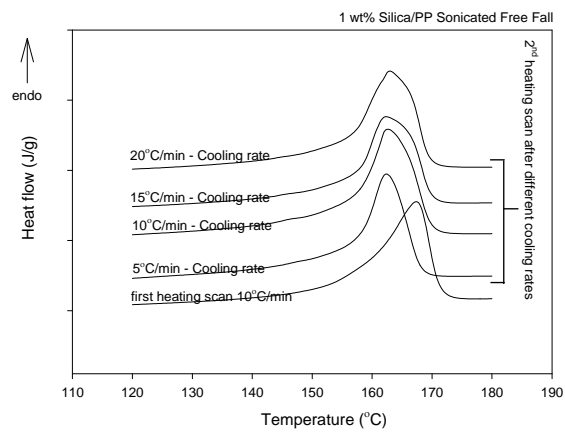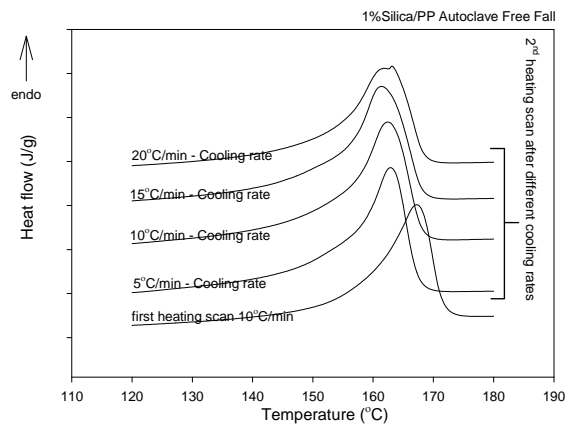
Figure 4.18 DSC heating curve of subsequent reheating (heating rate 10°C/min) after difference cooling rate; 5, 10, 15 and 20°C/min, of PP free-fall fiber, 1 wt% silica/PP free-fall fiber-prepared by sonication and 1 wt% silica/PP free-fall fiber-prepared by autoclave

Figure 4.19 Compare DSC heating curve of first and second scanning after difference

cooling rate; 5°C/min, 10°C/min, 15°C/min and 20°C/min of PP free-fall fiber, 1 wt%

silica/PP free-fall fiber-prepared by sonication and 1 wt% silica/PP free-fall fiber-

prepared by autoclave

4.7 A polarization microscope study of melt-mixed silica/PP composite

The spherulite crystal sizes of melt-mixed silica/PP composite were observed by polarized microscopy (Olymplus® SZ40) equipped with a hot stage. The polarized images of PP and silica/PP composites are shown in Fig. 4.20. Typically, sizes of neat PP spherulite are around 80-100 micrometers which are quite large. The large spherulite as revealed by SEM images is responsible for the problem of boundary crack of PP material. Therefore, the crystal size reduction is required by the addition of nucleating agent or by the application of shear stress. In this study, silica was loaded. The results in Fig. 4.20 show that the spherulite crystal sizes of 0.5, 1.0 and 2.5 wt.% silica/PP composites are found in a range between 30 and 40 micrometers which are relatively smaller than neat PP. In association with the size reduction, the number of spherulite crystals increases with an increase in the amount of silica content in PP. As seen, the masterbatch containing the highest amount of silica loading (5.6 wt.%) has the highest number of spherulite crystals compared with the others.
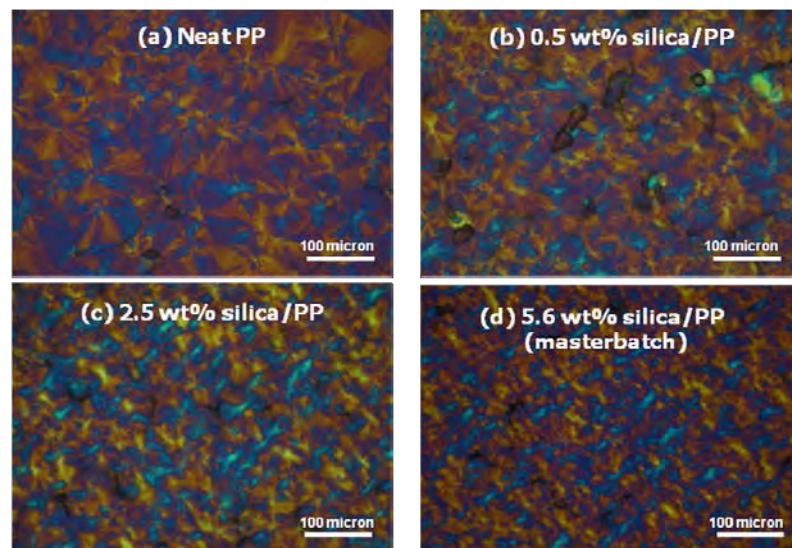

Figure 4.20 Polarized images of spherulite crystals in (a) neat PP, (b) 0.5%silica/PP
(c) 2.5 wt.% silica/PP (d) 5.6 wt.% silica/PP nanocomposite (masterbatch)

In case of solution mixed method, spherulite growth information was revealed earlier in SEM analysis section. In this section, the initial point of crystal growth was observed by hot stage analysis. Images of crystals are photographed and illustrated in Table 4.6. The initial point of autoclaved 1 wt% silica/PP was recorded at around 128°C which is higher than those of sonicated 1 wt% silica/PP (125°C) and neat PP (120°C). The highest initial point suggests that crystallization takes place; the higher the initial point the faster the crystallization capability. The faster initial point of crystal growth of silica/PP nanocomposite implies that nucleation process of the composite underwent faster. In addition, crystal sizes of nanocomposite are found smaller than those of neat PP and toluene PP. Therefore, the initial point data provide solid evidence to conclude that the addition of silica particles leads to an increase in crystallization rate of PP due to its heterogeneous nucleation effect (Bhattacharyya et al., 2003; Wang et al., 2005). The schematic diagram representing the nucleation effect of silica is shown in Fig. 4.21.
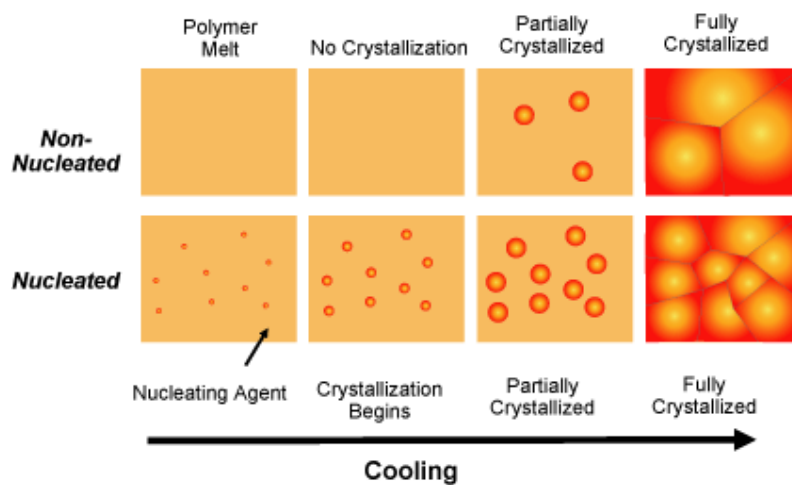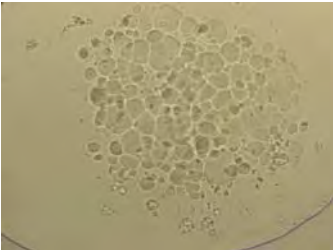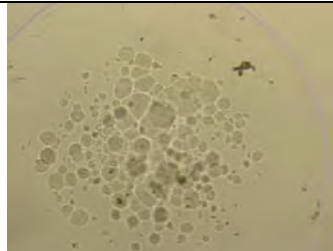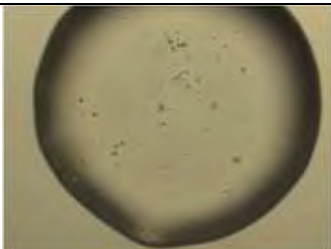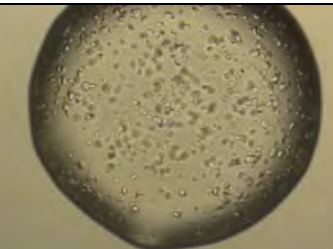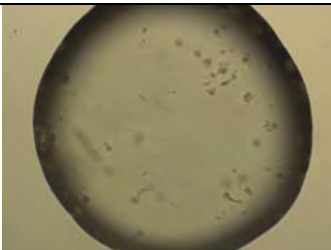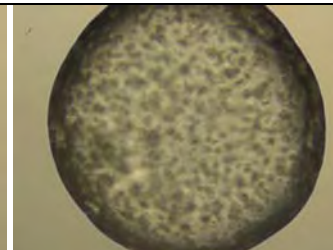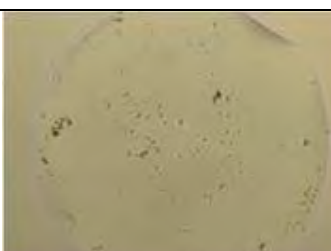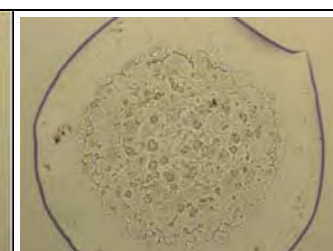

Figure 4.21 The scheme representing nucleation effect of silica particles

(from http://www.specialchem4polymers.com/tc/clarifiers/index.aspx?id=principle)

Table 4.6 Initial point of spherulite crystals for solution mixed silica/PP

	Initial point (°C)		
PP	120	120°C	110°C
PP – toluene	120	120°C	110°C
0.5% silica/PP – sonicated	120	120°C	110°C
1.0% silica/PP - sonicated	125	125°C	110°C
1.0% silica/PP – autoclave	128	128°C	120°C

4.8 Fiber molecular orientation by sonic modulus technique

4.8.1 Composite fibers from melt-mixed masterbatches

Sonic modulus technique was used to determine molecular orientation along fiber axis. The transit time of pulse sound was employed to calculate the sonic modulus. The results of sonic modulus values are presented in Fig. 4.22. The sonic modulus value increases with an increase in spinning speed, indicating polymer orientation along fiber axis due to an increase in drawing force. When considering the spun fibers taken at 1100 m/min, it is observed that sonic modulus of neat PP fiber is slightly more than that of composite fibers. The results indicate that the relatively decreased polymer chain orientation found in case of composite fibers is likely due to the molecular orientation interference caused by the presence of silica dispersion. Therefore, the addition of silica particle into PP fiber is likely to affect the fiber's mechanical properties, particularly the fiber elongation. (Joshi et al., 2004)
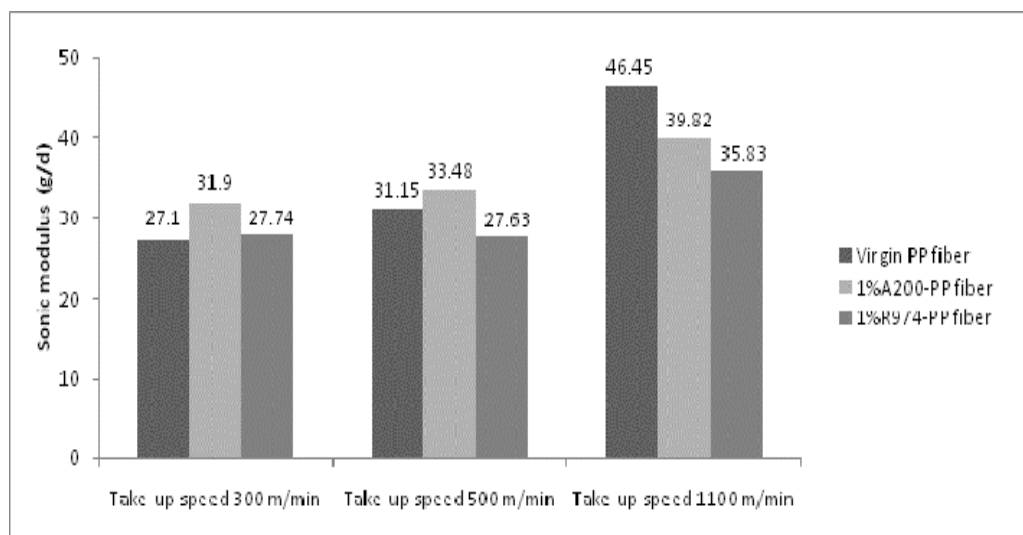

Figure 4.22 Sonic modulus of neat PP fiber, 1 wt% hydrophilic silica/PP composite fiber

and 1 wt% hydrophobic silica/PP composite fiber drawn at various spinning speeds

4.8.2 Nanocomposite monofilaments

To measurement polymer molecule orientation along the fiber, sonic modulus was employed. Results are shown in Table 4.7. The sonic modulus value of neat PP monofilament is 30.52 which is similar to that of neat PP fiber spun using high take-up speed. Control PP fiber spun from PP powder (obtained toluene route) possesses sonic modulus value of 46.76 which is higher than neat PP. For nanocomposite fibers, sonic modulus values exhibit no trend at all. It is difficult to explain the effect of silica nanoparticles addition on polymer orientation. The results shown that 0.75, 1 wt% silica/PP fiber, sonic modulus tended to lower than PP-toluene (control). The molecular orientation was disturbed in case of high silica content.

Table 4.7 Sonic modulus of silica/PP nanocomposite fibers form solution mixed resins

Fiber	Sonic Modulus (g/denier)
Neat PP	30.52
PP-toluene	46.76
Sonicated 0.25%Silica/PP	55.36
Sonicated 0.5%Silica/PP	55.67
Sonicated 0.75%Silica/PP	26.52
Sonicated 1.0%Silica/PP	32.93
Autoclaved 1.0%Silica/PP	36.53

4.9 Properties of composite fibers

4.9.1 Properties of composite fibers spun from masterbatches

The properties of the composite fibers were measured in terms of tensile strength, % elongation at break and shrinkage. The results are presented in Table 4.8. For tensile strength and percent elongation at break, the results are graphically illustrated in Fig. 4.23 and Fig. 4.24. As found, the tensile strength values of composite fibers containing 0, 0.5, 1.0 and 2.5 wt% silica are about 2.96, 2.97, 2.99 and 3.03 gf/den, respectively. The results show that the effect of silica addition neither enhances

nor impairs the tensile strength of composite fiber. Due to its very low aspect ratio as similar as titanium dioxide, silicon dioxide filler has insignificant effect on the resultant tensile strength. On the other hand, the % elongation values are 12.18, 14.65, 15.62 and 19.96 which increase with an increase in silica loading. An increase in percent elongation indicates that the polymer chain orientation in case of composite fibers during spinning was likely to be interfered by the presence of silica particles. As a consequence, the composite fiber is further elongated when applying shear stress. In addition to imperfect polymer orientation, fiber thermal stability is also likely to be affected. As seen in Table 4.8, percent hot air shrinkage tends to increase with an increase in silica loading, further confirming the effect of silica particles on the properties of composite fibers.

Table 4.8 Properties of composite fibers prepared from melt-mixed masterbatches

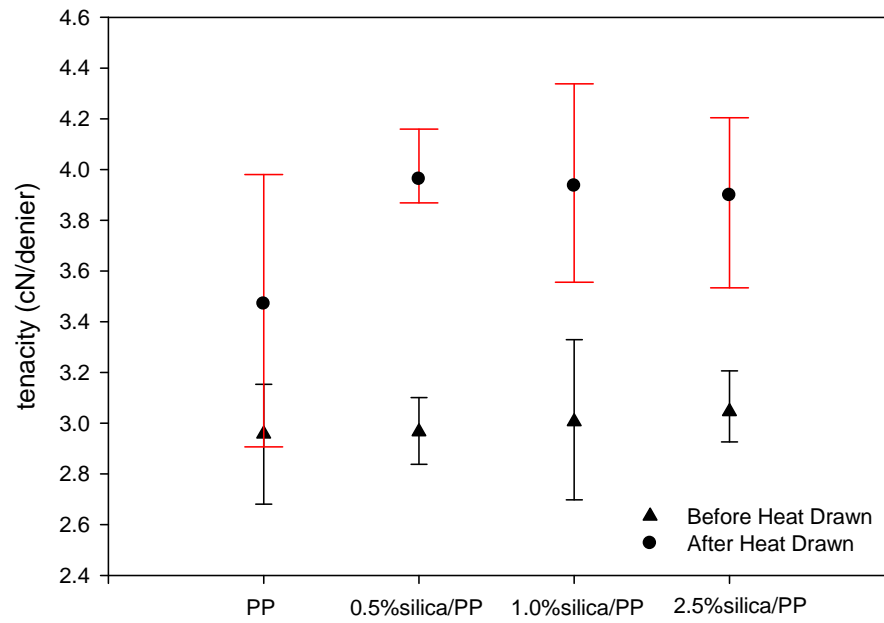| Hydrophobic SiO_2 (wt%)	Denier	Tensile strength (gf/den)	%E	Hot air shrinkage (%)	Ash (%)
0	96.9	2.96	12.18	3.31	0.017
0.5	96.6	2.97	14.65	3.32	0.517
1.0	97.5	2.99	15.52	3.47	0.969
2.5	97.3	3.03	19.96	3.66	2.221

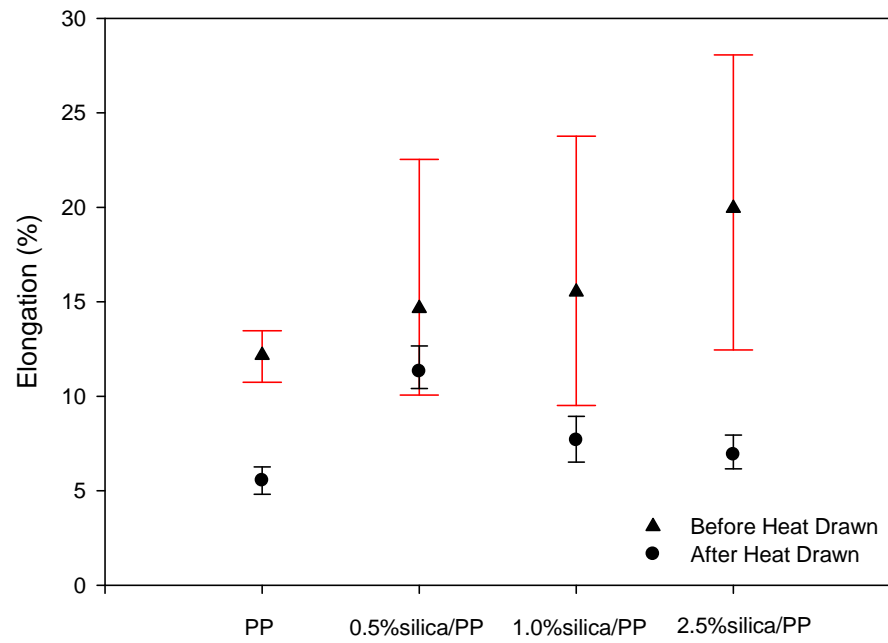Figure 4.23 Tensile strength of composite fibers containing 0.5 – 2.5 wt% silica

Figure 4.24 Percent elongation of composite fibers containing 0.5 – 2.5 wt% silica

4.9.2 Mechanical properties of nanocomposite fibers spun from solution-mixed resins

Tensile measurements were performed using the Instron tensile tester 5500 model with gauge length of 25 mm at a crosshead speed of 20 mm/min. Maximum force to breaking fiber (gram force) and elongation at break (%) were taken. Results are shown in Table 4.9. It is noticed that control PP fiber exhibits a sharp decrease in tensile strength when compared to neat PP fiber. This indicates that toluene combined with heat/or ultrasonication treatments severely depolymerize polypropylene chain molecule. An improvement of tensile strength could be achieved with an incorporation of silica nanoparticles. As found, the tensile strength values of nanocomposite fibers containing 0, 0.25, 0.5, 0.75 and 1.0 wt% silica are about 110.68, 85.58, 100.45, 88.70, and 107.12 MPa, respectively. The corresponding % elongation values are 932.05, 304.60, 574.22, 529.73 and 794.76, respectively. It can be said that an increase in tensile strength of nanocomposite fibers is related to the presence of silica particles, producing reinforcement effect on PP matrix. In a similar trend to composite fibers spun from melt-mixed resin, the results show that the incorporation of nanosized silica inhibits the polymer chain orientation along the fiber axis, resulting in an increase in % elongation value of the nanocomposite fibers.

Table 4.9 Tensile properties of nanocomposite fibers (draw ratio of 2)

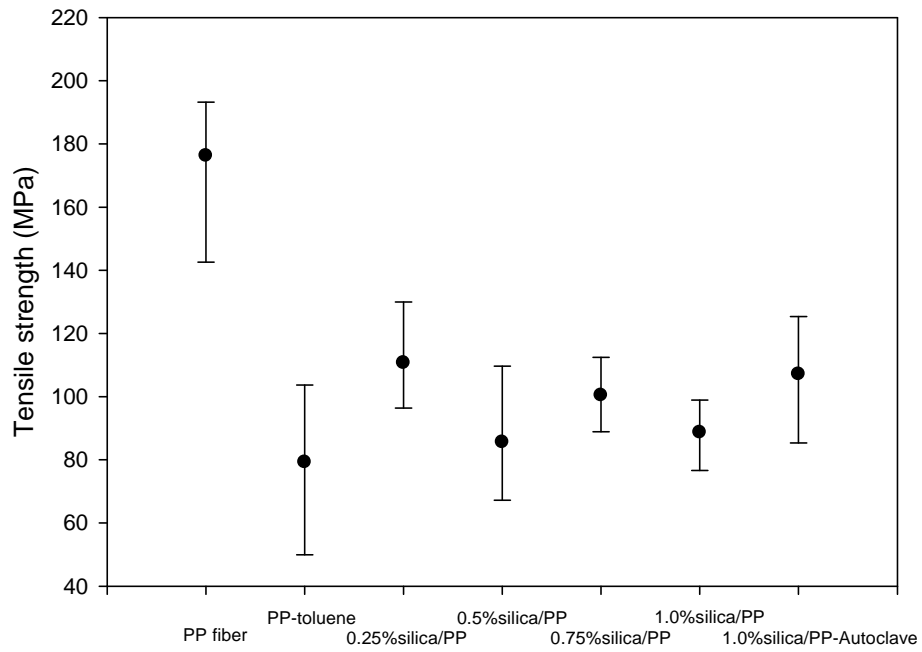|	Tensile properties	
	Tensile strength (MPa)	Elongation (%)
Neat fiber	176.27	604.07
Control PP fiber	79.25	427.64
0.25%Silica/PP Fiber (sonication)	110.68	932.05
0.50%Silica/PP Fiber (sonication)	85.58	304.60
0.75%Silica/PP Fiber (sonication)	100.45	574.22
1.0%Silica/PP Fiber (sonication)	88.70	529.73
1.0%Silica/PP Fiber (autoclave)	107.12	794.76

Figure 4.25 Tensile strength of nanocomposite fibers
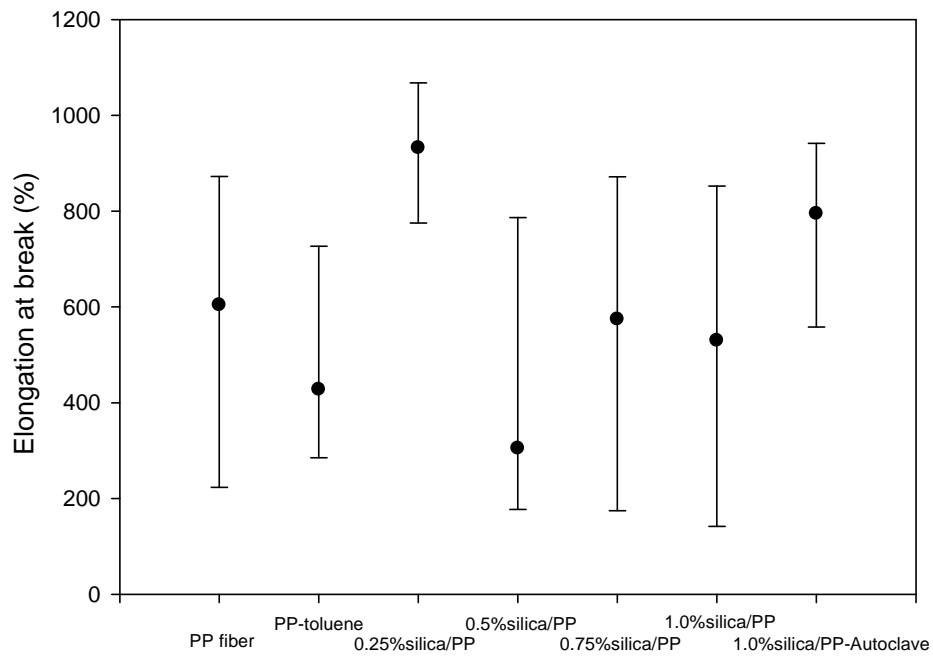
Figure 4.26 Elongation at break of nanocomposite fibers

4.10 Fiber Shrinkage Properties

4.10.1 Shrinkage properly of composite fibers from melt-mixed masterbatches

Figure 4.27 shows percent shrinkages of silica/PP composite fibers prepared from melt-mixed masterbatches. It is found that fibers tend to shrink slightly with an increase in silica loading. Namely, the percent shrinkage increases from 3.31, 3.32, 3.47 and 3.66 % for fibers containing 0, 0.5, 1.0, and 2,5 wt%, respectively. It was probable that polymer chain orientation along the fiber axis was restricted by silica particle, resulting in loosely packed polymer chains. As a consequence, the fibers with high silica loading are prone to shrink. These fibers were further heat-drawn to achieve fully drawn fibers. In the opposite direction, the fully drawn fibers exhibit improvement of shrink-resistance judged by the decrease in the percent shrinkage with an increase in silica loading. At the fully drawn state, the polymer chain reached the optimum level, resulting in densely packed polymer chains. Therefore, in this case, the silica particles played a role in reinforcing the polymer structure, leading to the dimensional stability of the fibers.
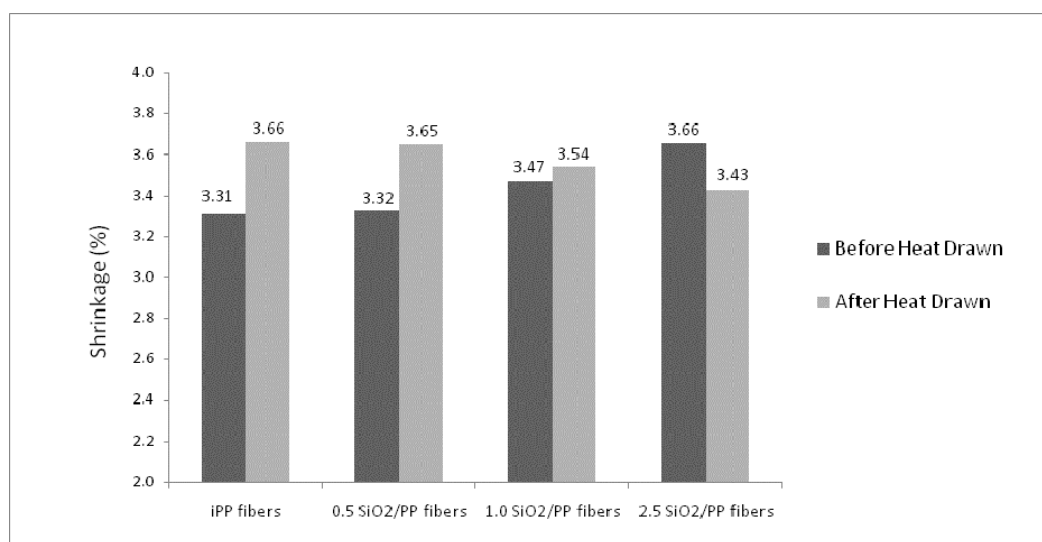

Figure 4.27 Percent shrinkages of silica/PP composite fibers spun from melt-mixed masterbatch (before and after heat drawing)

4.10.2 Fiber shrinkage of nanocomposite fibers spun from solution-mixed resins

Hot air shrinkage and hot water shrinkage of nanocomposite fibers were determined in a hot air oven at 110°C for 30 min and in boiling water for 30 min, respectively. The average percent shrinkages obtained from 5 specimens are presented in Table 4.10 It should be noted that the percent shrinkage of the nanocomposite fibers cannot be compared with those of the composite fibers spun from masterbatch due to the difference in the draw ratios. From the table, the shrinkage property of nanocomposite fibers is affected in a similar manner to the composite fibers; the higher the silica content the lower the % shrinkage. This phenomenon is obvious in the case of autoclaved 1 wt% silica/PP nanocomposite fiber where the % shrinkages are found as low as 6.80% and 4.60% for hot air shrinkage and water boiling shrinkage, respectively. It is understandable to say that autoclaved treated silica was extremely fine and evenly distributed in the polymer matrix, producing an effective reinforcement. In order to confirm the dimensional stability, the fibers were immersed into liquid nitrogen. The fiber images were observed by SEM analyze. The results shown in Fig 4.28 clearly confirm that autoclaved silica/PP nanocomposite fiber exhibits the excellent dimensional stability.

Table 4.10 Fiber shrinkages (hot air shrinkage and water boiling shrinkage)

	% shrinkage (hot air)	% Shrinkage (boiling water)
Neat Fiber	13.20	7.20
Neat fiber (toluene)	11.20	8.40
0.25%SiO$_2$/PP Fiber (sonication)	11.80	7.60
0.50%SiO$_2$/PP Fiber (sonication)	12.00	7.00
0.75%SiO$_2$/PP Fiber (sonication)	11.60	7.60
1.0%SiO$_2$/PP Fiber (sonication)	10.80	7.60
1.0%SiO$_2$/PP Fiber (autoclave)	6.80	4.60

Neat PP fiber   Neat PP fiber (toluene)

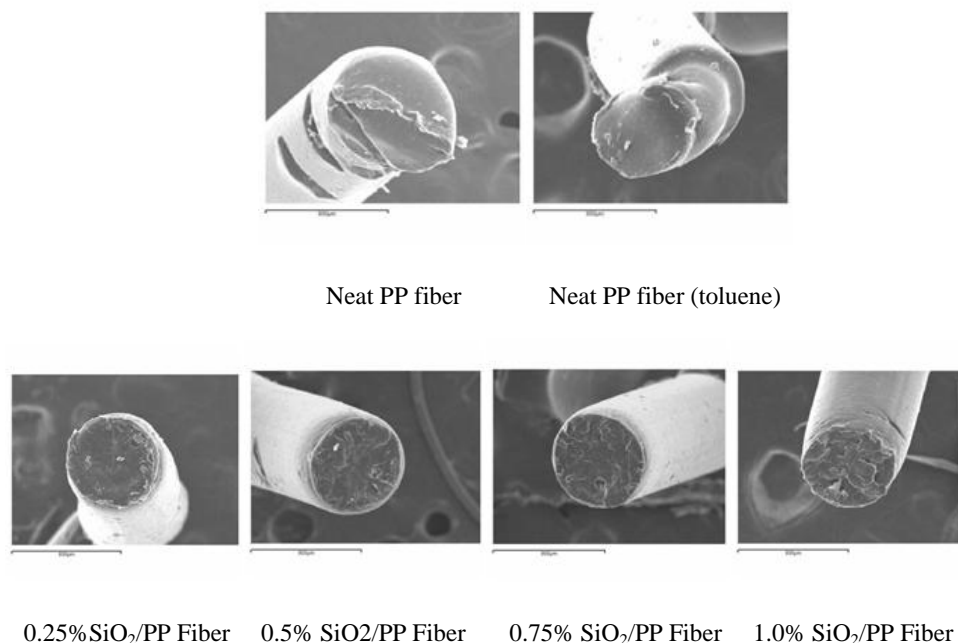0.25%SiO$_2$/PP Fiber   0.5% SiO2/PP Fiber   0.75% SiO$_2$/PP Fiber   1.0% SiO$_2$/PP Fiber

Figure 4.28 SEM images of liquid nitrogen treated fibers

(neat PP and nanocomposite fibers)

4.11 Contact angle measurement

Surface property of the nanocomposite fibers (melt mixing) and composites (solution mixing) was observed by contact angle measurement using Data Physics model PSL 250. 10 measurements were recorded and averaged. The average contact angles are presented in Table 4.11. Contact angles of neat PP, 0.5%silica/PP, 1.0%silica/PP and 2.5%silica/PP (melt mixing) are 86.99°, 85.05°, 100.38°, and 104.70°, respectively. The additional increase in surface hydrophobicity is believed to be involved with an incorporation of silica particles as well as the method of silica dispersion. While as in solution mixing, contact angles of neat PP, control PP (PP-toluene), 0.25%silica/PP (sonication), 0.5%silica/PP (sonication), 0.75%silica/PP (sonication), 1.0%silica/PP (sonication) and 1.0%silica/PP (autoclave) are 97.048°, 99.388°, 98.248°, 98.762°, 99.125° ,98.949°, 104.557°, respectively. Particularly, an increase in surface roughness was attributed to the presence of silica nanoparticles on

the fiber surface. From Fig 4.29 - 4.32 (contact angle), when compared to solution mixed silica/PP fiber, the autoclaved silica/PP fiber possesses a relatively higher contact angle which is governed by the predominant silica particles present on the fiber surface as revealed by AFM image. From these results, it is assured that autoclave mixing was the most effectiveness in disaggregating the silica agglomerate, resulting in even particle distribution. As a result, the surface and bulk properties of the resultant nanocomposite fiber were successfully modified.

Table 4.11 Contact angle of compressed sample from composite fiber by melt mixing and composites by solution mixing

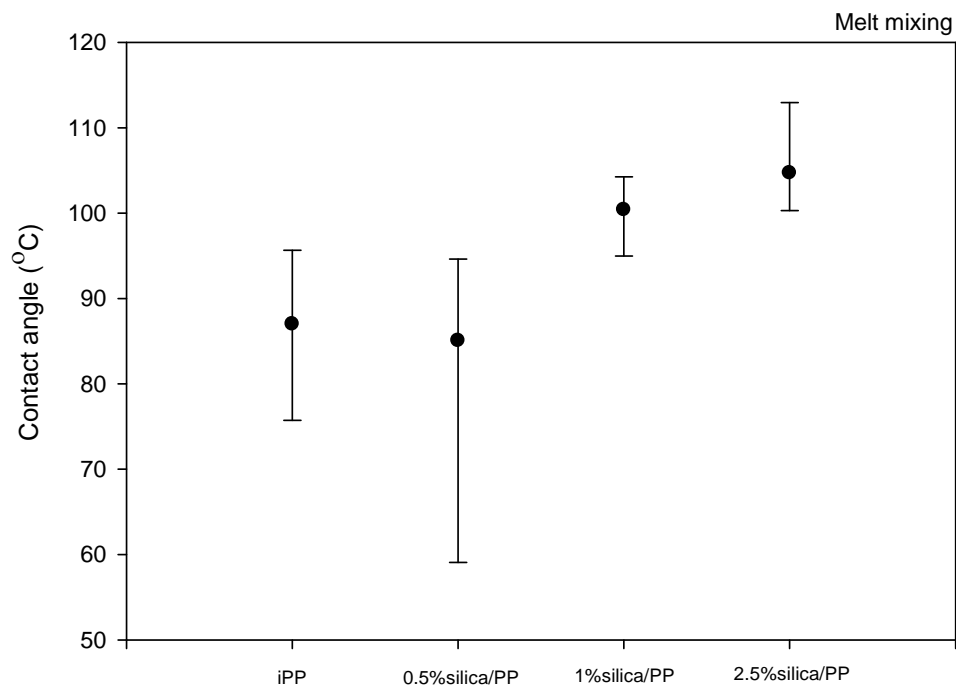|	Contact Angle (°C)
PP Fiber	86.996
0.5%silica/PP Fiber - Melt Mixing	85.058
1.0%silica/PP Fiber - Melt Mixing	100.387
2.5%silica/PP Fiber - Melt Mixing	104.700
PP Powder	97.048
PP Powder - Toluene	99.388
0.25%silica/PP Powder - Sonication	98.248
0.5%silica/PP Powder - Sonication	98.762
0.75%silica/PP Powder - Sonication	99.125
1.0%silica/PP Powder - Sonication	98.949
1.0%silica/PP Powder - Autoclave	104.557

Figure 4.29 Contact angle on compressed sample from composite fiber by melt mixing
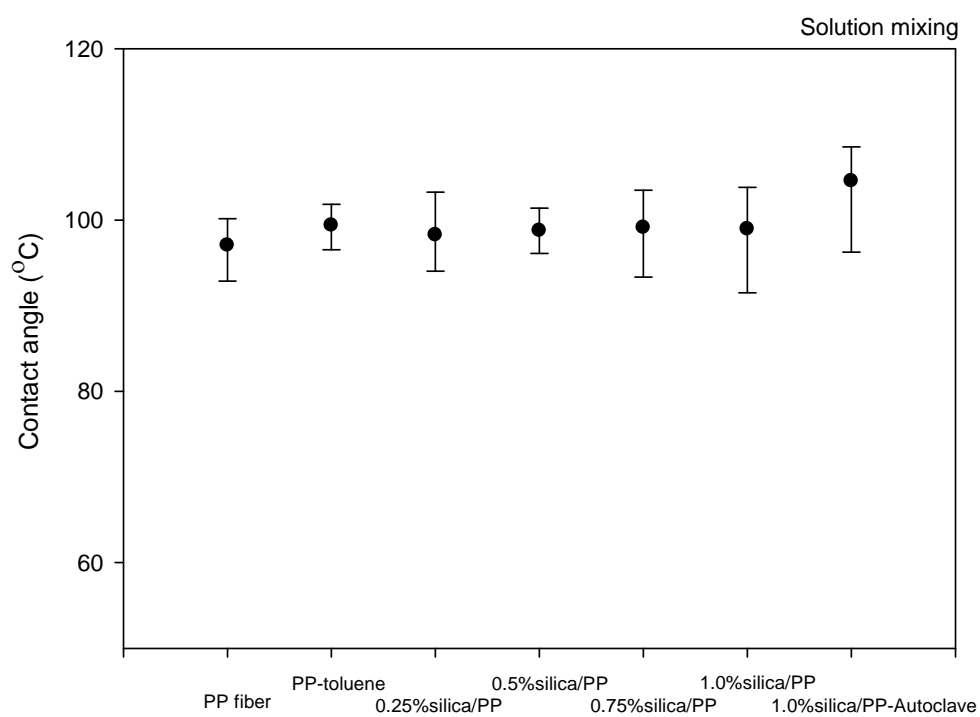

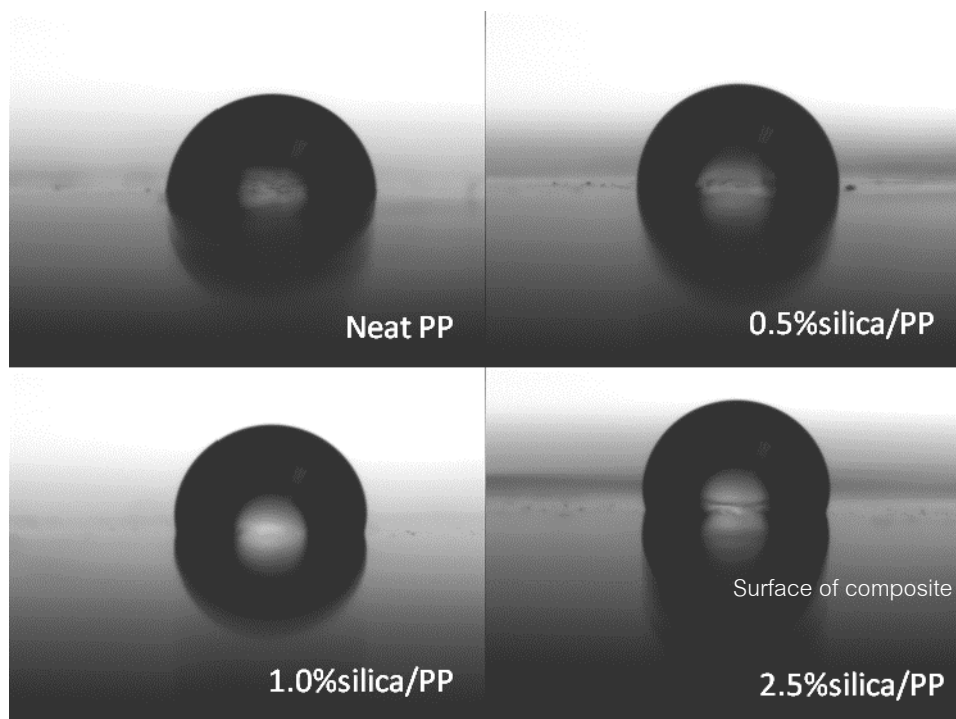Figure 4.30 Contact angle on compressed sample from composites by solution mixing

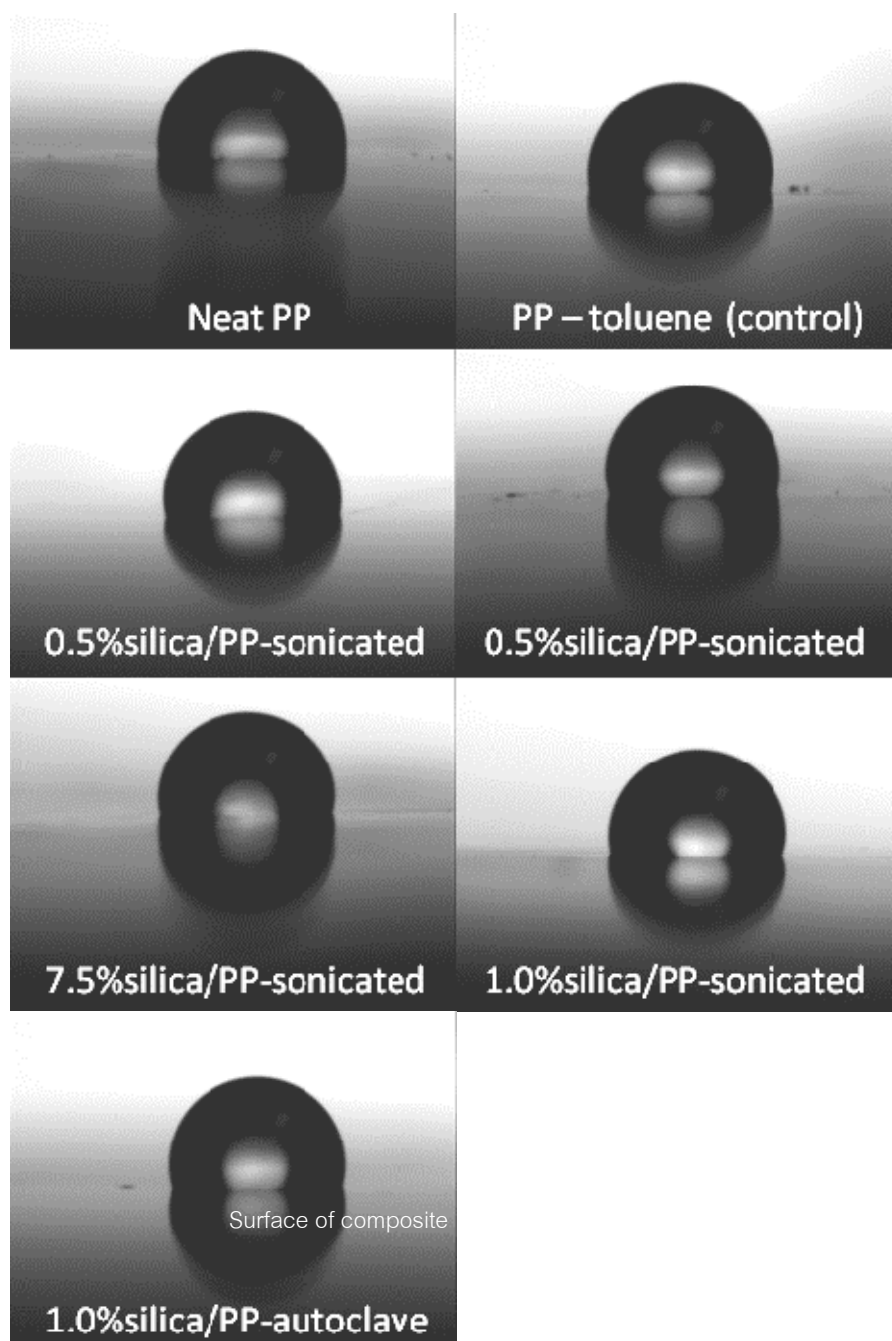Figure 4.31 Water drops on the compression samples – melt mixing

Figure 4.32 Water drops on the compression samples - autoclave

CHAPTER V

CONCLUSIONS

5.1 General conclusion

Propose of this work was to improve properties and understand the structure of polypropylene based nanocomposite fiber. Hydrophobic silica was selected as filler based on its similarity in terms of hydrophobicity. Mixing techniques were emphasized on melt mixing and solution mixing to prepare nanocomposite resins prior to fiber spinning. Melt mixing was carried out using twin screw extruder, resulting in composite masterbatch. Solution mixings were divided into two techniques, sonication (ultrasonic) and autoclave (high pressure vessels) to prepare nanocomposite resins. Toluene was used as solvent medium and temperature of 140°C was set to make polypropylene soluble.   Characterizations and properties evaluation were investigated. The results are summarized as follows:

Morphological study showed that the silica nanoparticle could be worked as a nucleating agent of polypropylene fiber, revealed by SEM images of fiber surfaces of free fall monofilament. In addition from hot stage, silica/polypropylene nanocomposite fiber exhibited the highest number of spherulites, especially in case of autoclave technique. The number of spherulites with reduced size increased with an increase in silica content. This behavior occurred only in free-fall monofilament spun from the single screw extruder, indicating that heterogeneous nucleation process was dominant. Spherulites disappeared from the surface of drawn fibers because of the combination effect between shear stress induced crystallization and heterogeneous nucleation. On the other hand, fibers spun from high spinning speeds showed no sign of spherulite on the fiber surface. This meaned that shear stress induced crystallization in spinline had more pronounced effect than heterogeneous crystallization. From DSC study, Crystallization temperature of silica filled resins increased with an increase silica content .The maximum effect was observed in case of autoclaved nanocomposite fiber as a result of well distribution of silica nanoparticles. Small spherulite size with highest

number especially in molding process generally is required to improve the properties of polypropylene products. Silica infused polypropylene fiber could exhibit improved properties particularly dimension stability as summarized later on.

The crystal structure of PP fibers was detected by XRD. In case of low speed spun fibers, neat fibers exhibited poor crystallinity since fibers were cooled quickly with partial crystallization induced by weak shear force. Crystalline form was clearly observed in case of composite fibers spun using low speed due to effect of heterogeneous nucleation. At the high speed spinning (1100 m/min), both neat PP and composite fibers showed up a strong crystalline peak, indicating that shear stress induced crystallization took a dominant role in inducing crystallization of PP. For crystalline structure of fibers from monofilament line, results support that the silica nanoparticles could be worked as a nucleating agent of polypropylene fiber. Especially in β-form could not be observed in other fibers, but β-form could found with the addition of nano-silica prepared via autoclave. However, α-form was still be major form of polypropylene fiber.

For crystallization and crystal size, numbers of spherical crystals increased with an increase in the amount of hydrophobic silica content in polypropylene. The initial point of spherical crystal of silica/polypropylene composite was around 125 °C higher than initial point of spherical crystal of neat PP around 122 °C. On the other hand, the solution mixing technique, the initial point of crystal was around 128 °C which was the highest nucleating point. It could be concluded that silica could work as a nucleating agent for PP, especially when incorporated using autoclaved method.

Thermal stability of polypropylene fiber could be improved when loaded with hydrophobic silica (compared to hydrophilic silica). The neat polypropylene started to decompose at 416 °C, while 1 %hydrophobic silica/polypropylene started to decompose at 430 °C. The degradation temperature recorded at 50% residual weight were found 446.33 °C and 459.33 °C of neat polypropylene fiber and 1 wt% hydrophobic silica/polypropylene, respectively. The nanocomposite fibers could be successfully prepared by solution mixing method, specifically autoclave technique. The

autoclave mixed 1wt% hydrophobic silica/polypropylene fiber exhibited the highest crystallization rate followed by sonication mixed 1wt% hydrophobic silica/polypropylene fiber. The crystallization temperature of neat polypropylene fiber, sonicated 1 wt% silica/polypropylene fiber and autoclaved 1 wt% silica/polypropylene fiber were 113.5, 115.1 and 118.3 °C, respectively. The subsequent reheating from difference cooling rate was found that increasing in cooling rate, reheat melting resulted in broad melting peak. This implied that polymer with poor particle distribution had a variety of crystal size and shape. In the other hand, sonicated 1 wt% silica/polypropylene and autoclaved 1% silica/polypropylene reheat melting peak shown narrow peak. It could be concluded that the addition of hydrophobic silica can improve the uniformity of fine structure of polypropylene. Note that, this effect is more important in case of molding process since cycle time to process of polypropylene could be faster when infusing with silica into polymer.

For molecular orientation, the molecular orientation along a fiber was interfered by silica particle especially in high speed and draw ratio in spinning process. Molecular orientation was interfered when hydrophobic silica was added.

For tensile properties, FDY fibers from hydrophobic silica filled polypropylene were not affected in terms of tensile strength but were affected a little bit for elongation at break of fiber. Tensile strength was 2.96 and 2.99 g/den for neat polypropylene FDY and 1 wt% silica/polypropylene FDY, respectively. Elongation at break was 12.18 and 15.52 % for neat polypropylene FDY and 1 wt% silica/polypropylene FDY, respectively. The autoclaved 1 wt% hydrophobic silica/polypropylene exhibited no change in tensile strength and elongation at break when compare with polypropylene-toluene (control sample).

For thermal stability, due to the interaction between silica nanoparticles and polymer matrix, TGA results showed that melt mixed 1wt% silica/polypropylene fiber started to degrade at higher temperature than neat PP fiber. This phenomenon was also observed in case of solution mixed nanocomposite fiber. The finding illustrated that autoclaved 1

wt% hydrophobic silica/polypropylene fiber exhibited the highest heat stability. As a result, shrinkage property of nanocomposite fibers was improved. Especially, hydrophobic silica prepared by autoclave technique had lowest values of percent shrinkage of 6.8 and 4.60 % when measured in hot air and boiling water. These properties were derived from the reinforcement effect of silica nanoparticle, leading to the dimensional stability.

Surface property of the composite fibers (melt mixing) and nanocomposites (solution mixing) was observed by contact angle measurement. The additional increase in surface hydrophobicity is believed to be involved with an incorporation of silica particles as well as the method of silica dispersion. When compared to sonication mixed silica/PP fiber, the autoclaved silica/PP fiber possessed a relatively higher contact angle which was governed by the predominant silica particles present on the fiber surface as revealed by AFM image. From these results, it was assured that autoclave mixing was the most effectiveness in disaggregating the silica agglomerate, resulting in even particle distribution. As a result, the surface and bulk properties of the resultant nanocomposite fiber were successfully modified.

5.2 Future work

Recommendations for future work are as follows

Cause of problem on cryo-technique sample preparation, this study was not investigated the dispersion of hydrophobic silica in the PP fiber. It should be studied by TEM technique.

The solution blending technique in autoclaved hydrophobic silica nanocomposite should to prepare more amount of composite enough in pilot scale spinning machine, for taking knowledge in commercialized scale.

Spinning conditions need to be consistent throughout the experiment so that the effect of hydrophobic silica prepared by autoclave on polypropylene fiber properties may be addressed. Experiments should be run to determine until the optimum processing conditions is occurred.

The effect of hydrophobic silica affecting other properties should be addressed; such as friction property of fiber, effect to texturing process etc.

Comparison on the effects of hydrophobic silica and hydrophilic silica prepared by autoclave technique may be further studied.

The studies in terms different type of polypropylene should be additional study, to find out the affect from hydrophobic silica.

REFERENCES

Amash, A., and Zugenmaier, P. Morphology and properties of isotropic and oriented samples of cellulose fibre–polypropylene composites. <u>Polymer</u>. 41, 4 (2000): 1589-1596.

Barthel, H. Surface Interactions of Dimethylsiloxy Group Modified Fumed Silica. <u>Colloids and Surfaces</u>, A. 101 (1995): 217-226.

Bhattacharyya, A.R., Sreekumar, T.V., Liu, T., Kumar, S., Ericson, L.M., Hauge, R.H., and Smaaley, R.E. Crystallization and Orientation Studies in Polypropylene/Single Wall Carbon Nanotube Composite. <u>Polymer</u>. 44 (2003): 2373-2377.

Bikiaris, D.N., Papageorgiou, G.Z., Pavlidou, E., Vouroutzis, N., Palatzoglou, P., and Karayannidis, G.P. Preparation by Melt Mixing and Characterization of Isotactic Polypropylene/SiO$_2$ Nanocomposites Containing Untreated and Surface-treated Nanoparticles. <u>Journal of Applied Polymer Science</u>. 100 (2006): 2584-2696.

Bikiaris, D.N., Papageorgiou, G.Z., Pavlidou, E., Vouroutzis, N., Palatzoglou, P., and Karayannidis, G.P. Preparation by Melt Mixing and Characterization of Isotactic Polypropylene/SiO$_2$ Nanocomposites Containing Untreated and Surface-Treated Nanoparticles. <u>Journal Applied Polymer Science</u>. 100 (2006): 2684-2696.

Bikiaris, D.N., Vassiliou, A., Pavlidou, E., and Karayannidis, G.P. Compatibilisation effect of PP-g-MA copolymer on iPP/SiO$_2$ Nanocomposites Prepared by Melt Mixing. <u>European Polymer Journal</u>. 41 (2005): 1965-1978.

Broda, J., and Wlochowicz, A. Influence of pigments on supermolecular structure of Polypropylene Fibres. <u>European Polymer Journal</u>. 36 (2000): 1283-1297.

Broda, J., Gawlowski, A., Slusarczyk, C., Wlochowicz, A., and Fabia, J. The Influence of Additives on the Structure of Polypropylene Fibres. <u>Dyes and Pigments</u>. 74 (2007): 508-511.

Bugnicourt, E. Development of Sub-micro Structured Composites Based on an Epoxy Matrix and Pyrogenic Silica. Thesis de Doctor of Philosophy. INSA of Lyon. 2005: 306p.

Caldas, V., Brown, G.R., Nohr, R.S., Macdonald, L.G., and Raboin, L.E. Enhancement of Tensile Properties of Isotactic Polypropylene Spunbonded Fabrics by a Surface-Modified Silica/Silicone Copolymer Additive. Journal Applied Polymer Science. 65 (1997): 1759-1772.

Campoy, I., Arribas, J.M., Zaporta, M.A.M., Marco, C., and Gomez, M.A. Crystallization Kinetics of Polypropylene-Polyamide Compatibilized Blends. European Polymer Journal. 31, 5 (1995): 475-478.

Chan, C.M., Wu, J., Li, J.X., and Cheung, Y.K. Polypropylene/Calcium Carbonate Nanocomposites. Polymer. 43 (2002): 2981-2992.

Chatterjee, A., and Deopura, B.L. Crystallization Behaviour of PP and Carbon Nanofibre Blends. Fibers and Polymers. 4, 3 (2003): 102-106.

Chen, M., Tian, G., Zhand, Y., Wan, C., and Zhang, Y. Effect of Silicon Dioxide on Crystallization and Melting Behaviour of Polypropylene. Journal of Applied Polymer Science. 100 (2006): 1889-1989.

Cho, J.W., and Paul, D.R. Nylon 6 Nanocomposites by Melt Compounding. Polymer. 42 (2001): 1083-1094.

Choi, S., Jeong, Y., Lee, G.W., and Cho, D.H. Thermal and Mechanical Properties of Polypropylene Filaments Reinforced with Multiwalled Carbon Nanotubes via Melt Compounding. Fiber and Polymers. 10, 4 (2009): 513-518.

Ellis, T.S., and Angelo, J.S.D. Thermal and Mechanical Properties of a Polypropylene Nanocomposite. Journal of Applied Polymer Science. 90 (2003): 1639-1647.

Ericson, J. <u>Incorporating Carbon Nanotubes into Polypropylene Fibers</u>. Master of Science Thesis. North Carolina State University. Raleigh (2003): 92p.

Esfandiari, A. The Statistical Investigation of Mechanical Properties of PP/Natural Fibers Composites. <u>Fibers and Polymers</u>. 9, 1 (2008): 48-54.

Gao, F. Clay/polymer Composites: The Story. <u>Materialstoday</u>. 7, 11 (2004): 50-55.

Garcia, M., G. van Vliet, Jain, S., Schrauwen, B.A.G., Sarkissov, A., W.E. van Zyl, and Boukamp, B. Polypropylene/SiO_2 Nanocomposites with Improved Mechanical Properties. <u>Review Advance Material Science</u>. 6 (2004): 169-175.

Gupta, V.B., and Kothari, V.K. ed. <u>Manufactured Fibre Technology</u>. London: Chapman & Hall, 1997.

Hasan, M.M., Zhou, Y., Mahfuz, H., and Jeelani, S. Effect of SiO_2 Nanoparticle on Thermal and Tensile Behavior of Nylon-6. <u>Materials Science and Engineering A</u>. 429 (2006): 181-188.

He, J.P., Li, H.M., Wang, X.Y., and Gao, Y. In Situ Preparation of Poly(ethylene terephthalate)-SiO_2 Nanocomposites. <u>European Polymer Journal</u>. 42 (2006): 1128-1134.

Huang, L., Zhan, R., and Lu, Y. Mechanical Properties and Crystallization Behavior of Polypropylene/Nano-SiO_2 Composites. <u>Journal of Reinforced Plastics and Composites</u>. Vol. 25. No. 9 (2006): 1001-1012.

Jain, S., Goossens, H., Martin van Duin, and Lemstra, P. Effect of In Situ Prepared Silica Nano-particles on Non-isothermal Crystallization of Polypropylene. <u>Polymer</u> 46 (2005): 8805-8818.

Janigova, I., and Chodak, I. Temperature Effect on Kinetics of Isothermal Crystallization of Crosslinked Filled LDPE-2. Particulate Silica with Surface Area as a Filler. <u>European Polymer Journal</u>. 31, 3 (1995): 271-274.

Jitputti, J., Pavasupree, S., Suzuki, Y., and Yoshikawa, S. Synthesis and Photocatalytic Activity for Water Splitting Reaction of Nanocrystalline Mesoporous Titania Prepared by Hydrothermal Method. Journal of Solid State Chemistry. 180 (2007): 1743-1749.

Joshi M., Shaw, M., and Butola, B.S. Studies on Composite Filaments from Nanoclay Reinforced Polypropylene. Fibers and Polymers. 5, 1 (2004): 59-67.

Joshi, M., Shaw, M., and Butola, B.S. Studies on Composite Filaments from Nanoclay Reinforced Polypropylene. Fibers and Polymers. 5, 1 (2004): 59-67.

Katz, H.S., and Milewski, J.V.. Handbook of Filler for Plastics, New York: Van Nostrand Reinhold, 1987, 467p.

Kearns, J.C., and Shambaugh, R.L. Polypropylene Fibers Reinforced with Carbon Nanotubes. Journal of Applied Polymer Science. 86 (2002): 2079-2084.

Kish, M.H., Shoushtari, S.A., and Kazemi, S. Effects of Cold-drawing and Heat-setting on the Structure and Properties of Medium Speed Spun Polypropylene Filaments. Iranian Polymer Journal. 9, 4 (2000): 239-248.

Kumar, S., Doshi, H., Srinivasarao, M., Park, J.O., and Schiraldi, D.O. Fibers from Polypropylene/Nano Carbon Fiber Composites. Polymer. 43 (2002): 1701-1703.

Kuriger, R.J., Alan, M.K., Anderson, D.P., and Jacobsen, R.L. Processing and Characterization of Aligned Vapor Grown Carbon Fiber Reinforced Polypropylene. Composites: Part A. 33 (2002): 53-62.

Li, J., Zhou, C., and Gang,W. Study on Nonisothermal Crystallization of Maleic Anhydride Grafted Polypropylene/Montmorillonite Nanocomposite. Polymer Testing. 22 (2003): 217-223.

Liu, W., Tian, X., Cui, P., Li, Y., Zheng, K., and Yang, Y. Preparation and Characterization of PET/Silica Nanocomposites. Journal of Applied Polymer Science. 91 (2004): 1229-1232.

Liu, X., and Wu, Q. PP/clay Nanocomposites Prepared by Grafting-melt Intercalation. Polymer, 42, 25. (2001): 10013-10019.

Liu, Z., Chen, K., and Yan, D. Crystallization, Morphology, and Dynamic Mechanical Properties of Poly(trimethylene terephthalate)/Clay Nanocomposites. European Polymer Journal. 39 (2003): 2359-2366.

Ma, H., Zeng, J., Realff, M.L., Kumar, S., and Schiraldi, D.A. Processing, Structure, and Properties of Fibers from Polyester/Carbon Nanofiber composites. Composites Science and Technology. 63 (2003): 1617-1628.

Mahfuz, H., Hasan, M.M., Rangari, V.K., and Jeelani, S. Reinforcement of Nylon-6 Filaments with SiO_2 Nanoparticles and Comparison of Young's Modulus with Theoretical Bounds. Macromolecular Materials and Engineering. 292 (2007): 437-444.

Moore, E.M., Ortiz, D.L., Mara, V.T., Shambaugh, R.L., and Grady, B.P. Enhancing the Strength of Polypropylene Fibers with Carbon Nanotubes. Journal of Applied Polymer Science. 93. (2004): 2926-2933.

Mukhopadhyay, S., Deopura, B.L., and Alagirusamy, R. Production and Properties of High-modulus-High-tenacity Polypropylene Filament. Journal of Industrial Textiles. 33, 4. (2004): 245-268.

Papageorgiou, G.Z., Achilias, D.S., Bikiaris, D.N., and Karayannidis, G.P. Crystallization Kinetics and Nucleation Activity of Filler in Polypropylene/surface-treated SiO_2 Nanocomposites. Thermochimica Acta. 427 (2005): 117-128.

Pavlikova, S., Thomann, R., Reichert, P., Mulhaupt, R., and Marcincin. Fiber Spinning from Poly(propylene)-Organoclay Nanocomposite. Journal of Applied Polymer Science. 89 (2003): 604-611.

Peng, Z., Kong, L.X., and Li, S.D. Thermal Properties and Morphology of a Poly(vinyl alcohol)/Silica Nanocomposite Prepared with a Self-Assembled Monolayer Technique. Journal of Applied Polymer Science. 96 (2005): 1436-1442.

Perez, C.J., Vazquez, A., and Alvarez, V.A. Isothermal Crystallization of Layered Silicate/Starch-Polycaprolactone Blend Nanocomposites. Journal of Thermal Analysis and Calorimetery. 91, 3 (2008): 749-757.

Potschke, P., Fornes, T.D., and Paul, D.R. Rheologigal Behaior of Multiwalled Carbon Nanotube/Polycarbonate Composites. Polymer. 43 (2002): 3247-3255.

Presting, H., and Konig, U. Future Nanotechnology Developments for Automotive Applications. Materials Science and Engineering C. 23 (2003): 737-741.

Qiu, W., Mai, K., and Zeng, H. Effect of Silane-Grafted Polypropylene on the Mechanical Properties and Crystallization Behavior of Talc/Polypropylene Composites. Journal of Applied Polymer Science. 77, 13 (2000): 2974-2977.

Qu, C., Yarg, H., Liang, D., Cao, W., and Fu, Q. Morphology and Properties of PET/PA-6/SiO$_2$ Ternary Composite. Journal of Applied Polymer Science. 104 (2007): 2288-2296.

Rosso, P., Ye, L., Friedrich, K., and Sprenger, S. A Toughened Epoxy Resin by Silica Nanoparticle Reinforcement. Journal of Applied Polymer Science. 100 (2006): 1849-1855.

Rothon, R. Particulate-Filled Polymer Composites. Polymer Science and Technology Series. Longman Science & Technical. 375p.

Rottstegge, J., Zhang, X., Zhou, Y., Xu, D., Han, C.C., and Wang, D. Polymer Nanocomposites Powders and Melt Spun Fibers Filled with Silica Nanoparticles. Journal Applied Polymer Science. 103 (2007): 218-227.

Sandler, J.K.W., Pegel, S., Cadek, M., Gojny, F., M. van Es, Lohmar, J., Blau, W.J., Schulte, K., Windle, A.H., and Shaffer, M.S.P. A comparative study of melt spun polyamide-12 fibres reinforced with carbon nanotubes and nanofibres. Polymer. 45 (2004): 2001-2015.

Schmidt, G., and Malwitz, M.M. Properties of Polymer-Nanoparticle Composites. Current Opinion in Colloid and Interface Science. 8 (2003): 103-108.

Sipaut, C.S., Ahmad, N., Adnan, R., Rahman, I.Ab., Bakar, M.A., Ismail, J., and Chee, C.K. Properties and Morphology of Bulk Epoxy Composite Filled with Modified Fumed Silica-Epoxy Nanocomposites. Journal of Applied Science. 7 (1) (2007): 27-34.

Sui, G., Fuqua, M.A., Ulven, C.A., and Zhong, W.H. A plant fiber reinforced polymer composite prepared by a twin-screw extruder. Bioresource Technology, 100, 3 (2009): 1246-1251.

Supahol, P., Thanomkiat, P., Junkasem, J., and Dangtungee, R. Non-isothermal Melt-crystallization and Mechanical Properties of Titanium (IV) oxide Nanoparticle-filled Isotactic Polypropylene. Polymer Testing. 26 (2007): 20-37.

Suzuki, Y., Pavasupree, S., Yoshikawa, S., and Kawahata, R. Direct Hydrothermal Processing of Long Titanate Nanofibers from Natural Rutile. Key Engineering Materials. 317-318 (2006): 243-246.

Suzuki, Y., Pavasupree, S., Yoshikawa, S., and Kawahata, R. Natural Rutile-Derived Titanate Nanofibers Prepared by Direct Hydrothermal Processing. Journal of Materials Research. 20 (2005): 1063-1070.

Tao, Y., Pan, Y., Zhang, Z., and Mai, K. Non-isothermal Crystallization, Melting Behaviour and Polymorphism of Polypropylene in β-nucleated Polypropylene/Recycled Poly(ethylene terephthalate) Blends. European Polymer Journal. 44 (2008): 1165-1174.

Thostenson, E.T., Li, C., and Chou, T.W. Nanocomposite in context. Composite Science and Technology. 65 (2005): 491-516.

Tian, X., Zhang, X., Liu, W., Zheng, J., Ruan, C., and Cui, P. Preparation and Properties of Poly(ethylene terephthalate)/Silica Nanocomposites. Journal of Macromolecular Science, Part B: Physics. 45 (2006): 507-513.

Velasco, J.I., Saja, J., and Martinez, A. Crystallization Behavior of Polypropylene filled with surface-modified talc. Journal of applied polymer science. 61 (1996): 125-132.

Vladimirov, V., Betchev, C., Vassiliou, A., Papageorgiou, G., and Bikiaris,D. Dynamic Mechanical and Morphological Studies of Isotactic Polypropylene/Fumed Silica Nanocomposites with enhanced Gas Barrier Properties. Composites Science and Technology. 66 (2006): 2935-2944.

Wang, Z., Li, G., Xie, G., and Zhang, Z. Dispersion Behaviour of TiO_2 Nanoparticles in LLDPE/LDPE/TiO_2 Nanocomposites. Macromolecular Chemistry and Physics. 206 (2005): 258-262.

Wu, C.L., Zhang, M.Q., Rong, M.Z., and Friedrich, K. Tensile Performance Improvement of Low Nanoparticles Filled-Polypropylene Composites. Composites Science and Technology. 62 (2002): 1327–1340

Wypych, G. Handbook of Fillers. New York. Plastics Design Library. (1999): 890p.

Yang, F., and Nelson, G.L. Polymer/Silica Nanocomposites Prepared Via Extrusion. Polymers for Advanced Technologies. 17 (2006): 320-326.

Yang, F., Ou, Y., and Yu, Z. Polyamide 6/silica Nanocomposites Prepared by In Situ Polymerization. Journal of Applied Polymer Science. 69 (1998): 355-361.

Yang, Y., and Gu, H. Preparation and Properties of Deep Dye Fibers from Poly(ethylene terephthalate)/SiO_2 Nanocomposites by In Situ Polymerization, Journal Applied Polymer Science. 105 (2007): 2363-2369.

Yoon, C.S., and Ji, D.S. Modification and Properties of Polypropylene Fibers Using Aluminosiloxane. <u>Fibers and Polymers</u>. 4 (2003): 210-214.

Yuan, Q., Rajan, V.G., and Misra, R.D.K. Nanoparticle Effects During Pressure-induced Crystallization of Polypropylene. <u>Materials Science and Engineering B</u>. 153 (2008): 88-95.

Zhang, X., Yang, M., Zhao, Y., Zhang, S., Dong, X., and Liu, X. Polypropylene/Montmorillonite Composites and Their Application in Hybrid Fiber Preparation by Melt-Spinning. <u>Journal of Applied Polymer Science</u>. 92 (2004): 552-558.

Zheng, H., and Wu, J. Preparation, Crystallization, and Spinnability of Poly(ethylene terephthalate/Silica Nanocomposites. <u>Journal Applied Polymer Science</u>. 103 (2007): 2564-2568.

APPENDIX

HMC Polymers
An associate of PTT & Basell

Moplen HP561R

Polypropylene Homopolymer Resin for Spunbond Fiber

Features

- High melt flow with very narrow MWD resin for high speed spin continuity of low denier fiber
- Very uniform melt flow rate and low gel
- Excellent processability and wide processing operating window
- Spinnability improved with enchanted fabric properties
- Very good gas fading resistance

Typical applications

- Spunbonded nonwoven fabric using for hygine products, medical, agriculture, geotextile, etc.

Resin properties (a)	*Moplen* HP561R	ASTM METHOD(b)
Melt flow rate (230 ℃ / 2.16 kg), dg/min	25	D1238
Density, g/cm^3	0.90	D792B
Tensile strength at yield, MPa	32	D638
Elongation at yield, %	11	D638
Flexural modulus, MPa	1240	D790A
Notched izod impact strength at 23 ℃, J/m	24	D256A
Deflection temperature, at 455 kPa, ℃	94	D648

(a) Values shown are averages and are not to be considered as specifications.

(b) ASTM test methods are the latest under Society's current procedures. All molded specimens are prepared by injection

FDA Statement

Moplen HP561R meets USF&DA requirements in the Code of Federal Regulations in 21 CFR 177.1520 for all food contact. All ingredients in *Moplen* HP561R meets the chemical registration requirements of TSCA (U.S.) and DSL (Canada).

Note: Due to the fact that different regulations in each country set different details of compliance, users of *Moplen* HP561R are recommended to undertake their own investigation of the requirements and comply with each regulation set forth, for instance, in applicable local F&DA requirements. Ultimately the users must make their own determination that their use of *Moplen* HP561R is safe, lawful and technically suitable in their intended applications.

Moplen is a trademark of Basell
HMC Polymers is certified according to ISO 9001 and 14001
Issued 10-Jul-07

The purpose of this document is only for technical support of the use of the product.

HMC Polymers Co., Ltd
20/F, Sathorn City Tower, 175 South Sathorn Road, Thungmahamek, Sathorn, Bangkok 10120, Thailand
Tel +66 2679 6388-89, 2614 3700   Fax +66 2679 6380
www.hmcpolymers.com

Product Information

▶AEROSIL® R 974

Hydrophobic Fumed Silica

AEROSIL® R 974 is a hydrophobic fumed silica aftertreated with DDS (Dimethyldichlorosilane) based on a hydrophilic fumed silica with a specific surface area of 200 m²/g

Applications and Properties

Applications

- Silicone rubber and silicone sealants
- Paints and coatings
- Negative toner
- Adhesives
- Coating polymers

Properties

- Hydrophobic component for thickening and reinforcement of RTV-1 pack silicone sealants.
- Improves shelf-life of silicone sealants.
- Water resistant, for thickening and hydrophobising of liquid systems.
- Rheology control of (complex) liquid systems.
- For use in coatings as anti-settling agent, for pigment stabilization and improvement of corrosion protection.
- Improves hydrophobicity and rheology of offset printing inks.
- Improvement and maintenance of free flow and anti-caking characteristics of powders.
- Due to large surface area improved thickening and thixotropic effect as well as transparency.

Physico-chemical Data

Properties	Unit	Typical Value
Specific surface area (BET)	m²/g	170 ± 20
Carbon content	wt.%	0.7 - 1.3
Average primary particle size	nm	12
Tapped density *(approx. value)** acc. to DIN EN ISO 787/11, Aug. 1983	g/l	approx. 50
Moisture* 2 hours at 105 °C	g/l	≤ 0.5
Ignition loss 2 hours at 1000 °C based on material dried for 2 hours at 105 °C	wt.%	≤ 2.0
pH in 4% dispersion		3.7 - 4.7
SiO₂-content based on ignited material	wt.%	≥ 99.8

* explant
The data represents typical values and not production parameters.

AEROSIL
Invented to improve®

Safety and Handling

With every sample or initial shipment of our products we will send a Material Safety Data Sheet. Of course, you can also request an MSDS or any other information regarding product safety at any time, or download it as a registered user at www.aerosil.com.

Packaging and Storage

AEROSIL® R 974 is supplied in multiple layer 10 kg bags. We recommend to store the product in closed containers under dry conditions and to protect the material from volatile substances. AEROSIL® R 974 should be used within 2 years after production.

Registration

AEROSIL® R 974					
CAS-No.	EINECS	TSCA (USA), AICS (Australia), DSL (Canada)	PICCS (Philippines), IECS (China)	ENCS (Japan)	ECL (Korea)
68 611-44-9	271-893-4	Registered	Registered	1-548/ 7-476	KE-10116

▶ **For further information please contact:**

Commercial Contact

	NAFTA	Asia (without Japan)	Japan
Evonik Degussa GmbH Business Line Aerosil Weissfrauenstrasse 9 D-60287 Frankfurt am Main, Germany Phone: +49 69/218-2532 Fax: +49 69/218-2533 E-Mail: aerosil@evonik.com http://www.aerosil.com	**Evonik Degussa Corporation** Business Line Aerosil 379 Interpace Parkway, P. O. Box 677 Parsippany, NJ 07054-0677 Phone: +1 (800) AEROSIL Phone: +1 (973) 541-8510 Fax: +1 (973) 541-8501	**Aerosil Asia Marketing Office** c/o NIPPON AEROSIL CO., LTD. P. O. Box 7015 Shinjuku Monolith 13F 3-1, Nishi-Shinjuku 2-chome Shinjuku-ku, Tokyo 163-0913 Japan Phone: +81-3-3342-1786 Fax: +81-3-3342-1761	NIPPON AEROSIL CO., LTD. Sales & Marketing Division P. O. Box 7015 Shinjuku Monolith 13F 3-1, Nishi-Shinjuku 2-chome Shinjuku-ku, Tokyo 163-0913 Japan Phone: +81-3-3342-1763 Fax: +81-3-3342-1772

Technical Contact

	NAFTA	Asia (without Japan)	Japan
Evonik Degussa GmbH Technical Service Aerosil Rodenbacher Chaussee 4 P. O. Box 1345 D-63403 Hanau-Wolfgang, Germany Phone: +49 6181/59-3936 Fax: +49 6181/59-4489	**Evonik Degussa Corporation** Technical Service Aerosil 2 Turner Place Piscataway, NJ 08855-0365 Phone: +1 (888) SILICAS Phone: +1 (732) 981-5000 Fax: +1 (732) 981-5275	**Evonik Degussa GmbH** Technical Service Aerosil Rodenbacher Chaussee 4 P. O. Box 1345 D-63403 Hanau-Wolfgang, Germany Phone: +49 6181/59-3936 Fax: +49 6181/59-4489	NIPPON AEROSIL CO., LTD. Applied Technology Service 3 Mita-cho Yokkaichi, Mie 510-0841 Japan Phone: +81-593-45-5270 Fax: +81-593-46-4657

Please visit our website www.aerosil.com to find your local contact.

AEROSIL® R 974 / Apr 08 / www.aerosil.com

AEROSIL

Product Information

▶AEROSIL® 200

Hydrophilic Fumed Silica

AEROSIL® 200 is a hydrophilic fumed silica with a specific surface area of 200 m²/g.

Applications and Properties

Applications

- Paints and coatings
- Unsaturated polyester resins, laminating resins and gel coates
- HTV- and RTV-2K-silicone rubber
- Adhesives and sealants
- Printing inks
- Cable compounds and cable gels
- Plant protection
- Food and cosmetics

Properties

- Rheology and thixotropy control of liquid systems, binders, polymers, etc.
- Used as anti-settling, thickening and anti-sagging agent.
- Reinforcement of HTV- and RTV-2K silicone rubber.
- Improvement of free flow and anticaking characteristics of powders.

Physico-chemical Data

Properties	Unit	Typical Value
Specific surface area (BET)	m²/g	200 ± 25
Average primary particle size	nm	12
Tapped density (approx. value)* acc. to DIN EN ISO 787/11, Aug. 1983	g/l	approx. 50
Moisture* 2 hours at 105 °C	wt.%	≤ 1.5
Ignition loss 2 hours at 1000 °C based on material dried for 2 hours at 105 °C	wt.%	≤ 1.0
pH in 4% dispersion		3.7 - 4.7
SiO₂ - content based on ignited material	wt.%	≥ 99.8

* ex plant
The data represents typical values and not production parameters.

AEROSIL
Invented to Improve®

Safety and Handling

With every sample or initial shipment of our products we will send a Material Safety Data Sheet. Of course, you can also request an MSDS or any other information regarding product safety at any time, or download it as a registered user at www.aerosil.com.

Packaging and Storage

AEROSIL® 200 is supplied in multiple layer 10 kg bags. We recommend to store the product in closed containers under dry conditions and to protect the material from volatile substances. AEROSIL® 200 should be used within 2 years after production.

Registration

AEROSIL® 200

CAS-No.	EINECS	TSCA (USA), AICS (Australia), DSL (Canada)	ENCS (Japan)	ECL (Korea)	IECS (China)
112 945-52-5 7631-86-9	231-545-4	Registered	1-548	KE-30953 (KE-31032)	Registered

▶ For further information please contact:

Commercial Contact

Evonik Degussa GmbH
Business Line Aerosil
Weissfrauenstrasse 9
D-60287 Frankfurt am Main,
Germany
Phone: +49 69/218-2532
Fax: +49 69/218-2533
E-Mail: aerosil@evonik.com
http://www.aerosil.com

NAFTA
Evonik Degussa Corporation
Business Line Aerosil
379 Interpace Parkway,
P. O. Box 677
Parsippany, NJ 07054-0677
Phone: +1 (800) AEROSIL
Phone: +1 (973) 541-8510
Fax: +1 (973) 541-8501

Asia (without Japan)
Aerosil Asia Marketing Office
c/o NIPPON AEROSIL CO., LTD
P. O. Box 7015
Shinjuku Monolith 13F
3-1, Nishi-Shinjuku 2-chome
Shinjuku-ku, Tokyo
163-0913 Japan
Phone: +81-3-3342-1786
Fax: +81-3-3342-1761

Japan
NIPPON AEROSIL CO., LTD.
Sales & Marketing Division
P. O. Box 7015
Shinjuku Monolith 13F
3-1, Nishi-Shinjuku 2-chome
Shinjuku-ku, Tokyo
163-0913 Japan
Phone: +81-3-3342-1763
Fax: +81-3-3342-1772

Technical Contact

Evonik Degussa GmbH
Technical Service Aerosil
Rodenbacher Chaussee 4
P. O. Box 1345
D-63403 Hanau-Wolfgang,
Germany
Phone: +49 6181/59-3936
Fax: +49 6181/59-4489

NAFTA
Evonik Degussa Corporation
Technical Service Aerosil
2 Turner Place
Piscataway, NJ 08855-0365
Phone: +1 (888) SILICAS
Phone: +1 (732) 981-5000
Fax: +1 (732) 981-5275

Asia (without Japan)
Evonik Degussa GmbH
Technical Service Aerosil
Rodenbacher Chaussee 4
P. O. Box 1345
D-63403 Hanau-Wolfgang,
Germany
Phone: +49 6181/59-3936
Fax: +49 6181/59-4489

Japan
NIPPON AEROSIL CO., LTD.
Applied Technology Service
3 Mita-cho
Yokkaichi, Mie
510-0841 Japan
Phone: +81-593-45-5270
Fax: +81-593-46-4657

Please visit our website www.aerosil.com to find your local contact.

AEROSIL® 200 / N oo 0 T / www.aerosil.com

AEROSIL
invented to improve

BIOGRAPHY

Name: Natee Srisawat

Date of Birth: December 22, 1969

Nationality: Thai

University Education:

Bachelor Degree: Textile Chemistry Engineering, Rajamangala University of Technology, Thailand.

Master Degree: Appropriate Technology for Resource Development, Mahidol University, Thailand.

Master Degree: Material Technology, King Mongkut's University of Technology Thonburi, Thailand.

Publication:

Natee Srisawat, Manit Nititanakul and Kawee Srikulkit. Characterizations of Fibers Produced from Polypropylene/Silica Composite, <u>Journal of Metals, Materials and Minerals</u>. 19, 1 (2009): 53-58.